SYNTHESIS AND EVALUTION OF C-2 ARYLIDENE/ ARYL CONGENERS OF LANTADENES AS ANTICANCER AGENTS

By

NAVIN KUMAR TAILOR

A THESIS SUBMITTED IN FULFILLMENT OF THE REQUIREMENTS FOR

THE DEGREE OF DOCTOR OF PHILOSOPHY

IN

PHARMACY

JAYPEE UNIVERSITY OF INFORMATION TECHNOLOGY
WAKNAGHAT

MAY, 2014

CERTIFICATE

This is to certify that the thesis entitled, "**Synthesis and evaluation of C-2 arylidene/aryl congeners of Lantadenes as anticancer agents**" which is being submitted by Navin Kumar Tailor for the award of degree of Doctor of Philosophy in Pharmacy by the Jaypee University of Information Technology at Waknaghat, is a record of the candidate's own work, carried out by him under my supervision. This work has not been submitted partially or wholly to any other University or Institute for the award of this or any other degree or diploma.

Dr. Manu Sharma

ACKNOWLEDGEMENTS

First and foremost I thanks to my GOD for the miraculous ways; He led me throughout this journey. Without His presence, this would not have been possible. His grace, strength, love, care and all the blessings are uncountable in the untrodden path.

It is my great pleasure to express my deep sense of gratitude and sincere thanks to my respected research guide ***Dr. Manu Sharma****, Assistant Professor, Department of Pharmacy, Jaypee University of Information Technology, Waknaghat, Solan, for his guidance, profound interest, meticulous care, support, creative criticism and encouragement.*

I express my sincere gratitude to ***Prof. R. S. Chauhan****, Professor and Head, Dept. of Biotechnology, Bioinformatics & Pharmacy, for his support and valuable suggestions during the work.*

I am delighted to express my thanks to COO. ***Dr. Y. Medury****, Director,* ***Brig (Retd). Balbir Singh*** *and Vice Chancellor,* ***Dr. Ravi Prakash****, Jaypee University of Information Technology, for providing all the necessary facilities, and creating research environment to carry out research.*

I thankful to Department of Biotechnology, Government of India for providing financial assistance for this project.

I also thankful to National Cancer Institute, USA and Cancer Research Initiative Foundation, Drug Discovery Laboratory, Malaysia, to carryout anticancer screening of compounds.

I would like to acknowledge the support of my friends ***Jeet, Varun, Aseem, Tarun*** *&* ***Madan*** *for their cherishable friendship.*

I extend my heart felt thanks to ***my parents & family*** *for their continuous help in various ways during this journey.*

Finally, I would like to thank everybody who was important to the successful realization of work, as well as expressing my apology that I could not mention personally one by one.

Date:

Place: Waknaghat **Navin Kumar Tailor**

TABLE OF CONTENTS

LIST OF TABLES

LIST OF FIGURES

CHAPTER 1

INTRODUCTION AND REVIEW OF LITERATURE

1. Natural products and drug discovery

Nature is known as rich sources of compounds with unique chemical features and pronounced biological activities, found in millions of species of plants, animals, marine organisms and micro organisms. Natural products (NPs) have played, and continue to play, a dominant role in the discovery of lead for the development of conventional drugs for the treatment of the human disease [Harvey, 2008]. NPs have unique diversity with specific stereochemistry, complexity and these are generally derived through specific biosynthetic pathways like shikimate, polyketide or mevalonate, leading to particular class of compounds [Tailor and Sharma, 2013]. They have been extensively used to elucidate complex cellular mechanisms, including signal transduction and cell cycle regulation, leading to the identification of important targets for therapeutic intervention [Chin *et al.,* 2006]. They continue to be of great utility as biological tools as well as therapeutic agents and in this context, the diversity of natural structures continues to impress and inspire medicinal chemistry.

In many cases, structural modifications of natural products imparts new physicochemical properties with improved biological effects, fewer side effects and provide more structural insight to established structure-activity relationships [Huryn and Wipf, 2008]. Integration of combinatorial chemistry, computational chemistry and high-throughput screening are able to afford compounds that are far more efficient than those currently used in clinical practice. Likewise, advances in genomics and the advent of biotechnology have improved both the discovery and production of new natural compounds. Despite the ever-increasing demand of new natural products, their isolation and structure elucidation still remain a labor-intensive process. As an alternative, chemists are now enlisting the tools of solid-phase combinatorial synthesis to construct libraries of natural product analogues and natural product like compounds [Cragg and Newman, 2005].

Within the spheres of cancer, a number of compounds (>60%) were obtained directly or indirectly from natural origin with significant anticancer activity. On the basis of encouraging results of vinca alkaloids and podophyllotoxins, National Cancer Institute initiated an extensive plant collection program in 1960, focused mainly in temperate regions, which led to the discovery of many novel chemo types showing a range of

cytotoxic activities [Balunas and Kinghorn, 2005]. Despite major limitations of NPs including poor solubility in biological fluids, undesirable pharmacokinetics and associated toxicity, structural and chemical diversity of NPs are well suited to provide the core scaffolds for future cancer chemotherapeutics development. Modulation of the transcription factors (e.g., NF- κB, AP-1, STAT3), anti-apoptotic proteins (e.g., Akt, Bcl-2, Bcl-XL), proapoptotic proteins (e.g., caspases, PARP), protein kinases (e.g., IKK, EGFR, HER2, JNK, MAPK), cell cycle proteins (e.g., cyclins, cyclin-dependent kinases), cell adhesion molecules, COX-2, and growth factor signaling pathways by NPs are believed to responsible for their cancer protective role [Aggarwal and Shishodia, 2006]. Several natural products have been investigated as promising anticancer activity and were discussed on the basis of their origin from plant, marine- and microorganism.

The role of weeds in the present pharmacopeia has been overlooked, despite significant evidence that weeds in particular, are an important source of medicines for indigenous peoples and have a highly significant over representation in indigenous pharmacopoeias in relation to other types of plants [Stepp and Moerman, 2001]. There are numbers of evidences that weeds are relatively high in bioactive secondary compounds and are thus likely to hold promise for drug discovery. One such weed, which has attracted a lot of interest of scientists, is *Lantana camara* L. (Verbenaceae). It is a rich source of a number of biologically active triterpenoids. Lantadene A and B are the pentacyclic triterpenoids isolated from the leaves of *Lantana camara* L. and these compounds have attracted lot of interest in last three decades because of their anticancer properties [Inada *et al.,* 1995; Sharma *et al.,* 2007; Kaur *et al.,* 2008; Kaur *et al.,* 2010]. Recent research has indicated that the NF-κB, AP-1, Bcl-2, signaling pathway are suppressed in tumor cells during treatment with these compounds [Sharma *et al.,* 2007; Kaur *et al.,* 2008; Kaur *et al.,* 2010]. Several congeners of lantadene have been synthesized and evaluated for antitumor activity [Sharma *et al.,* 2007 a, b, c; Sharma *et al.*, 2008]. Therefore, the secondary metabolites of such weeds can provide lead molecules for various diseases.

2. Antioxidant and oxidative stress

Reactive species (RS), including reactive oxygen (ROS) and reactive nitrogen species (RNS), are constantly generated during normal oxidative metabolism in aerobic organisms and in response to environmental stimuli. These are small molecules or ions formed by the

incomplete one-electron reduction of oxygen, and include free radicals such as superoxide anion ($O_2^{\bullet-}$), hydroxyl radical ($OH^{\bullet}$), peroxyl radical ($RO_2^{\bullet}$), and alkoxyl radical ($RO^{\bullet}$) as well as non-radical species that are oxidizing agents and/or easily converted into radicals, such as hydrogen peroxide (H_2O_2), hypochlorous acid (HOCl), ozone (O_3), and singlet oxygen ($^1O_2$) [Simonian and Coyle, 1996]. ROS are generated by exogenous source (UV light, ionizing radiation and inflammatory cytokine) and endogenous source such as mitochondria [Inoue *et al.,* 2003], xanthine oxidase [Li and Jackson, 2002], neutrophils, eosinophils, macrophages, CP450 [Conner and Grisham, 1996], microsomes and peroxisomes [Gupta *et al*., 1997]. There are several other factors have also been investigated to elicit production of ROS [Morel and Barouki, 1999].

Furthermore, some of transition metals such as iron, copper, chromium, cobalt, vanadium, cadmium, arsenic, and nickel have been investigated to play important role in generation of free radicals via Fenton chemistry [Halliwell and Guteridge 1990; Leonard *et al*., 2004; Valko *et al*., 2005]. Under physiological conditions, intricate defense systems composed of antioxidant enzyme systems (superoxide dismutase, catalase, and glutathione peroxidase) and non-enzymatic antioxidants such as glutathione (GSH), vitamins (A, E and C), melatonin, uric acid, lipoic acid, carotenoids, and polyphenols (flavonoids, curcumin, resveratrol and others), impart balance between generation and neutralization of reactive oxygen species [Mates *et al*., 1999; McCall and Frei, 1999]. Inadequate antioxidant defense systems, improper intake of dietary antioxidant supplements and excessive generation of ROS, leads to so called "oxidative stress" (OS). RS also cause interact and damage to cellular macromolecules such as nucleic acid, protein and lipids [Levine and Stadtman, 2001; Stadtman, 2001; Welch *et al.,* 2001].

Cysteine residues and protein bound metals, including heme iron are the primary targets of ROS, as it readily (reversibly or irreversibly) oxidized to a disulfide bond (–SSR), sulfenic acid (–SOH), sulfinic acid ($–SO_2H$) or sulfonic acid ($–SO_3H$) [Thannickal and Fanburg, 2000; Poli *et al.,* 2004]. Cystein residue containing signaling enzymes and proteins include phospholipase C [Zhao *et al.,* 2005; Cheng *et al.,* 2006], phospholipase A_2 [Akiyama *et al.,* 2006; Muralikrishna and Hatcher, 2006] and phospholipase D [Tappia *et al.,* 2006]. Ion channels [Moudgil *et al.,* 2006; Thomas *et al.,* 2007], including calcium channels [Hajnoczky *et al.,* 2006], have been proposed potential target for ROS. Further,

signaling mechanisms that respond to changes in the thiol/disulfide redox state, such as Src family kinase [Nakamura *et al.,* 1993; O'Hara *et al.,* 2003], MAPKs [Chang and M. Karin, 2001; Schmitz *et al.,* 2002], activator protein-1 (AP-1) [Okuno *et al.,* 1993] and nuclear factor-κB (NF-κB) [Schreck *et al.,* 1991] transcription factors can also be targets. Apart from deleterious nature, ROS play central role in intracellular signal transduction pathways for variety of pathophysiological cellular responses and pathophysiology of various diseases such as acute respiratory distress syndrome [Wilson *et al.,* 2001], aging [Dugan and Quick, 2005], Alzheimer [Hensley *et al.,* 1996; Multhaup *et al.,* 1997], atherosclerosis [Halliwell, 1989], cancer [Yoshizumi *et al.,* 2001; Touyz, 2004], cardiovascular disease [Di Virgilio, 2004; Muhammad *et al.,* 2009], diabetes [Moulton, 1996], inflammation [Bolanos *et al.,* 2009], inflammatory joint disease [Atabek *et al.,* 2004], neurological disease [Furukawa *et al.,* 2004], obesity [Kamp *et al.,* 1992; Tabner *et al.,* 2001], Parkinson [Gelderman *et al.,* 2007], pulmonary fibrosis [Haurani and Pagano, 2007], rheumatoid arthritis [Jeremy *et al.,* 2004], and vascular disease [Perez-Gregorio *et al.,* 2011; Figueiredo-Gonzalez *et al.,* 2012]. Since, endogenous antioxidant defense system is not always completely effective and there is continuous exposure to various environmental factors, there is always a need to search new drug candidates to counter oxidative damage.

In this quest, co-administration of antioxidant enzyme system and non-enzymatic antioxidant or their integration or covalently attachment with existing drug candidates played a pivotal role. In this context, antioxidant hybrid approach may provide possibilities for generating a diverse array of new types of molecules as promising therapeutic agents in oxidative stress induced diseases.

2.1. Biological effects of antioxidants and their mechanism

A variety of enzymatic and non-enzymatic antioxidants have been investigated from natural or unnatural origins with potential role in biological systems. Mainly following three mechanism of action have been proposed of antioxidants against RS induced oxidative damage: - (i) modulation of signaling pathways that mediated gene regulation in response to ROS, (ii) quenching of free radicals, (iii) direct chemical interaction of the antioxidant with signaling enzymes and transcription factors [Leonarduzzi *et al.,* 2010]. The mechanism of some of the important antioxidants is discussed here. The α-tocopherol is an important antioxidant which plays a vital role in

various inflammations and it directly binds with phospholipase A_2 (PLA_2) [Chandra *et al.,* 2002]. At the same time, it leads to modulation of NADPH oxidase, protein kinase C (PKC), protein kinase B (PKB) via inhibition of subunit assembly [Zingg, 2007; Linnewiel *et al.,* 2009]. The trans-retinoic acid regulates the physiology of cells differentiation and apoptosis via directly binding with protein kinase C (PKCα and PKCβ) [Ochoa *et al.,* 2003; Kambhampati *et al.,* 2003].

Similarly, ascorbic acid potentiates enzymatic degradation of hypoxia inducible factor-1 (HIF-1α) via proline and asparagine hydroxylase [Vissers *et al.,* 2007]. Curcumin is another important antioxidant which has attracted various research groups in recent times and it has been observed that it modulates PKC, NF-κB and AP-1 by direct binding [Mahmmoud, 2007; Conboy *et al.,* 2009], and by inhibition of IκBα proteasome [Hussain *et al.,* 2008; Milacic *et al.,* 2008] and Fos-Jun-DNA complex formation [Hahm *et al.,* 2002]. Resveratrol modulate c-Src, PK (by direct binding) [Yu *et al.,* 2001], NF-κB (by inhibition of the pathway and/or of IκBα proteasome degradation) [Hauptmann *et al.,* 1996; Shakibaei *et al.,* 2008], and AP-1 by alteration in its composition [Yang and Meyskens, 2005]. Inhibition of NADP oxidase subunit translocation by epigallocatechin gallate imparts its mast stabilizing and antiallergic activity [Nishikawa *et al.,* 2007]. Flavonoids regulate RTK, MAPKs, PI3K/Akt by direct action [Teillet *et al.,* 2008; Labbe *et al.,* 2009], and modulation of NF-κB by inhibition of the pathway and/or of IκBα proteasome degradation [Banerjee *et al.,* 2008]. Antiinflammatory effects of kaempferol and quercetin exerted by direct binding with vascular cell adhesion molecule-1 (VCAM-1), intercellular adhesion molecule-1 (ICAM-1), endothelial cell selectin (E-selectin), inducible NO synthase (iNOS) and cyclo-oxygenase-2 (COX-2) [Crespo *et al.,* 2008]. GSH play its crucial role against oxidative damage via S-glutathionylation of PKCs [Chu *et al.,* 2001], MAPKs [Cross and Templeton, 2004], IKKβ, p65, NF-κB [Reynaert *et al.,* 2006; Qanungo *et al.,* 2007] and p53 [Velu *et al.,* 2007].

Apart from these molecular targets there is another important pathway which plays an important role in oxidative stress. Nrf2 is a nuclear transcription factor that controls the expression and coordinated induction of a battery of defensive genes encoding detoxifying enzymes and antioxidant proteins. This is a mechanism of critical importance for cellular protection and cell survival. Nrf2 is retained in the cytoplasm by an inhibitor, INrf2 which

functions as an adapter for Cul3/Rbx1-mediated degradation of Nrf2. In response to oxidative/ electrophilic stress, Nrf2 is switched on and then off by distinct early and delayed mechanisms. Oxidative/ electrophilic modification of INrf2 cysteine 151 and/or protein kinase C phosphorylation of Nrf2 serine 40 results in the escape or release of Nrf2 from INrf2. Nrf2 is stabilized and translocates to the nucleus, forms heterodimers with unknown proteins, and binds the antioxidant response element, which leads to coordinated activation of gene expression. The switching on and off of Nrf2 protects cells against free radical damage, prevents apoptosis, and promotes cell survival. Recently, various antioxidants such as curcumin, caffeic acid, resveratrol, lipoic acid, catechin and their congeners result in up-regulation of Nrf2 in various *in-vitro* and *in-vivo* models [Balogun *et al.,* 2003; Kang *et al.,* 2007; Farombi *et al.,* 2008]. The Nrf2 have been found as an important activator of phase II antioxidant genes.

2.2. Antioxidant hybrid systems

Hybrid systems are constructing of different molecular entities from natural or unnatural origin to transform or augment different entities or to generate a molecule with bifunctional feature with new properties. This design of antioxidant enzymes or non-enzymatic antioxidants conjugation with other bioactive molecules/ drug used in oxidative stress induced diseases might be helpful to increase the potencies and diversity of drug candidates/ molecules [Mehta and Singh, 2002].

2.2.1. Hybrids based on 1, 2-dithiolone moiety

Alpha-lipoic acid (ALA), also known as 1, 2-dithiolane-3-pentanoic acid, is a natural antioxidant that scavenges reactive oxygen species (ROS) and regenerates or recycles endogenous antioxidants, and exists as R- and S-enantiomeric forms. However, only R-LA is conjugated to conserved lysine residues in an amide linkage of mitochondrial multi-enzyme complexes that catalyze the oxidative decarboxylation of α-keto acids (e.g. pyruvate dehydrogenase, 2-oxo-glutarate dehydrogenase, and transketolase) and glycine cleavage, thus plays a critical role in mitochondrial energy metabolism. ALA **1** is readily taken up and reduced in cells and tissues to dihydrolipoic acid **2** (DHLA), and exert oxidative protection in both intracellular and extracellular environments. Furthermore, they have also been involved in regeneration of other antioxidants (vitamin C and vitamin E) via redox coupling and increase intracellular glutathione levels [Suzuki *et al.,* 1991; Kagan

et al., 1992; Yan *et al.,* 1996]. Thiol functionality of glutathione has been proposed for major contributor to oxidative defense in brain, but glutathione cannot be directly administered whereas ALA can be administered directly. *In-vitro*, animal, and reliminary human studies indicate that alpha-lipoate may be effective in numerous neurodegenerative disorders [Packer *et al.,* 1997].

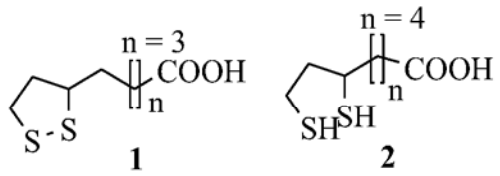

1 **2**

2.2.1.1. Hybrids with 1, 2-dithiolone moiety as neuroprotective agent

In an effort to design potential neuroprotective agents with 1, 2-dithiolone scaffold, Koufaki M. and co-workers conjugated ALA **1** with catechol **3** and were screened on glutamate-challenged hippocampal HT22 cells [Koufaki *et al.,* 2007]. Interestingly, neuroprotective potential were increased on bioisosteric replacement of the amide group with heteroaromatic rings such as triazole, 1, 2, 4-oxadiazole, 1, 3, 4-oxadiazole, tetrazole or thiazole **4a-e** in comparison to parent ALA. Similarly, bioisosteric replacements of amide functionality with heteroaromatic ring in LA-chroman conjugates **5** were done to observe influence in oxidative stress-induced cell death of glutamate-challenged HT22 hippocampal neurons by Koufaki M. and co-workers [Melagraki *et al.,* 2009]. The results showed that in case of **4d** (EC_{50} 2.99 ± 0.14 μM) and **5**, the effect of housing a hetero aromatic ring and free phenolics moiety in one molecule gives synergistic effect rather than additive.

Cholinesterase enzyme (Acetylcholinesterase, AChE and Butyrylcholinesterase, BuChE), are key regulators of acetylcholine level in synaptic region, and have significant contribution in many neurodegenerative disorder especially in Alzheimer's disease (ADs). Recognizing the importance of the polyphenolic moiety in many biologically active natural/synthetic products, and their well establish neuroprotective ability, Woo, Y.J. *et al.* have crafted LA-polyphenolic hybrids and concluded that cinnamate based polyphenolic compounds were potential cholinesterase inhibitor, which might be due to the presence of *α,β*-unsaturated carbonyl moiety [Woo *et al.,* 2011]. Acetylated caffeic acid conjugate **6** was ~800 fold selective potential inhibitor of BuChE (IC_{50} = 0.5 ± 0.2 μM and K_i = 1.52 ±

0.18 μM) over AChE. In another report, Decker, M. *et al.* designed [2, 1-b] quinazolinimines **7** and ALA **1** hybrids connected through varying length of methylene spacer (n = 2-6) [Decker *et al.,* 2008] and it was observed that spacer chain length is proportional to selectivity towards BuChE. The hybrid bearing octamethylene spacer **8** exhibit ~10 fold and ~1000 fold more potent AChE and BChE inhibitory activity in contrast to parent quinazolinimines, respectively.

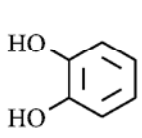

3

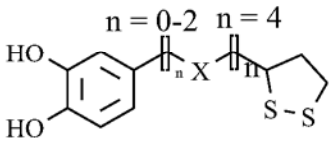

4a X = 1,2,4-oxadiazole
4b X = 1,3,4-oxadiazole
4c X = 1,2,3-triazole
4d X = Tetrazole
4e X = Thiazole

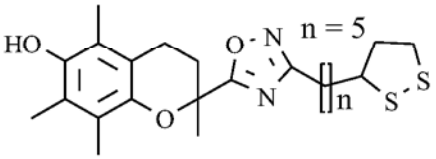

5

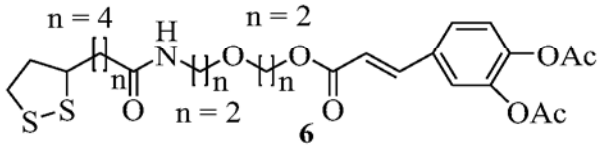

6

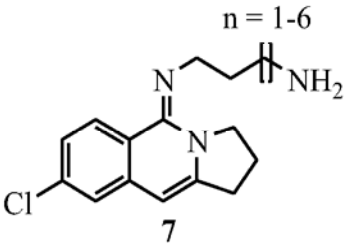

7

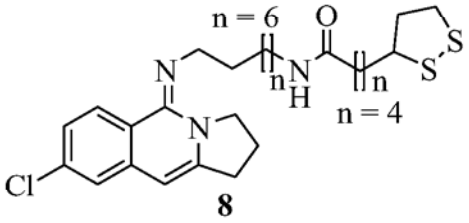

8

2.2.1.2. Hybrids with 1, 2-dithiolone moiety as cardioprotective agent

Coronary artery occlusion results from deposition of fatty materials or damage to vasculature endothelial lining, leading to myocardium infraction. In general, treatment of acute myocardial ischemia involves the use of either thrombolytic agents or percutaneous transluminal coronary balloon angioplasty (PTCA), which effectively restores blood flow to the myocardium and reduce overall mortality. However, these therapies do not protect the heart from the damage caused by ROS, produced upon the readmission of oxygenated blood into the ischemic myocardium (reperfusion). Furthermore, it was found that oxygen free radicals react with the phospholipids components of the myocardium affecting selective permeability of cell membranes and resulting in the development of life

threatening ventricular arrhythmias and/or fibrillation. On the other hand, experimental findings support the hypothesis that lipid peroxidation inhibitors such as vitamin E protect the myocardium from I/R injury [Koufaki *et al.,* 2003].

In order to explore role of lipoic acid on cardiovascular damage, Koufaki, M. *et al.* conjugate ALA **1** with trolox 9 **(**6-hydroxy-2,5,7,8-tetramethylchroman-2-carboxylic acid), an analogue of vitamin E **10**, and evaluated for lipid peroxidation inhibition and antioxidant capacities (measured as contents of malondialdehyde) [Koufaki *et al.,* 2004]. Lipoic acid substitution with amide functionality at C-2 and C-5 position by methylene spacer **11a-b** and **12-15**, were assessed as essential feature in order to total suppression of reperfusion arrhythmias while compounds with direct attachment on C-4 position **13** and trolox/lipoic acid mixture reduced the arrhythmia score by 63.5% and 53%, respectively. Furthermore, antioxidant and inhibitory lipid peroxidation capacity of hybrid compounds were comparable to trolox/lipoic acid mixture.

2.2.1.3. Hybrids with 1, 2-dithiolone moiety as radioprotective agent

Melatonin (*N*-acetyl-5-methoxytryptamin) **16**, pineal gland hormone which regulates circadian rhythms and critically controlling the sleep-wake cycle [Altun and Ugur-Altun, 2007] and also have the capacity to protect nuclear and mitochondrial DNA from oxidative damage [Reiter *et al.,* 2001]. Furthermore, significant application in cancer, immune disorders, cardiovascular diseases, depression, seasonal affective disorder (SAD), circadian rhythm sleep disorders, and sexual dysfunction make it interesting biomolecule. The radioprotective activity of melatonin was increased by conjugating 1, 2-dithiolane moiety (ALA) with melatonin to form new hybrid molecule melatoninolipoamide **17** [Venkatachalam *et al.,* 2006]. Pulse radiolysis induced one-electron oxidation and reduction of **17** showed that the melatonin moiety in the conjugate is more susceptible for the oxidation, while the lipoic acid moiety for the reduction.

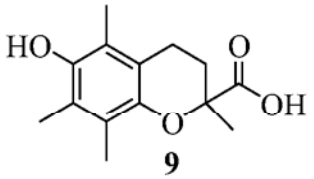

9

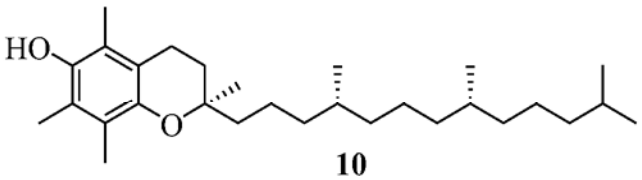

10

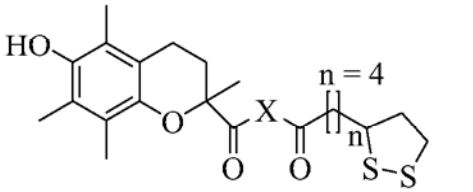

11a X = $HN(CH_2)_2NH(CH_2)_2NH_2$
11b X = $HN(CH_2)_2C_4H_9N_2$

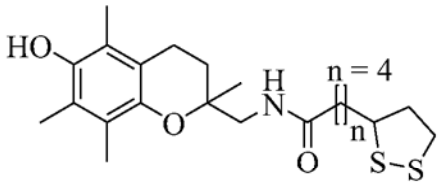

12

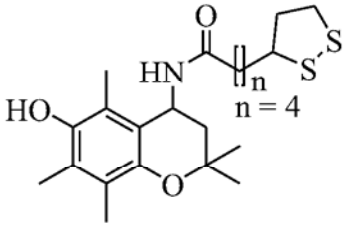

13

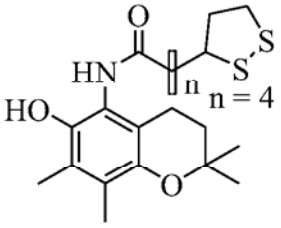

14

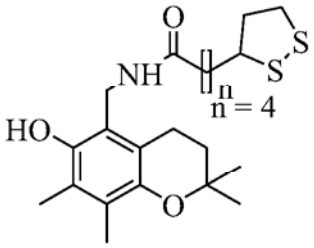

15

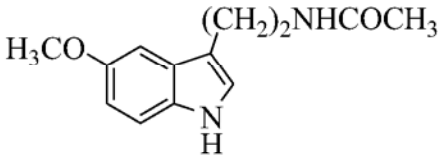

16

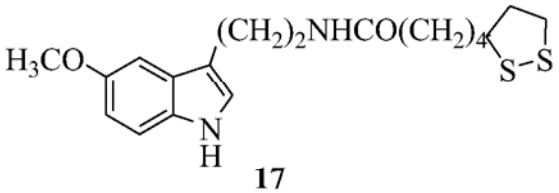

17

2.2.1.4. Hybrids with 1, 2-dithiolone moiety as antiinflammatory agent

In recent years role of antioxidants are well established in combating inflammatory disorders. There are many hetero aromatic ring containing compounds from natural and synthetic origin, which have been shown potential inflammation inhibitory activity [Todeschini *et al.,* 1998; Rani *et al.,* 2004]. In view of fact that, hetero aromatic ring conjugates with lipoic acid via amide linkage might give potential drug candidates, in this direction, quinolinone-3-aminoamides **18** [Detsi *et al.,* 2007] and coumarin-3-aminoamides **19** [Melagraki *et al.,* 2009] were conjugated with lipoic acid and tested for their inhibitory ability to lipoxinagenase (LOX %, 0.1 mM) and Carrageenin rat paw edema (CPE %, 0.01 mmol/Kg body weight). Results indicated that compounds with aromatic diamine (especially 1, 2-phenylene diamine) were more potent in comparison to aliphatic diamine while vice versa in case of LOX %. Lipoxinagenase inhibitory capacities of quinolinone-3-aminoamides-lipoic acid hybrid **20** were observed higher (100%) in comparison to corresponding parent amino amides while vice versa in case of CPE inhibition. In case of CPE inhibition %, coumarin-3-aminoamides-lipoic acid hybrid **21** was observed more

potential (73%) in comparison to corresponding parent amino amides, while vice versa in case of inhibitory LOX %.

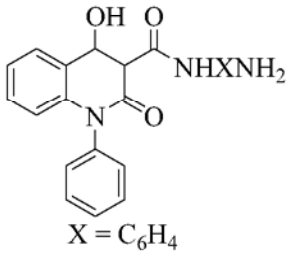

18

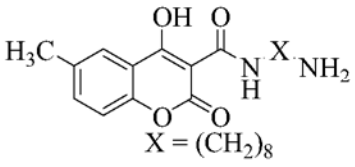

19

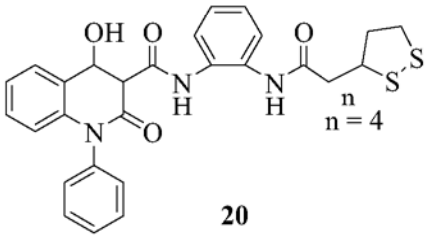

20

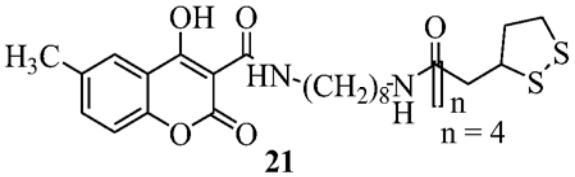

21

2.2.2. Hybrids based on *α,β*-unsaturated carbonyl moiety

α,β-unsaturated carbonyl moiety bearing compounds comprise a wide group of naturally occurring compounds includes coumarin (benz-α-pirone) **22**, flavones **23**, chalcone **24**, and curcumin **25**. Remarkable array of biological activities and associated low toxicity of these compounds seems special place in nature. Mode of biological action of this class of compounds has long been believed to be due to their interaction with thiol groups of enzymes via Michael addition at ketovinyl double bond [Opletalova, 2000].

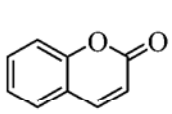

22

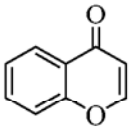

23

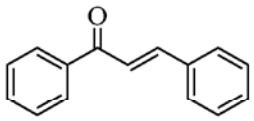

24

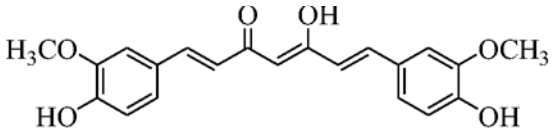

25

SAR studies showed that electron withdrawal (EW) group is favorable because it will increase the electrophilicity of the C-β and thus facilitate the nucleophilic attack of the cellular thiols groups and opposite is true for the electron donating (ED) groups. Coumarin (1, 2-benzopirone) is one of the important class of *α,β*-unsaturated carbonyl group. Several natural and synthetic coumarins have been found to exhibit variety of pharmacological activities like anti-HIV, anticoagulant, antibacterial, antioxidant, anti-inflammatory, and fluorescent labeling [Lee *et al.,* 1994; Kalkhambkar *et al.,* 2008; Roussaki *et al.,* 2010].

2.2.2.1. Hybrids with *α,β*-unsaturated carbonyl moiety as anticancer agent

Among the diverse biological activities of coumarin, the most intriguing bioactivity is the effect against breast cancer [Musa *et al.,* 2009]. Tamoxifen **26** is a selective estrogen receptor modulator (SERM) and used thoroughly in breast cancer for more than three decades [Jaiyesimi *et al.,* 1995]. The side effects and drug resistance are major concerns of tamoxifen [Fisher *et al.,* 1994; Filardo *et al.,* 2000]. Recently, 667 COUMATE **27** and neo-tanshinlactone **28** are in phase I clinical trials with increase in 10-fold potency and 20-fold selectivity in comparison to Tamoxifen **27** [Stanway *et al.,* 2006]. In order to explore role of *α,β*-carbonyl moiety in cancer, Sashidhara, K.V. *et al.* synthesized a series of coumarin-chalcone hybrids and evaluated their cytotoxic potential against KB (Oral squamous cell carcinoma), C33A (cervical carcinoma), MCF-7 (Breast adenocarcinoma), A549 (lung) and one normal human NIH3T3 (Mouse embryo fibroblast) [Sashidhara *et al.,* 2010]. Overview of the results proposed that a chalcone-coumarin hybrid with electron withdrawing group **29** was more potent in comparison to parent coumarin.

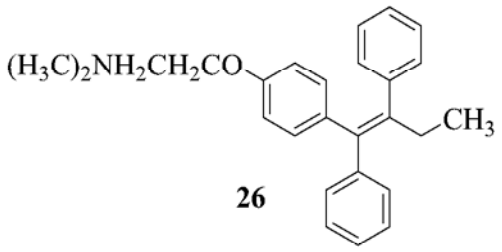

26

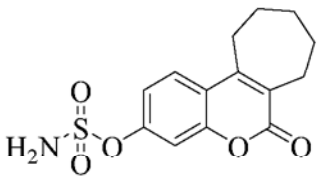

27

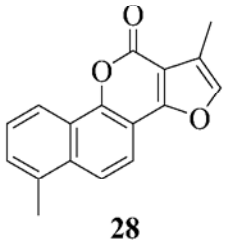

28

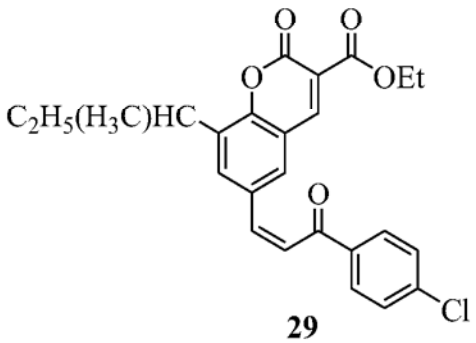

29

Structure activity relationship (SAR) studies of various anticancer agents auspicate that methoxy group is one of important functional group responsible for cytotoxic potency and it was backed by significant role of resveratrol (3,5,4'-trihydroxy-trans-stilbene) **30**, and 3,4,5,4'-tetramethoxystilbene (DMU-212, **31**) in various types of cancer. In this context, Belluti, F. *et al.* have inserted substituted *trans*-vinylbenzene moiety on coumarin

backbone and screened for antiproliferative activity against lung carcinoma H460, squamous cell carcinoma A431 and melanoma JR8 [Belluti *et al.,* 2010]. 3,5-dimethoxy- **32a** and 3,5-dimethylstilbin **32b** substitution on 7-methoxycoumarin scaffolds at C-4 position was found to exert optimum inhibitory action against H460 (0.45 ± 0.09 μM), A431 (3.44 μM) and JR8 (3.2 μM).

Estrogens (oestrogen) are primary female sex hormone; stimulate the proliferation of normal and malignant cells *via* induction of nucleic acid synthesis and activation of growth regulatory genes namely ERα and ERβ. Steroidal framework of estradiol (E2) provide site of attachment of variety of substituents such as cytotoxic moieties, radioisotopes, dietary antioxidants, affinity and photo affinity-labeling groups, of which several E2 conjugates have advanced as synthetic ligands for targeting the ER [el Amouri *et al.,* 1992; Bodine *et al.,* 2002]. In this direction flavones and coumarins have been conjugated with ER to obtain hybrid molecules **33**, **34** and it leads to enhancement of potency and selective towards ERα in comparison to estradiol [Ahmed *et al.,* 2007; Musa *et al.,* 2009].

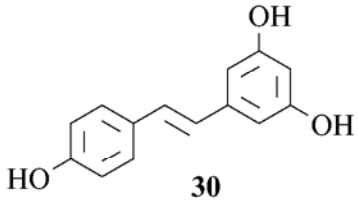

30

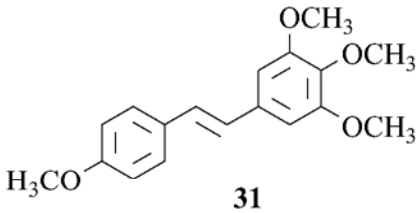

31

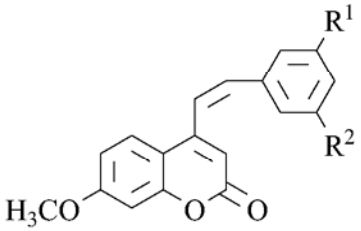

32a $R^1 = OCH_3$ $R^2 = OCH_3$
32b $R^1 = CH_3$ $R^2 = CH_3$

Aqueous solubility (log W) is an important consideration in formulation and development phase of drug candidates as most of drugs are orally administered and is likely to hamper bioavailability [Allen and Smith, 2001]. Various approaches have been employed to improve aqueous solubility such as salt formation, amino acid conjugate and prodrug approach. Paclitaxel, potential mitotic inhibitors, have been used in chemotherapy of patient suffering from lung, ovarian, breast cancer, and advanced forms of Kaposi's sarcoma [Saville *et al.,* 1995]. Complex structural feature of paclitaxel renders its hydrophobicity, allergic reaction and precipitation on aqueous dilution on intravenous administration with non-aqueous vehicle containing detergent like Cremophor EL [Singla *et al.,* 2002]. Paclitaxel also have serious side effects such as unusual bruising or bleeding,

pain/redness/swelling at the injection site, fever, chills, cough, sore throat, difficulty in swallowing, dizziness, shortness of breath, severe exhaustion, skin rash, facial flushing, female infertility by ovarian damage [Ozcelik *et al.,* 2010] which enforce for further structural modification or develop new delivery systems to reduce its toxicity. In this direction, Noguchi, M. *et al.* prepared photoliable 7-N,N-diethylamino-4-hydroxymethyl coumarin (DECM) hybrid of paclitaxel **35** to improve water solubility along with enhancement of target specificity [Noguchi *et al.,* 2008].

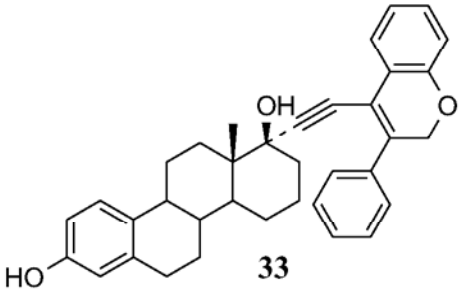

33

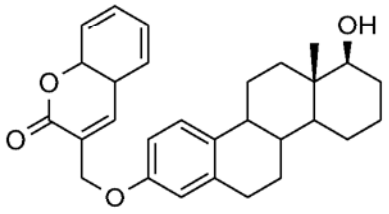

34

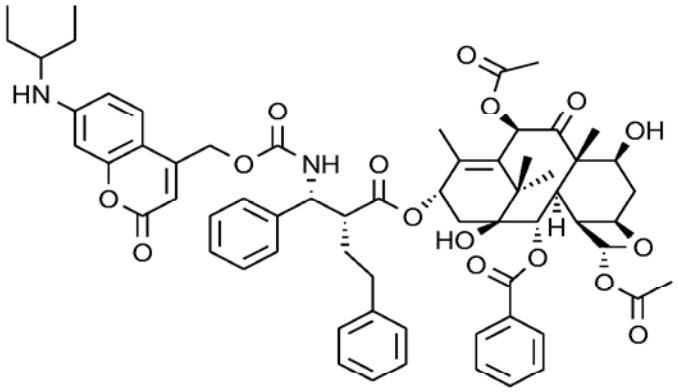

35

Fluorescent labeling involves covalent attachment of drug with antibodies, protein, amino acid, and peptide which are used as specific probes for detection of a particular target via fluorescence microscopy, flow cytometer or some other fluorescence reading instrument [Brush]. Commonly used fluorescent dyes are fluorescein, rhodamine, Alexa Fluors, Dylight fluors, ATTO dyes (labeling of DNA, RNA and protein), BODIPY dyes (4,4-difluoro-4-bora-3a,4a-diaza-s-indacene), and 6-FAM phosphoramidite. Presence of chromophore, α,β-unsaturated carbonyl moiety in coumarin and structure resemblance with fluorescent dyes imparts significant fluorescent characteristic to them.

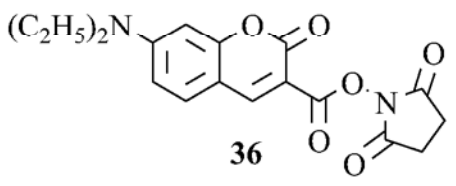

36

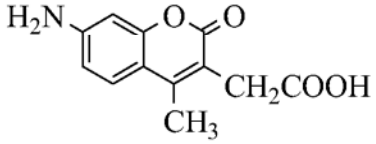

37

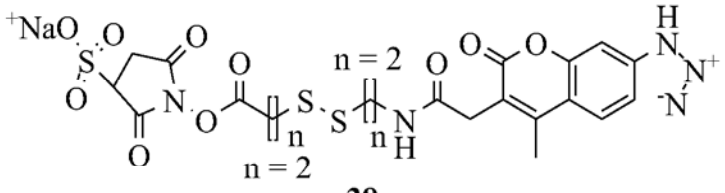

38

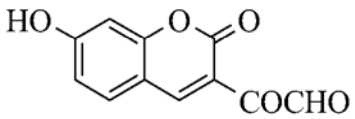

39

There are several examples such as 7-diethylaminocoumarin succinimidyl ester (DEAC-SE) **36**, 7-amino-4-methyl coumarin-3-acetic acid **37** (AMCA) [Eldaw and Khalfan, 1988], sulfosuccinimidyl-2(7-azido-4-methycoumarin-3-acetamido)-ethyl-1,3′-dithiopropionate (SAED) **38** [Thevenin *et al.,* 1992], 7-hydroxycoumarinyl-3-glyoxal **39** (HOCGO), 7-(dimethylamino)coumarinyl-3-glyoxal (DMACGO) **40** [Baburaj *et al.,* 1994], and 4-bromometyl-7-methoxy-coumarin **41** (BrMMC) [Stratford and Dennis, 1992] which shows wild applicability of coumarin and similar moieties in the biological fields. Recently in 2008, Wells, G. *et al.* observed supportive role of 7-diethylaminocoumarin in nuclear penetration on conjugation with sequence-selective DNA-targeting agents pyrrolo [2, 1-c] [1, 4] benzodiazepine (PBD) **42** via varying length of spacer [Wells *et al.,* 2008].

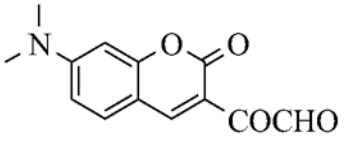

40

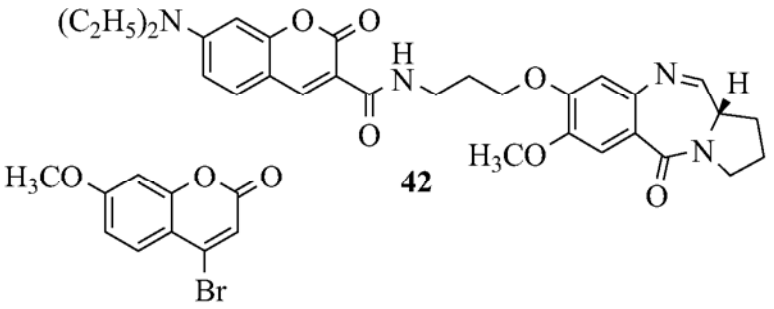

41

42

2.2.2.2. Hybrids with α,β-unsaturated carbonyl moiety as cardioprotective agent

Limited success of antiarrhythmic drugs in suppression of reperfusion arrhythmia and sudden cardiac death is due to the associated increased risk of proarrhythmia and lack of selectivity towards ion channels, which enforce to find out new drug candidates. Similarly, vitamin E has been shown protective role in myocardium from ischemia/

reperfusion (I/R) injury, but hydrophobicity impedes it to gain access to the intracellular compartment. In this context, Koufaki M. *et al.* have conjugated α-tocopherol (Vitamin E, **10**) with class I antiarrhythmics namely procainamide **43** and lidocaine **44** in order to obtain bifunctional antiarrhythmic antioxidants [Koufaki *et al.,* 2003]. Phytyl chain of vitamin E was replaced with different alkyl chain of one, six or twelve carbon atoms. Among procainamide analogue (**45a-c**, **46a-c**) only C-2 methyl substituted analogue **45a** was able to decrease in premature beats (5 ± 2 and 7 ± 3.5 at 100 and 30 mM, respectively), in comparison to procainamide (5 ± 3 and 6 ± 2.5 at 100 and 30 mM, respectively).

Similarly, only **45a** was able to increase in QRS intervals which were comparable to that of procainamide (**45a**: 60 ± 6, 54 ± 8 ms at 100 and 30 mM, respectively; procainamide: 66 ± 10, 58 ± 5 ms at 100 and 30 mM, respectively). While both lidocaine analogue (**47a-b**) showed potential to decrease premature beats (**47a**: 7 ± 2 and 8 ± 2.1 at 100 and 30 mM, respectively; **47b**: 6 ± 2.5 and 6 ± 3 at 100 and 30 mM, respectively) which was slightly less than lidocaine (4 ± 3 and 5 ± 3 at 100 and 30 mM, respectively). The hybrids **47a** and **47b** showed 100% inhibition of lipid peroxidation 10 μM. At the same time, QRS intervals were comparable to parent drug lidocaine. Substitution at C-5 position with methylene spacer between amino amide groups is key feature of these hybrids against reperfusion arrhythmias.

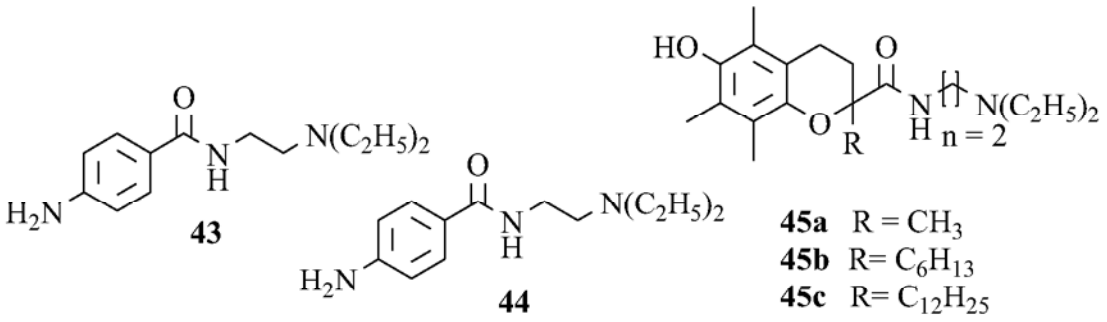

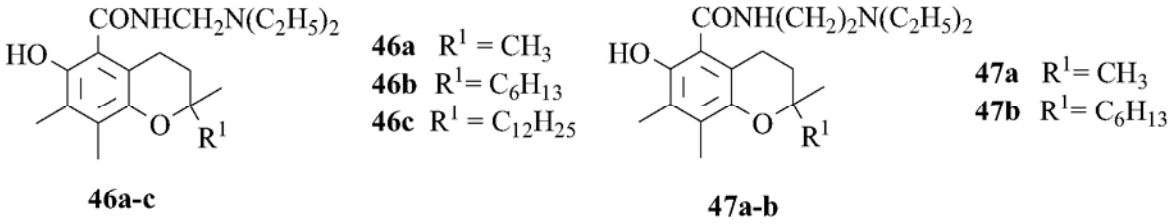

2.2.2.3. Hybrids with *α,β*-unsaturated carbonyl moiety as antimicrobial agent

Hepatitis C virus (HCV), the major etiological agent of the non-A non-B hepatitis, was identified at the molecular level at the end of the 1980s [Choo *et al.,* 1989]. Presently, it is estimated that HCV infects more than 170 million persons worldwide and thus represents a viral pandemic that is about five times more widespread than infection by the human immunodeficiency virus (HIV) [Wasley and Alter, 2000]. RNA-dependent RNA polymerase (RdRP) is essential for viral replication and no functional equivalent in uninfected mammalian cells make validated drug target to block HCV replication with negligible associated toxicity [De Francesco *et al.,* 2003]. Currently three classes of inhibitors are used namely; nucleoside analogues, non-nucleoside inhibitors (NNIs) and pyrophosphate inhibitors. Non-nucleoside inhibitors include structurally heterogeneous compounds having benzimidazole **48, 49** [Hashimoto *et al.,* 2001, Beaulieu *et al.,* 2002], benzothiadiazine derivative **50** [Dhanak *et al.,* 2001]. In order to optimize structure of benzimidazole based RNA-dependent RNA polymerase (RdRP) inhibitors against hepatitis C virus. Hwua, J.R. *et al.* synthesized a series of benzimidazole-coumarin conjugates by one-flask methods and evaluated against hepatitis C virus [Hwu *et al.,* 2008]. SAR analysis concluded that (a) introduction of a Br group on the coumarin ring (e.g., **51b** *versus* **51a**) enhanced HCV inhibition by 6.7-fold and also the selectivity by 2.9-fold; (b) introduction of an OMe group on the coumarin ring (e.g., **51d** *versus* **51c**) further improved the antiviral activity; (c) enhancement of the selectivity resulting from substitution in the coumarin nucleus (cf. **51d**, **51a**, and **51c**) followed the order OMe <H <Br; (d) incorporation of β-D-glucose peracetate moiety into the benzimidazole-coumarin conjugate (e.g., **51c** *versus* **52**) resulted in a 4.8-fold increase in anti-HCV activity.

2.2.2.4. Hybrids with α,β-unsaturated carbonyl moiety as radical quenching agent

Fullerene also known as buckminsterfullerene is composed of C_{60} carbon exists in the form of a hollow sphere, ellipsoids, or tube. The ability of C_{60} and its congeners to scavenge a large number of radicals per molecule [Morton, *et al.,* 1998] makes them potential drug candidates in pathophysiology of oxidative stress induced disorder, namely cardiovascular [Wang *et al.,* 1999; Hsu *et al.,* 2000] and neurodegenerative diseases [Dugan *et al.,* 1997; Dugan *et al.,* 2001]. Recently, researcher have succeeded in conjugation of fullerenes with number of radical scavenging agents such as flavonoids **53**,

54 [De La Torre *et al.,* 2004], and quercetin **55, 56** [De La Torre *et al.,* 2002]. In further advancement, Enes, R.F. *et al.* integrated 3, 5-di-tert-butyl-4- hydroxyphenyl groups (BHT) with C_{60}-flavonoid conjugate **57-59** [Enes *et al.,* 2009]. These hybrids **57-59** showed synergistic free radical scavenging ability.

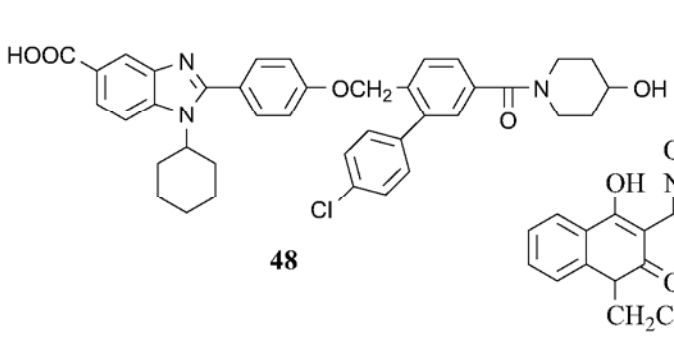

48

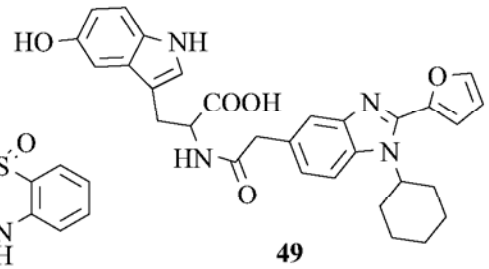

49

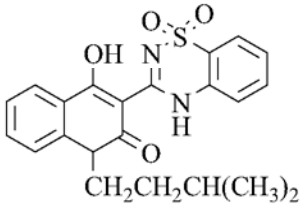

50

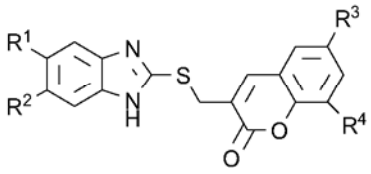

51a-d

	R^1	R^2	R^3	R^4
51a	H	H	H	H
52b	H	H	Br	H
53c	Cl	Cl	H	H
54d	Cl	Cl	H	OCH_3

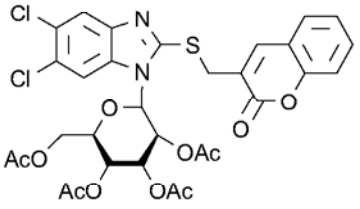

52

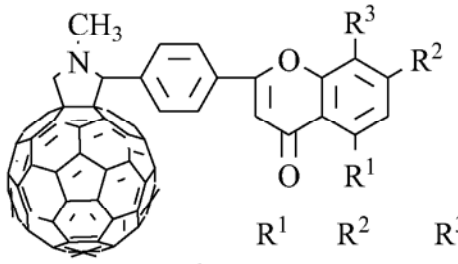

	R^1	R^2	R^3
53a	H	H	H
53b	Bn	H	H
53c	H	OBn	OBn

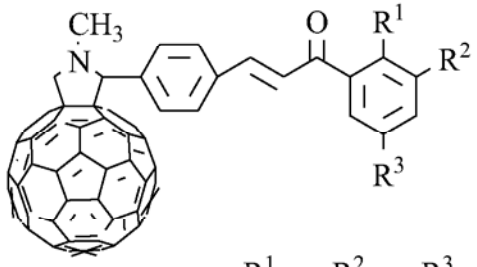

	R^1	R^2	R^3
54a	OH	H	H
54b	OBn	OBn	OBn

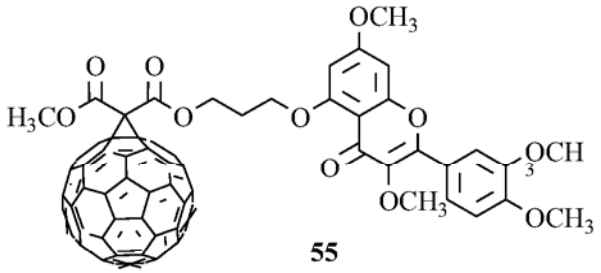

55

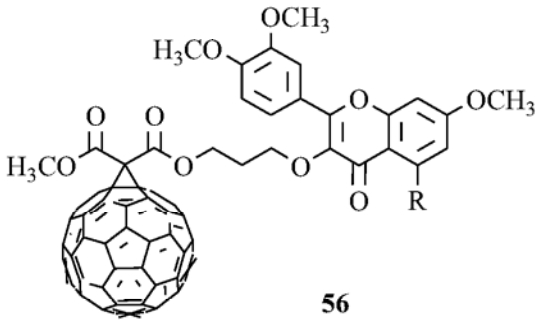

56

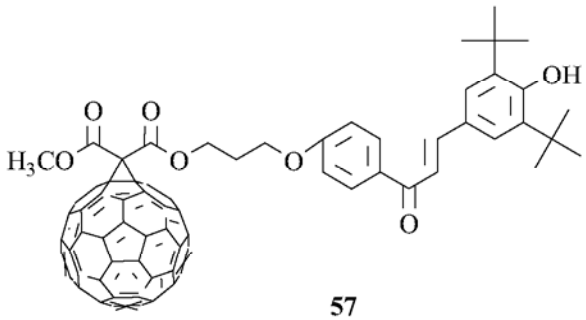

57

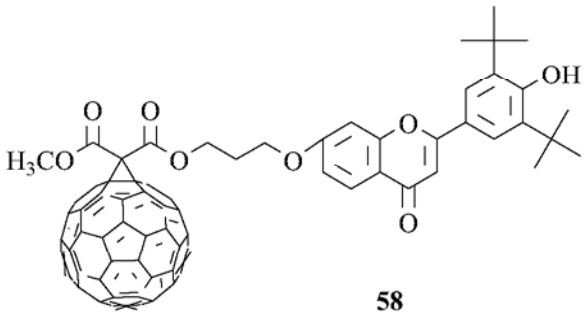

58

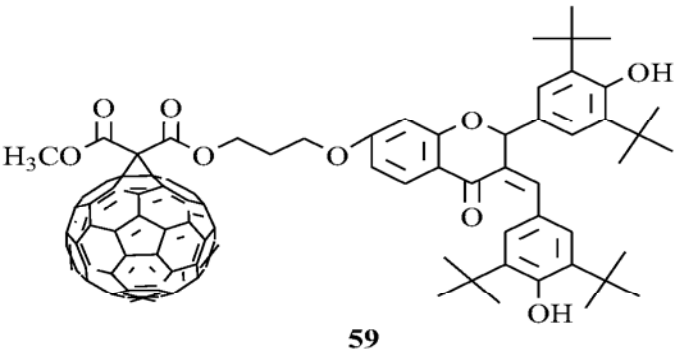

59

2.2.3. Hybrids based on cinnamate moiety

2.2.3.1. Hybrids with cinnamate moiety as neuroprotective agent

Presence of olefinic bond with carbonyl functionality in cinnamate based compounds such as cinnamic acid, ferulic acid, and synapic acid, impart wide range of biological application. Tacrine is one of potential drug candidates used in neurodegenerative disorder like ADs. Further structural optimization of tacrine **60** was done by conjugating with ferulic acid **61** via varying length of methylene spacer [Fang *et al.,* 2008]. It was postulated that conjugation with octamethylene spacer **62** exhibited a reversible and non-competitive inhibition to acetylcholinesterase (AChE) whereas,

reversible and competitive inhibitory activity was observed to butyrylcholinesterase (BChE) with IC_{50} (nM) 9.6 ± 2.1 and 12.7 ± 2.6, respectively.

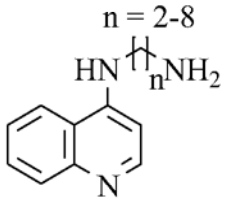

60

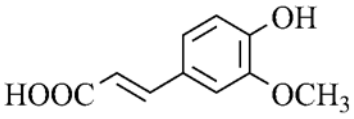

61

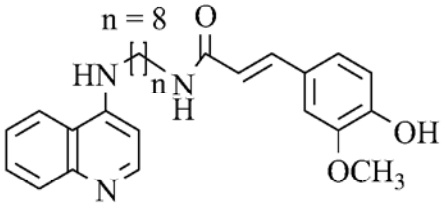

62

Calpain is Ca^{+2}-activated cystein protease typically associated with cellular necrosis. One of the major causes of neurodegenerative disorder is ROS mediated activation of calpain, which is involved in various neurological disorders such as stroke, Parkinson's disease and Alzheimer [Croall and DeMartino, 1991; Lipton, 1999; Goll *et al.,* 2003]. Lee, K.S. *et al.* has synthesized chromone carboxamide **63** and has shown potential calpain inhibitory activity [Lee, *et al.,* 2005]. To elucidate structural requirements for μ-calpain inhibition, Yoo, Y.J. *et al.* synthesized acyclic variants of chromone ring in **63** by conjugating cinnamoyl functionality on α-position [Yoo *et al.,* 2011]. Potential role of acyclic variants of chromone carboxamide **64** against neurodegeneration and increasing role of cinnamate based compounds as neuroprotective agents, a series of cinnamoyl ketoamides were synthesized with varying substitution at α-position of ketoamides group Calpain inhibitory activity was increased in order of propyl ≡ isopropyl > ethyl ≡ butyl as alkyl substituent at α-position of ketoamides group and hydroxyl group on aromatic ring system. Compound **65** showed most potent inhibitory activity (IC_{50} = 0.13 μM) against m-calpain and its potency was 4-fold higher than that of acyclic variant **64** (IC_{50} = 0.52 mM) and 2-fold lower than that of parent compound **63** (IC_{50} = 0.07 mM).

2.2.3.2. Hybrids with cinnamate moiety as cardioprotective agent

Angiotensin converting enzyme (ACE) inhibitors are mostly used antihypertensive agents. Selective inhibition of Angiotensin-II (AT-II) by Sartans with absence of side effects (coughing) makes it superior over other ACE inhibitor. Garcia, G. *et al.* have synthesized polyphenolic compounds conjugate with losartan **66** [Garcia *et al.,* 2009]. Integration of phenolics functionalities on losartan improves 4-8 fold antioxidant capacity than losartan. Hybrids were less efficient to oppose to bind radiolabelled AT-II to receptor than losartan except **67a** (41%) and **67b** (40%) which exhibit equivalent potential

as losartan (47%). 3-(3,4-Dihydroxyphenyl) propionic acid was potential candidate among all integrated polyphenolic compounds and its structural resemblance with cinnamate based compounds revealed out that structural optimization of losartan with cinnamate based compounds might improve *its* basic properties as an AT-II receptor blocker.

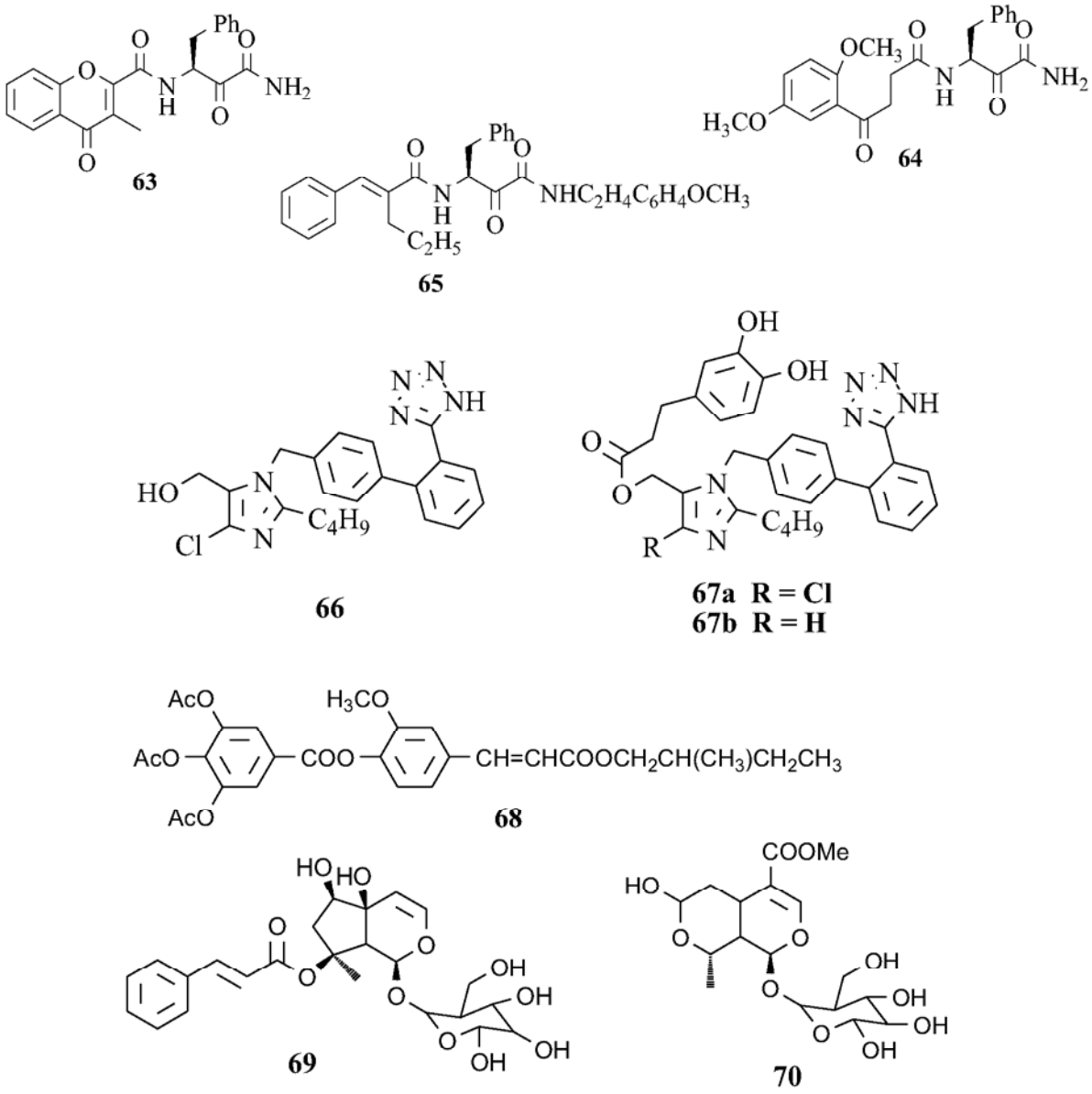

2.2.3.2. Hybrids with cinnamate moiety as anticancer/anti-inflammatory agent

Nomura, E. *et al.* have synthesized gallic acid-ferulic acid ester and investigated their inhibitory effects on 12-*O*-tetradecanoylphorbol-13-acetate (TPA)-induced Epstein-Barr virus (EBV) activation and superoxide (O_2^-) generation and **68** was observed

promising chemopreventive agent [Nomura *et al.,* 2002]. Harpagoside **69**, naturally occurring phenylpropanoids-conjugated iridoide glycoside have potential anti-inflammatory agent and structural characterization revealed that cinnamate moiety might be responsible for activity. Takeda, Y. *et al.* conjugated cinnamate moiety on morroniside **70** (iridoide glycoside) and showed potential TNF-α induced E-selectin expression inhibition (IC_{50} = 49.3μM) over harpagoside (IC_{50} = 88.2μM) [Takeda *et al.,* 2010].

2.2.4. Miscellaneous hybrids

Various natural and synthetic polymers such as gelatin, albumin, cellulose, poly (2-hydroxyethyl methacrylate), chitosan, and polyethylene glycol (PEG) have wide range of pharmaceutical and biomedical applications, due to their biocompatibility, biodegradation, non toxicity, and non immunogenicity. Some of polymeric products, especially medical equipment and food packaging, sterilization by radiation results in potential risk of degradation, i.e., chain scission and/or cross linking, resulting in discoloration, cracking of the surface, stiffening, and loss of mechanical properties [Jahan and McKinny, 1999]. Furthermore, protein composite polymers (i.e. gelatin, pectin) and poly (2-hydroxyethyl methacrylate (important constituents of contact lens) are liable to oxidative damage.

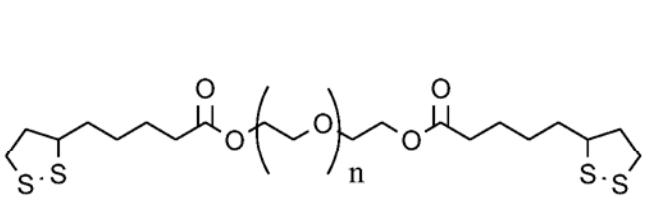

71

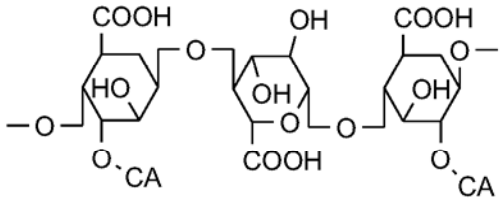

72

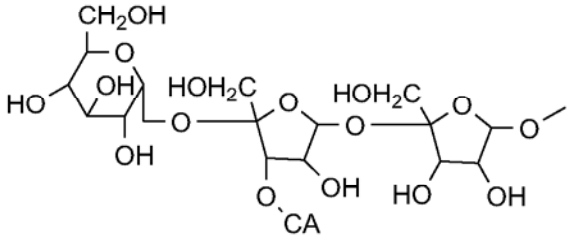

73

CA = Catechin

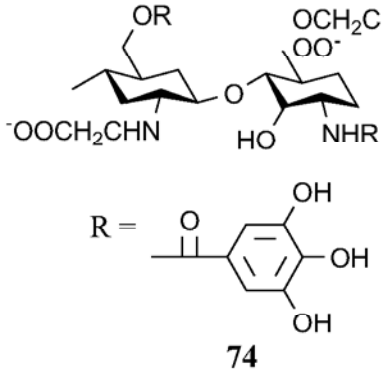

74

Various strategies had been employed to protect these biomolecules from oxidative damage [Atkinson and Lehrle, 1992; Al-Malaika and Suharty, 1995; Ortiz *et al.,* 1999].

Currently, grafting of antioxidant moiety on polymeric side chain has been used to overcome oxidative damage. Researcher have been tried various polymeric-antioxidant combination to improved physical, chemical and biological properties such as PEG-lipoic acid conjugates **71** [Youk *et al.,* 2005], gallic acid-gelatin and catechin-gelatin [Spizzirri *et al.,* 2009], poly (2-hydroxyethyl methacrylate)-quercetin [Curcio *et al.,* 2011], catechin-alginate **72** and catechin-inulin **73** [Spizzirri *et al.,* 2010], chitosan-gallic acid **74** [Yu *et al.,* 2011] via grafting and other technique. Improvement in radical scavenging capacity of antioxidant polymer in comparison to parent polymer indicated that covalent attachment of antioxidant moieties on polymer might improve their oxidative resistance and introduce new features for specific applications in pharmaceutical, cosmetic and food industry.

2.2.5. Structure-activity relationship (SAR) analysis of antioxidant hybrid compounds

From above mentioned detailed investigation, it was concluded that many antioxidant hybrid compounds have been synthesized and observed significant and to moderate range of biological action in comparisons to parent one. Some key structure activity relationship features are as under:-

1. The presence of 1,2-dithiolone functionality is important for neuroprotective action.
2. Numbers of free phenolics functionality are proportional to their radical quenching capacity.
3. Insertion of α,β-unsaturated carbonyl moiety in compounds impart wide range of biological application, along with this presence of electron withdrawing groups potential electrophilicity of Cβ-carbon which results in enhance Michel interaction with cellular/enzymatic thiol groups.
4. Potential role of cinnamate based compounds in neuroprotection, antimicrobial and inflammation again giving witness of double bonds and carbonyl functionality.

CHAPTER 2

RESEARCH ENVISAGED AND PRESENT WORK

Review of literature in the preceding section reveals the contribution of antioxidative and signalling modulatory functionalities in discovery and development of drug candidates as promising therapeutic intervention in oxidative stress induced diseases. Structural description of anticancer agents and their SAR study indicates that certain functionalities including cinnamoyl (**75**), vanillyl (**76**), caffeoyl (**77**), syringyl (**78**), ferulyl (**79**) and many more can play a promising role in the drug development against cancer and other diseases.

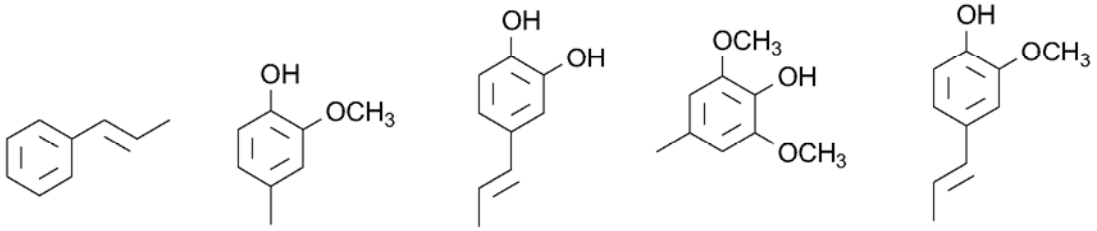

75 **76** **77** **78** **79**

Nature is known as rich sources of compounds with unique chemical features and pronounced biological activities, found in millions of species of plants, animals, marine, micro organisms. The natural products have played, and continue to play, a dominant role in the discovery of lead for the development of conventional drugs for the treatment of the human diseases. In addition to medicinally important plants, various weeds have also attracted the attention of many medicinal chemists for discovery and development of new drug candidates. One of such weed, which has attracted lot of interest of scientists in last three decade, is *Lantana camara* L. (Verbenaceae). It has encroached upon vast expanse of land area including pastures, orchards, tea gardens forests and agricultural lands in tropical and subtropical parts of the world and has imposed a great threat to grazing livestock and overall ecological balance. It is a rich source of a number of biologically active triterpenoids. Lantadene A **80** and lantadene B **81** are the major triterpenoids of the leaves of common pink-edged red flowering variety of weed *Lantana camara* L. (Verbenaceae). These compounds inhibited Epstein-Barr virus action in Raji cells induced by 12-*O*-tetradecanoylphorbcol-13-acetate (TPA). LA **80** and LB **81** have also been reported to exhibit inhibitory effects on the two stage carcinogenesis of the mouse skin papiloma using 7,12-dimethylbenz[a]anthracene (DMBA) as inducer and TPA as promoter. These observations indicated that lantadenes have the potential to develop antitumor agents.

These compounds have structural difference in the side chain attached to C-22 position through ester linkage and this structural variation plays an important role in the activity.

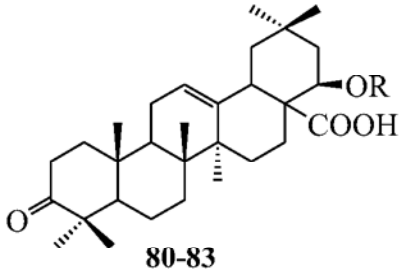

80-83

(**80**) R = $COC(CH_3)=CHCH_3$
Lantadene A
(**81**) R = $COCH=C(CH_3)_2$
Lantadene B
(**82**) R = $COCH(CH_3)CH_2CH_3$
Lantadene C
(**83**) R = $COCH(CH_3)_2$
Lantadene D

Based on these observations, some of important functionalities were selected and proposed structure of lantadenes and hybrid compounds were submitted to DTP National Cancer Institute (NCI, Bethesda, USA). Selected lantadenes and hybrid compounds were synthesized and screened for *in-vitro* cytotoxic evaluation over a panel of 60 cell lines composite of nine different type of cancers including leukemia, non-small cell lung cancer, colon cancer, CNS cancer, melanoma, ovarian cancer, renal cancer, prostate cancer and breast cancer. NCI's COMPARE analysis was performed to find out probable anticancer molecular mechanism. As no molecular targets have been reported for these target vectors, which suggested that anticancer activity of test compounds were might be due to new molecular mechanistic targets. Furthermore, significance of lantadenes and integrated vanillyl and cinnamoyl functionalities was explored by selective cancer cytotoxicity and molecular mechanistic inhibitory potential on NF-κB and Akt. Probable molecular interaction with protein was determined by using automated molecular docking software Auto Dock 4.2. The compound **93** was evaluated for *in-vitro* cytotoxicity and apoptotic study including DNA fragmentation, Caspase-3 dependent induction of apoptosis and modulation of NF-κB, c-jun, Bax, Bcl-2 and caspase-3 protein expression in B16F10 cells. The compound **93** was further evaluated for its *in-vivo* antitumor activity in B16F10 induced melanoma in C57BL/6 mice along with effects on liver enzyme and blood cells were also observed.

CHAPTER 3

EXPERIMENTALS

3.1. General

Melting points were determined on a Buchi melting point apparatus and are uncorrected. Reactions were monitored on Merck aluminium thin layer chromatography plates and visualized by exposure to iodine vapors. Column chromatography was carried on silica gel (100-200 mesh, MERCK chemicals). IR spectra were recorded on a Perkin-Elmer 882 spectrometer using potassium bromide pellets. ^{1}H NMR and ^{13}C NMR spectra were recorded with a Bruker Avance II 400 MHz spectrometers using $CDCl_3$/DMSO-*d6* as solvent, and tetramethylsilane was used as internal standard. Mass spectra were obtained with Micromass 70-VSE mass spectrometer at 70 eV using electron ionization (EI). Elemental analysis of compound was within 0.04% of the theoretical values. All solvents were freshly distilled and dried prior to use according to standard procedures.

3.2. Extraction and isolation of lantadene A & B

The leaves of *Lantana camara* were collected in September 2010 from Palampur (HP), India. The leaves were dried in the shade and powdered. Lantana leaf powder was extracted with methanol and the extract obtained was treated with charcoal to remove the green pigments which gave golden yellow colored extract. The solvent was removed under reduced pressure and the residue was suspended in methanol-water (1:7) mixture and extracted with chloroform. The organic layer was dried over anhydrous sodium sulphate and the solvent was removed under reduced pressure. The solid residue obtained was crystallized from methanol to obtain partially purified lantadenes as a white crystalline product [Sharma *et al.*,1987].

Isolation of Lantadene A (22*β*-[(2-methyl-1-oxo-2-butenyl)oxy]-3-oxoolean-12-en-28-oic acid 80)

1g of partially purified lantadenes were chromatographed over silica gel (100-200 mesh) and eluted with hexane: ethyl acetate (4:1) to obtain **22*β*-[(2-methyl-1-oxo-2-butenyl)oxy]-3-oxoolean-12-en-28-oic acid 80** as white solid (520 mg, 52%), R_f 0.63 (hexane: ethyl acetate :: 4:1), mp. 283-285 ^{0}C.

Analysis

IR (KBr) *ν* max: 2952.45 (C-H aliphatic), 1715.85 (C=O, ester), 1702.14 (C=O, 3-keto) cm^{-1}.

^{1}H NMR ($CDCl_3$: 400 MHz): δ 0.82 (s, 3H, CH_3), 0.85 (s, 3H, CH_3), 1.00 (s, 3H, CH_3), 1.05 (s, 6H, 2 x CH_3), 1.09 (s, 3H, CH_3), 1.17 (s, 3H, CH_3), 3.05 (d, *J* = 10.40 Hz, 1H, C-18-H), 5.09 (s, 1H, C-22α-H), 5.38 (s, 1H, C-12-H), 6.00 (q, 1H, *J* = 7.28 Hz, C-3′-H).

^{13}C NMR ($CDCl_3$, 100 MHz): δ 37.72 (C-1), 34.14 (C-2), 217.72 (C-3), 38.45 (C-4), 55.29 (C-5), 21.48 (C-6), 30.19 (C-7), 39.21 (C-8), 50.59 (C-9), 36.78 (C-10), 24.19 (C-11), 122.49 (C-12), 143.10 (C-13), 45.94 (C-14), 26.44 (C-15), 23.51 (C-16), 46.88 (C-17), 41.99 (C-18), 47.45 (C-19), 30.05 (C-20), 33.69 (C-21), 75.84 (C-22), 27.56 (C-23), 16.84 (C-24), 15.67 (C-25), 19.48 (C-26), 26.14 (C-27), 179.28 (C-28), 32.19 (C-29), 25.79 (C-30), 166.26 (C-1'), 127.58 (C-2'), 139.06 (C-3'), 15.10 (C-4'), 20.58 (C-5').

ESI-MS (*m/z*): 551.4 (M-1).

Elemental anal.: $C_{35}H_{52}O_5$ (552.5): C 76.05%; H 9.48%; found: C 76.03%; H 9.50%.

Isolation of Lantadene B (22*β*-[(3-methyl-1-oxo-2-butenyl)oxy]-3-oxoolean-12-en-28-oic acid 81)

1g of partially purified lantadenes were chromatographed over silica gel (100-200 mesh) and eluted with hexane: ethyl acetate (4:1) to obtain **22*β*-[(3-methyl-1-oxo-2-butenyl)oxy]-3-oxoolean-12-en-28-oic acid 81** as white solid (390 mg, 39%), R_f 0.61 (hexane: ethyl acetate :: 4:1), mp. 293-295 ^{0}C.

Analysis

IR (KBr) *v* max: 2950.12 (C-H aliphatic), 1713.45 (C=O, ester), 1703.09 (C=O, 3-keto) cm^{-1}.

^{1}H NMR ($CDCl_3$, 400 MHz): δ 0.83(s, 3H, CH_3), 0.88 (s, 3H, CH_3), 1.00 (s, 3H, CH_3), 1.05 (s, 6H, 2 x CH_3), 1.09 (s, 3H, CH_3), 1.17 (s, 3H, CH_3), 3.02 (d, *J* = 9.96 Hz, 1H, C-18-H), 5.04 (s, 1H, C-22α-H), 5.37 (s, 1H, C-12-H), 5.55 (s, 1H, C-2′-H).

^{13}C NMR ($CDCl_3$, 100 MHz): δ 38.54 (C-1), 33.75 (C-2), 217.81 (C-3), 39.16 (C-4), 55.30 (C-5), 21.50 (C-6), 32.26 (C-7), 39.24 (C-8), 50.57 (C-9), 37.63 (C-10), 25.77 (C-11), 122.37 (C-12), 143.09 (C-13), 45.97 (C-14), 27.46 (C-15), 24.13 (C-16), 46.87 (C-17), 42.07 (C-18), 47.45 (C-19), 30.07 (C-20), 36.77 (C-21), 75.20 (C-22), 27.59 (C-23), 16.85 (C-24), 15.16 (C-25), 19.52 (C-26), 26.44 (C-27), 178.84 (C-28), 34.16 (C-29), 26.28 (C-30), 165.32 (C-1'), 115.96 (C-2'), 157.15 (C-3'), 20.25 (C-4'), 23.56 (C-5').

ESI-MS (*m/z*): 551.5 (M-1).

Elemental anal.: $C_{35}H_{52}O_5$ (552.5): C 76.05%; H 9.48%; found: C 76.07%; H 9.49%.

3.3. Synthesis of bioactive intermediates and C-2 arylidene/aryl congeners of lantadenes

Synthesis of 22*β*-[(2-methyl-1-oxo-2-butenyl)oxy]-3*β*-hydroxyolean-12-en-28-oic acid (84)

To a solution of LA **80** (100 mg, 0.18 mM) in methanol and tetrahydrofuran mixture (20 ml, 1:1), 6.80 mg (0.18 mM) sodium borohydride was added and stirred at room temperature. After reaction completion, the solvent was removed *in vacuo* and the residue was diluted with water (15ml). The mixture was acidified with dilute HCl and extracted with ethyl acetate (3 x 15ml). The combined organic layer was dried over anhydrous sodium sulfate and evaporated to dryness. The residue was chromatographed over silica gel (100-200 mesh) and eluted with hexane : ethyl acetate (4:1) to obtain **22*β*-[(2-methyl-1-oxo-2-butenyl)oxy]-3*β*-hydroxyolean-12-en-28-oic acid 84** as white solid (84 mg, 83.7%), R_f 0.58 (hexane : ethyl acetate :: 4:1), mp. 278-279 ^{0}C.

Analysis

IR (KBr) *ν* max: 3482.87 (O-H), 2948.99, 2827.53 (C-H aliphatic), 1717.87 (C=O, ester) cm^{-1}.

^{1}H NMR (DMSO-*d6*, 400 MHz): δ 0.73 (s, 3H, CH_3), 0.80 (s, 3H, CH_3), 0.89 (s, 6H, 2 x CH_3), 0.94 (s, 3H, CH_3), 0.99 (s, 3H, CH_3), 1.16 (s, 3H, CH_3), 3.00 (dd, *J* = 11.32, 8.04 Hz, 1H, C-18-H), 3.09 (t, *J* = 7.24 Hz, 1H, C-3α-H), 4.99 (s, 1H, C-22α-H), 5.31 (s, 1H, C-12-H), 6.00 (q, *J* = 6.08 Hz, 1H, C-3′-H).

^{13}C NMR ($CDCl_3$, 100 MHz): δ 38.77 (C-1), 36.51 (C-2), 79.28 (C-3), 45.71 (C-4), 54.77 (C-5), 20.11 (C-6), 32.30 (C-7), 40.25 (C-8), 47.06 (C-9), 38.09 (C-10), 23.74 (C-11), 121.53 (C-12), 158.43 (C-13), 41.46 (C-14), 27.90 (C-15), 25.40 (C-16), 49.59 (C-17), 38.99 (C-18), 43.96 (C-19), 29.59 (C-20), 38.29 (C-21), 75.60 (C-22), 26.96 (C-23), 15.57 (C-24), 15.18 (C-25), 16.49 (C-26), 26.68 (C-27), 177.14 (C-28), 33.43 (C-29), 25.77 (C-30), 165.70 (C-1′), 127.50 (C-2′), 137.42 (C-3′), 15.00 (C-4′), 22.89 (C-5′).

ESI-MS (*m/z*): 553.4 (M-1).

Elemental anal.: $C_{35}H_{54}O_5$ (554.4): cal. C 75.77%; H 9.81%; found C 75.75%; H 9.80%.

Synthesis of 22*β*-[(3-methyl-1-oxo-2-butenyl)oxy]-3*β*-hydroxyolean-12-en-28-oic acid (85)

To a solution of LB **81** (100 mg, 0.18 mM) in methanol and tetrahydrofuran mixture (20 ml, 1:1), 6.80 mg (0.18 mM) sodium borohydride was added and stirred at room temperature. After reaction completion, the solvent was removed *in vacuo* and the residue was diluted with water (15ml). The mixture was acidified with dilute HCl and extracted with ethyl acetate (3 x 15ml). The combined organic layer was dried over anhydrous sodium sulfate and evaporated to dryness. The residue was chromatographed over silica gel (100-200 mesh) and eluted with hexane : ethyl acetate (4:1) to obtain **22*β*-[(3-methyl-1-oxo-2-butenyl)oxy]-3*β*-hydroxyolean-12-en-28-oic acid 85** as white solid (80 mg, 79.8%), R_f 0.56 (hexane : ethyl acetate :: 4:1), mp. 276-278 ^{0}C.

Analysis

IR (KBr) *v* max: 3480.79 (O-H), 2949.59, 2875.08 (C-H aliphatic), 1717.98 (C=O, ester) cm^{-1}.

^{1}H NMR ($CDCl_3$, 400 MHz): δ 0.71 (s, 6H, 2 x CH_3), 0.81 (s, 3H, CH_3), 0.85 (s, 3H, CH_3), 0.93 (s, 6H, 2 x CH_3), 1.09 (s, 3H, CH_3), 2.94 (dd, *J* = 6.32, 1.60 Hz, 1H, C-18-H), 3.15 (dd, *J* = 4.92, 2.96 Hz, 1H, C-3α-H), 4.96 (s, 1H, C-22α-H), 5.29 (s, 1H, C-12-H), 5.48 (s, 1H, C-2′-H).

^{13}C NMR ($CDCl_3$, 100 MHz): δ 38.75 (C-1), 33.77 (C-2), 79.05(C-3), 38.75 (C-4), 55.18 (C-5), 19.20 (C-6), 30.57 (C-7), 39.24 (C-8), 50.52 (C-9), 38.44 (C-10), 25.89 (C-11), 122.85 (C-12), 143.05 (C-13), 46.03 (C-14), 27.47 (C-15), 25.89 (C-16), 47.63 (C-17), 41.92 (C-18), 50.52 (C-19), 30.07 (C-20), 37.04 (C-21), 75.00 (C-22), 28.10 (C-23), 16.97 (C-24), 15.59 (C-25), 18.26 (C-26), 27.16 (C-27), 177.10 (C-28), 31.01 (C-29), 26.30 (C-30), 165.17 (C-1'), 115.99 (C-2'), 152.24 (C-3'), 20.24 (C-4'), 24.12 (C-5').

ESI-MS (*m/z*): 553.3 (M-1).

Elemental anal.: $C_{30}H_{48}O_4$ (554.3): cal. C 75.77%; H 9.81%; found C 75.72%; H 9.82%.

Synthesis of 22*β*-hydroxy-3-oxoolean-12-en-28-oic acid (86)

A solution of LA **80** or LB **81** (100 mg, 0.18 mM) in ethanolic potassium hydroxide (10% w/v, 25 ml) was refluxed. After reaction completion, the solvent was removed *in vacuo* and the residue was diluted with water (15ml). The mixture was acidified with dilute HCl and extracted with ethyl acetate (3 x 15 ml). The combined

organic layer was dried over anhydrous sodium sulfate and evaporated to dryness. The residue was chromatographed over silica gel (100-200 mesh) and eluted with hexane : ethyl acetate (2:1) to obtain **22*β*-hydroxy-3-oxoolean-12-en-28-oic acid 86** as white solid (54.2 mg, 63.9%); R_f 0.35 (hexane : ethyl acetate :: 1:1), mp. 234-236 ^{0}C.

Analysis

IR (KBr) ν max: 3434 (O-H), 2946 (C-H aliphatic), 1703 (C=O, keto) cm^{-1}.

^{1}H NMR ($CDCl_3$, 400 MHz): δ 0.78 (s, 3H, CH_3), 0.83 (s, 3H, CH_3), 0.97 (s, 3H, CH_3), 0.99 (s, 3H, CH_3), 1.02 (s, 3H, CH_3), 1.05 (s, 3H, CH_3), 1.09 (s, 3H, CH_3), 2.28-2.33 (m, 1H, C-2a-H), 2.44-2.51 (m, 1H, C-2b-H), 2.94 (dd, *J* = 13.80, 4.08 Hz, 1H, C-18-H), 3.85 (t, *J* = 3.24 Hz, 1H, C-22α-H), 5.29 (t, *J* = 3.44 Hz, 1H, C-12-H).

^{13}C NMR ($CDCl_3$, 100 MHz): δ 39.28 (C-1), 34.16 (C-2), 217.84 (C-3), 47.44 (C-4), 55.30 (C-5), 19.54 (C-6), 32.22 (C-7), 39.15 (C-8), 46.90 (C-9), 36.79 (C-10), 24.32 (C-11), 122.41 (C-12), 143.28 (C-13), 42.13 (C-14), 27.80 (C-15), 23.56 (C-16), 52.32 (C-17), 41.23 (C-18), 46.02 (C-19), 30.15 (C-20), 38.00 (C-21), 74.34 (C-22), 26.48 (C-23), 21.48 (C-24), 15.13 (C-25), 16.93 (C-26), 25.75 (C-27), 180.70 (C-28), 33.88 (C-29), 27.16 (C-30).

ESI-MS (*m/z*): 469.3 (M-1).

Elemental anal.: $C_{30}H_{46}O_4$ (470.68): cal. C 76.55%; H 9.85%; found: C 76.55%; H 9.84%.

Synthesis of 3*β*,22*β*-dihydroxy-3-oxoolean-12-en-28-oic acid (87)

To a solution of compound **86** (100 mg, 0.21 mM) in methanol and tetrahydrofuran mixture (20 ml, 1:1), ~7.00 mg (0.21 mM) sodium borohydride was added and stirred at room temperature. After reaction completion, the solvent was removed *in vacuo* and the residue was diluted with water (15ml). The mixture was acidified with dilute HCl and extracted with ethyl acetate (3 x 15ml). The combined organic layer was dried over anhydrous sodium sulfate and evaporated to dryness. The residue was chromatographed over silica gel (100-200 mesh) and eluted with hexane : ethyl acetate (2:1) to obtain **3*β*,22*β*-dihydroxy-3-oxoolean-12-en-28-oic acid 87** as white solid (71.2 mg, 70.7%), R_f 0.32 (hexane : ethyl acetate :: 1:1), mp. 210-212 ^{0}C.

Analysis

IR (KBr) *ν* max: 3446 (O-H), 2948 (C-H aliphatic), 1707 (C=O, acid) cm^{-1}.

^{1}H NMR (DMSO-*d6*, 400 MHz): δ 0.73 (s, 3H, CH_3), 0.85 (s, 3H, CH_3), 0.89 (s, 3H, CH_3), 0.93 (s, 3H, CH_3), 1.07 (s, 3H, CH_3), 1.10 (s, 3H, CH_3), 1.24 (s, 3H, CH_3), 2.94 (d, *J* = 11.76 Hz, 1H, C-18-H), 3.07 (t, *J* = 6.48 Hz, 1H, C-3α-H), 3.58 (s, 2H, C-3β-OH and C-22α-H), 4.00 (s, 1H, C-22β-OH), 5.23 (s, 1H, C-12-H).

^{13}C NMR (DMSO-*d6*, 100 MHz): δ 38.09 (C-1), 27.04 (C-2), 77.20 (C-3), 38.29 (C-4), 54.79 (C-5), 17.89 (C-6), 32.41 (C-7), 40.23 (C-8), 51.02 (C-9), 37.91 (C-10), 23.89 (C-11), 120.99 (C-12), 143.78 (C-13), 41.62 (C-14), 27.31 (C-15), 22.89 (C-16), 46.03 (C-17), 41.09 (C-18), 47.09 (C-19), 29.78 (C-20), 36.52 (C-21), 72.72 (C-22), 27.93 (C-23), 15.60 (C-24), 15.01 (C-25), 16.67 (C-26), 26.79 (C-27), 176.30 (C-28), 33.70 (C-29), 25.37 (C-30).

ESI-MS (*m/z*): 471.3 (M-1).

Elemental anal.: $C_{30}H_{48}O_4$ (472.40): cal. C 76.23%; H 10.24%; found: C 76.21%; H 10.25%.

Synthesis of 2-benzylidene-22*β*-hydroxy-3-oxoolean-12-en-28-oic acid (88)

To a solution of compound **86** (100 mg, 0.21 mM) in ethanolic potassium hydroxide solution (5% w/v, 25 ml), benzaldehyde (1.1 eq.) was added and stirred at room temperature. After reaction completion solvent was removed *in vacuo* and the residue was diluted with water (15 ml). The mixture was acidified with dilute HCl and extracted with ethyl acetate (3 x 15 ml). The combined organic layer was dried over anhydrous sodium sulfate and evaporated to dryness. The residue was chromatographed over silica gel (100-200 mesh) and eluted with hexane : ethyl acetate (2:1) to obtain the **2-benzylidene-22*β*-hydroxy-3-oxoolean-12-en-28-oic acid 88** as white solid (83.4 mg, 71.2%), R_f 0.39 (hexane : ethyl acetate :: 1:1), mp.152-154 ^{0}C.

Analysis

IR (KBr) *v* max: 3525 (O-H), 2952 (C-H aliphatic), 1671 (C=O, arylidene) cm^{-1}.

^{1}H NMR ($CDCl_3$, 400 MHz): δ 0.85 (s, 3H, CH_3), 0.87 (s, 3H, CH_3), 0.90 (s, 3H, CH_3), 1.12 (s, 3H, CH_3), 1.14 (s, 3H, CH_3), 1.18 (s, 3H, CH_3), 1.21 (s, 3H, CH_3), 3.02 (t, *J* = 7.66 Hz, 1H, C-18-H), 3.92 (s, 1H, C-22α-H), 5.39 (s, 1H, C-12-H), 7.31-7.44 (m, 5H, Ar-H), 7.53 (s, 1H, vinylic H).

^{13}C NMR ($CDCl_3$, 100 MHz): δ 39.23 (C-1), 137.59 (C-2), 207.92 (C-3), 41.29 (C-4), 53.00 (C-5), 22.70 (C-6), 31.90 (C-7), 42.35 (C-8), 52.42 (C-9), 38.18 (C-10), 24.38 (C-

11), 122.44 (C-12), 143.44 (C-13), 45.20 (C-14), 27.82 (C-15), 23.78 (C-16), 45.44 (C-17), 44.21 (C-18), 46.14 (C-19), 30.22 (C-20), 36.32 (C-21), 74.36 (C-22), 29.83 (C-23), 16.59 (C-24), 15.40 (C-25), 20.36 (C-26), 27.20 (C-27), 180.74 (C-28), 33.93 (C-29), 25.71 (C-30), 135.95 (ArCH), 133.67 (C-1''), 128.49 (C-2''), 130.47 (C-3''), 128.59 (C-4''), 130.47 (C-5''), 128.49 (C-6'').

ESI-MS (m/z): 557.3 (M-1).

Elemental anal.: $C_{37}H_{50}O_4$ (558.2): cal. C 79.53%; H 9.02%; found: C 79.51%; H 9.04%.

Synthesis of 2-(4-methoxybenzylidene)-22*β*-hydroxy-3-oxoolean-12-en-28-oic acid (89)

To a solution of compound **86** (100 mg, 0.21 mM) in ethanolic potassium hydroxide solution (5% w/v, 25 ml), 4-methoxybenzaldehyde (1.1 eq.) was added and stirred at room temperature. After reaction completion solvent was removed *in vacuo* and the residue was diluted with water (15 ml). The mixture was acidified with dilute HCl and extracted with ethyl acetate (3 x 15 ml). The combined organic layer was dried over anhydrous sodium sulfate and evaporated to dryness. The residue was chromatographed over silica gel (100-200 mesh) and eluted with hexane : ethyl acetate (2:1) to obtain the **2-(4-methoxybenzylidene)-22*β*-hydroxy-3-oxoolean-12-en-28-oic acid 89** as yellow solid (81.12 mg, 65.7%), R_f 0.38 (hexane : ethyl acetate :: 1:1), mp. 188-191 ^{0}C.

Analysis

IR (KBr) *v* max: 3501 (O-H), 2951 (C-H aliphatic), 1675 (C=O, arylidene) cm^{-1}.

^{1}H NMR ($CDCl_3$, 400 MHz): δ 0.78 (s, 6H, 2 x CH_3), 0.83 (s, 3H, CH_3), 1.05 (s, 6H, 2 x CH_3), 1.10 (s, 3H, CH_3), 1.14 (s, 3H, CH_3), 2.93 (d, *J* = 15.24 Hz, 1H, C-18-H), 3.76 (s, 3H, OCH_3), 3.85 (s, 1H, C-22α-H), 5.33 (s, 1H, C-12-H), 6.85 (d, *J* = 7.72 Hz, 2H, Ar-H), 7.34 (d, *J* = 7.72 Hz, 2H, Ar-H), 7.44 (s, 1H, vinylic H).

^{13}C NMR ($CDCl_3$, 100 MHz): δ 39.20 (C-1), 137.48 (C-2), 207.83 (C-3), 41.20 (C-4), 52.82 (C-5), 22.63 (C-6), 31.87 (C-7), 42.32 (C-8), 52.40 (C-9), 38.18 (C-10), 24.34 (C-11), 122.36 (C-12), 143.48 (C-13), 45.01 (C-14), 27.80 (C-15), 23.79 (C-16), 45.47 (C-17), 44.39 (C-18), 46.14 (C-19), 30.19 (C-20), 36.20 (C-21), 74.31 (C-22), 29.93 (C-23), 16.56 (C-24), 15.41 (C-25), 20.35 (C-26), 27.19 (C-27), 180.85 (C-28), 33.91 (C-29), 25.68 (C-30), 55.35 (OCH_3), 132.33 (ArCH), 128.61 (C-1''), 132.33 (C-2''), 113.96 (C-3''), 159.88 (C-4''), 113.96 (C-5''), 131.44 (C-6'').

ESI-MS (m/z): 587.3 (M-1).

Elemental anal.: $C_{37}H_{50}O_5$ (588.7): cal. C 77.31%; H 8.77%; found: C 77.30%; H 8.79%.

Synthesis of 2-(4-methylbenzylidene)-22*β*-hydroxy-3-oxoolean-12-en-28-oic acid (90)

To a solution of compound **86** (100 mg, 0.21 mM) in ethanolic potassium hydroxide solution (5% w/v, 25 ml), 4-methylbenzaldehyde (1.1 eq.) was added and stirred at room temperature. After reaction completion solvent was removed *in vacuo* and the residue was diluted with water (15 ml). The mixture was acidified with dilute HCl and extracted with ethyl acetate (3 x 15 ml). The combined organic layer was dried over anhydrous sodium sulfate and evaporated to dryness. The residue was chromatographed over silica gel (100-200 mesh) and eluted with hexane : ethyl acetate (2:1) to obtain the **2-(4-methylbenzylidene)-22*β*-hydroxy-3-oxoolean-12-en-28-oic acid 90** as yellow solid (97.7 mg, 81.4%,), R_f 0.37 (hexane : ethyl acetate :: 1:1), mp. 165-167 ^{0}C.

Analysis

IR (KBr) *v* max: 3473 (O-H), 2949 (C-H aliphatic), 1675 (C=O, arylidene) cm^{-1}.

^{1}H NMR (DMSO-*d6*+$CDCl_3$, 400 MHz): δ 0.85 (s, 3H, CH_3), 0.88 (s, 6H, 2 x CH_3), 1.12 (s, 6H, 2 x CH_3), 1.14 (s, 3H, CH_3), 1.21 (s, 3H, CH_3), 2.99 (d, *J* = 16.04 Hz, 1H, C-18-H), 3.81 (s, 1H, C-22α-H), 4.06 (br s, 1H, C-22β-OH), 5.34 (s, 1H, C-12-H), 7.22 (d, *J* = 7.96 Hz, 2H, Ar-H), 7.33 (d, *J* = 7.96 Hz, 2H, Ar-H), 7.42 (s, 1H, vinylic H).

^{13}C NMR (DMSO-*d6*+$CDCl_3$, 100 MHz): δ 38.65 (C-1), 138.21 (C-2), 206.78 (C-3), 41.03 (C-4), 52.19 (C-5), 20.94 (C-6), 31.45 (C-7), 41.89 (C-8), 51.18 (C-9), 38.13 (C-10), 23.87 (C-11), 120.81 (C-12), 143.76 (C-13), 44.44 (C-14), 27.28 (C-15), 22.23 (C-16), 44.76 (C-17), 43.61 (C-18), 45.92 (C-19), 29.76 (C-20), 35.66 (C-21), 72.76 (C-22), 29.28 (C-23), 16.19 (C-24), 14.88 (C-25), 19.84 (C-26), 26.98 (C-27), 176.47 (C-28), 33.61 (C-29), 23.11 (C-30), 25.10 (Ar<u>C</u>H$_3$), 132.43 (Ar<u>C</u>H), 132.38 (C-1''), 128.80 (C-2''), 129.96 (C-3''), 136.68 (C-4''), 129.96 (C-5''), 128.80 (C-6'').

ESI-MS (m/z): 571.3 (M-1).

Elemental anal.: $C_{38}H_{52}O_4$ (572.3); cal. C 79.68%; H 9.15%; found: C 79.66%; H 9.17%.

Synthesis of 2-(4-chlorobenzylidene)-22*β*-hydroxy-3-oxoolean-12-en-28-oic acid (91)

To a solution of compound **86** (100 mg, 0.21 mM) in ethanolic potassium hydroxide solution (5% w/v, 25 ml), 4-chlorobenzaldehyde (1.1 eq.) was added and stirred at room temperature. After reaction completion solvent was removed *in vacuo* and the residue was diluted with water (15 ml). The mixture was acidified with dilute HCl and

extracted with ethyl acetate (3 x 15 ml). The combined organic layer was dried over anhydrous sodium sulfate and evaporated to dryness. The residue was chromatographed over silica gel (100-200 mesh) and eluted with hexane : ethyl acetate (2:1) to obtain the **2-(4-chlorobenzylidene)-22*β*-hydroxy-3-oxoolean-12-en-28-oic acid 91** as yellow solid (83.5 mg, 67.8%), R_f 0.37 (hexane : ethyl acetate :: 1:1), mp. 132-134 ^{0}C.

Analysis

IR (KBr) *v* max: 3224.81 (O-H), 1627.96 (C=O arylidene), 781.39 (C-Cl) cm^{-1}.

^{1}H NMR ($CDCl_3$, 400 MHz): δ 0.79 (s, 6H, 2 x CH_3), 0.84 (s, 3H, CH_3), 1.06 (s, 3H, CH_3), 1.10 (s, 3H, CH_3), 1.14 (s, 3H, CH_3), 1.18 (s, 3H, CH_3), 2.97 (dd, *J* = 13.88, 3.88 Hz, 1H, C-18-H), 3.87 (t, *J* = 3.44 Hz, 1H, C-22α-H), 5.34 (t, *J* = 3.18 Hz, 1H, C-12-H), 7.19 (s, 1H, vinylic H), 7.36 (dd, *J* = 6.84, 1.8 Hz, 2H, Ar-H), 7.94 (dd, *J*= 6.76, 1.76 Hz, 2H, Ar-H).

^{13}C NMR ($CDCl_3$, 100 MHz): δ 39.30 (C-1), 143.38 (C-2), 207.74 (C-3), 41.30 (C-4), 52.95 (C-5), 22.64 (C-6), 31.85 (C-7), 42.32 (C-8), 52.39 (C-9), 38.20 (C-10), 25.64 (C-11), 122.33 (C-12), 140.24 (C-13), 45.19 (C-14), 27.77 (C-15), 23.74 (C-16), 45.39 (C-17), 44.13 (C-18), 46.07 (C-19), 30.17 (C-20), 36.29 (C-21), 74.35 (C-22), 29.72 (C-23), 16.43 (C-24), 15.37 (C-25), 20.30 (C-26), 27.16 (C-27), 180.88 (C-28), 33.87 (C-29), 24.35 (C-30), 136.17 (Ar<u>C</u>H), 134.18 (C-1''), 128.70 (C-2''), 131.57 (C-3''), 134.32 (C-4''), 128.86 (C-5''), 127.84 (C-6'').

ESI-MS (m/z): 591.3 (M-2).

Elemental anal.: $C_{37}H_{49}ClO_4$ (593.3); cal. C 74.91%; H 8.33%; found: C 74.90%; H 8.31%.

Synthesis of 2-(4-hydroxy-3-methoxybenzylidene)-22*β*-hydroxy-3-oxoolean-12-en-28-oic acid (92)

To a solution of compound **86** (100 mg, 0.21 mM) in ethanolic potassium hydroxide solution (5% w/v, 25 ml), 4-hydroxy-3-methoxybenzaldehyde (1.1 eq.) was added and stirred at room temperature. After reaction completion solvent was removed *in vacuo* and the residue was diluted with water (15 ml). The mixture was acidified with dilute HCl and extracted with ethyl acetate (3 x 15 ml). The combined organic layer was dried over anhydrous sodium sulfate and evaporated to dryness. The residue was chromatographed over silica gel (100-200 mesh) and eluted with hexane : ethyl acetate

(2:1) to obtain the **2-(4-hydroxy-3-methoxybenzylidene)-22*β*-hydroxy-3-oxoolean-12-en-28-oic acid 92** as yellow solid (94.6 mg, 74.6%), R_f 0.24 (hexane : ethyl acetate :: 1:1), mp. 147-149 ^{0}C.

Analysis

IR (KBr) *v* max: 3437 (O-H), 2969 (C-H aliphatic), 1691 (C=O, arylidene), 1275 (C-O-C) cm^{-1}.

^{1}H NMR ($CDCl_3$, 400 MHz): δ 0.85 (s, 3H, CH_3), 0.89 (s, 3H, CH_3), 0.91 (s, 3H, CH_3), 1.08 (s, 3H, CH_3), 1.13 (s, 3H, CH_3), 1.17 (s, 3H, CH_3), 1.21 (s, 3H, CH_3), 3.02 (t, *J* = 8.88 Hz, 1H, C-18-H), 3.92 (s, 3H, OCH_3), 3.94 (s, 1H, C-22α-H), 5.39 (s, 1H, C-12-H), 6.94 (dd, *J* = 5.44, 4.08 Hz, 2H, Ar-H), 7.02 (d, *J* = 1.04 Hz, 1H, Ar-H), 7.48 (1H, s, vinylic H).

^{13}C NMR ($CDCl_3$, 100 MHz): δ 38.12 (C-1), 137.59 (C-2), 207.70 (C-3), 39.20 (C-4), 52.34 (C-5), 22.64 (C-6), 30.18 (C-7), 41.28 (C-8), 46.10 (C-9), 36.26 (C-10), 24.35 (C-11), 122.34 (C-12), 143.43 (C-13), 44.27 (C-14), 27.78 (C-15), 23.75 (C-16), 45.06 (C-17), 42.28 (C-18), 45.55 (C-19), 29.83 (C-20), 33.89 (C-21), 74.33 (C-22), 29.69 (C-23), 16.52 (C-24), 15.41 (C-25), 20.34 (C-26), 27.16 (C-27), 180.36 (C-28), 31.83 (C-29), 25.68 (C-30), 55.98 (OCH_3), 131.91 (Ar<u>C</u>H), 128.85 (C-1''), 110.86 (C-2''), 149.51 (C-3''), 148.64 (C-4''), 114.09 (C-5''), 123.47 (C-6'').

ESI-MS (m/z): 603.4 (M-1).

Elemental anal.: $C_{38}H_{52}O_6$ (604.5): cal. C 75.46%; H 8.67%; found: C 75.44%; H 8.69%.

Synthesis of 2-(3-phenylprop-2-en-1-ylidene)-22*β*-hydroxy-3-oxoolean-12-en-28-oic acid (93)

To a solution of compound **86** (100 mg, 0.21 mM) in ethanolic potassium hydroxide solution (5% w/v, 25 ml), cinnamaldehyde (1.1 eq.) was added and stirred at room temperature. After reaction completion solvent was removed *in vacuo* and the residue was diluted with water (15 ml). The mixture was acidified with dilute HCl and extracted with ethyl acetate (3 x 15 ml). The combined organic layer was dried over anhydrous sodium sulfate and evaporated to dryness. The residue was chromatographed over silica gel (100-200 mesh) and eluted with hexane : ethyl acetate (2:1) to obtain the **2-(3-phenylprop-2-en-1-ylidene)-22*β*-hydroxy-3-oxoolean-12-en-28-oic acid 93** as yellow solid (105.9 mg, 86.7%), R_f 0.39 (hexane : ethyl acetate :: 1:1), mp. 90-92 ^{0}C.

Analysis

IR (KBr) *v* max: 3662 (O-H), 2998 (C-H aliphatic), 1686 (C=O, arylidene), 1583 (C=C) cm^{-1}.

^{1}H NMR ($CDCl_3$, 400 MHz): δ 0.94 (s, 3H, CH_3), 0.97 (s, 3H, CH_3), 1.14 (s, 3H, CH_3), 1.15 (s, 6H, 2 x CH_3), 1.20 (s, 3H, CH_3), 1.25 (s, 3H, CH_3), 3.05 (dd, *J* = 13.72, 9.92 Hz, 1H, C-18-H), 3.93 (t, *J* = 2.96 Hz, 1H, C-22α-H), 5.44 (t, *J* = 3.16 Hz, 1H, C-12-H), 6.93 (q, *J* = 8.72 Hz, 2H, ArC<u>H</u>CH, ArCHC<u>H</u>), 7.25 (d, *J* = 11.20 Hz, 1H, ArCHCHC<u>H</u>), 7.26 (dd, *J* = 9.24, 4.84 Hz, 1H, Ar-H), 7.36 (dd, *J* = 8.00, 1.00 Hz, 2H, Ar-H), 7.48 (d, *J* = 7.16 Hz, 2H, Ar-H).

^{13}C NMR ($CDCl_3$, 100 MHz): δ 39.19 (C-1), 136.68 (C-2), 207.33 (C-3), 41.22 (C-4), 53.06 (C-5), 22.63 (C-6), 31.94 (C-7), 42.33 (C-8), 52.42 (C-9), 38.24 (C-10), 24.36 (C-11), 122.38 (C-12), 143.42 (C-13), 45.08 (C-14), 27.79 (C-15), 23.76 (C-16), 45.35 (C-17), 42.42 (C-18), 46.11 (C-19), 30.19 (C-20), 36.07 (C-21), 74.33 (C-22), 29.64 (C-23), 16.61 (C-24), 15.50 (C-25), 20.29 (C-26), 27.20 (C-27), 180.74 (C-28), 33.90 (C-29), 25.64 (C-30), 140.66 (ArCHCH<u>C</u>H), 132.76 (Ar<u>C</u>H), 123.37 (ArCH<u>C</u>H), 137.25 (C-1''), 127.15 (C-2''), 128.84 (C-3''), 128.79 (C-4''), 128.82 (C-5''), 127.13 (C-6'').

ESI-MS (*m/z*): 583.3 (M-1).

Elemental anal.: $C_{39}H_{52}O_4$ (584.3): cal. C 80.09%; H 8.96%; found: C 80.06%; H 8.97%.

Synthesis of 2-(4-dimethylaminobenzylidene)-22*β*-hydroxy-3-oxoolean-12-en-28-oic acid (94)

To a solution of compound **86** (100 mg, 0.21 mM) in ethanolic potassium hydroxide solution (5% w/v, 25 ml), 4-dimethylaminobenzaldehyde (1.1 eq.) was added and stirred at room temperature. After reaction completion solvent was removed *in vacuo* and the residue was diluted with water (15 ml). The mixture was acidified with dilute HCl and extracted with ethyl acetate (3 x 15 ml). The combined organic layer was dried over anhydrous sodium sulfate and evaporated to dryness. The residue was chromatographed over silica gel (100-200 mesh) and eluted with hexane : ethyl acetate (2:1) to obtain the **2-(4-dimethylaminobenzylidene)-22*β*-hydroxy-3-oxoolean-12-en-28-oic acid 94** as yellow solid (89.10 mg, 70.6%), R_f 0.31 (hexane : ethyl acetate :: 1:1), mp. 175-177 ^{0}C.

Analysis

IR (KBr) *v* max: 3456 (O-H), 2998 (C-H aliphatic), 1668 (C=O, arylidene) cm^{-1}.

^{1}H NMR ($CDCl_3$, 400 MHz): δ 0.79 (s, 3H, CH_3), 0.80 (s, 3H, CH_3), 0.83 (s, 3H, CH_3), 1.05 (s, 6H, 2 x CH_3), 1.10 (s, 3H, CH_3), 1.14 (s, 3H, CH_3), 2.94 (s, 6H, 2 x NH_3), 2.98 (s, 1H, C-18-H), 3.86 (s, 1H, C-22α-H), 5.34 (s, 1H, C-12-H), 6.64 (d, *J* = 8.76 Hz, 2H, Ar-H), 7.33 (d, *J* = 8.92 Hz, 2H, Ar-H), 7.46 (s, 1H, vinylic H).

^{13}C NMR ($CDCl_3$, 100 MHz): δ 38.21 (C-1), 138.65 (C-2), 207.59 (C-3), 40.23 (C-4), 52.75 (C-5), 22.66 (C-6), 31.92 (C-7), 41.25 (C-8), 52.44 (C-9), 37.09 (C-10), 25.73 (C-11), 122.51 (C-12), 143.49 (C-13), 44.85 (C-14), 27.83 (C-15), 23.84 (C-16), 45.59 (C-17), 42.35 (C-18), 46.19 (C-19), 30.22 (C-20), 36.14 (C-21), 74.34 (C-22), 30.11 (C-23), 15.46 (C-24), 16.59 (C-25), 20.42 (C-26), 27.23 (C-27), 180.98 (C-28), 33.95 (C-29), 24.41 (C-30), 132.62 (Ar<u>C</u>H), 123.97 (C-1''), 132.62 (C-2''), 111.78 (C-3''), 150.40 (C-4''), 111.78 (C-5''), 128.94 (C-6''), 39.24 (NCH_3), 39.31 (NCH_3).

ESI-MS (*m/z*): 600.4 (M-1).

Elemental anal.: $C_{39}H_{55}NO_4$ (601.4): cal. C 77.83%; H 9.21%; found: C 77.81%; H 9.19%.

Synthesis of 2-(pyridine-4-ylmethylidene)-22*β*-hydroxy-3-oxoolean-12-en-28-oic acid (95)

To a solution of compound **86** (100 mg, 0.21 mM) in ethanolic potassium hydroxide solution (5% w/v, 25 ml), pyridine-4-aldehyde (1.1 eq.) was added and stirred at room temperature. After reaction completion solvent was removed *in vacuo* and the residue was diluted with water (15 ml). The mixture was acidified with dilute HCl and extracted with ethyl acetate (3 x 15 ml). The combined organic layer was dried over anhydrous sodium sulfate and evaporated to dryness. The residue was chromatographed over silica gel (100-200 mesh) and eluted with hexane : ethyl acetate (2:1) to obtain the **2-(pyridine-4-ylmethylidene)-22*β*-hydroxy-3-oxoolean-12-en-28-oic acid 95** as yellow solid (75.81 mg, 64.7%), R_f 0.18 (hexane : ethyl acetate :: 1:1), mp. 123-125 ^{0}C.

Analysis

IR (KBr) *v* max: 3479 (O-H), 2948 (C-H aliphatic), 1667 (C=O, arylidene) cm^{-1}.

^{1}H NMR (DMSO-d_6+$CDCl_3$, 400 MHz): δ 0.79 (s, 3H, CH_3), 0.84 (s, 3H, CH_3), 0.93 (s, 3H, CH_3), 0.99 (s, 3H, CH_3), 1.04 (s, 3H, CH_3), 1.08 (s, 3H, CH_3), 1.10 (s, 3H, CH_3), 2.93 (dd, *J* = 13.92, 3.92 Hz, 1H, C-18-H), 3.73 (s, 1H, C-22α-H), 4.08 (br s, 1H, C-22β-OH),

5.26 (t, *J* = 3.12 Hz, 1H, C-12-H), 6.85 (s, 1H, vinylic H), 7.02 (d, *J* = 5.84 Hz, 2H, Ar-H), 8.36 (d, *J* = 5.68 Hz, 2H, Ar-H).

^{13}C NMR (DMSO-d_6+$CDCl_3$, 100 MHz): δ 38.49 (C-1), 156.17 (C-2), 203.39 (C-3), 41.05 (C-4), 52.47 (C-5), 21.23 (C-6), 31.97 (C-7), 41.37 (C-8), 51.15 (C-9), 38.16 (C-10), 27.00 (C-11), 120.37 (C-12), 144.17 (C-13), 43.85 (C-14), 27.88 (C-15), 23.81 (C-16), 43.85 (C-17), 42.00 (C-18), 45.77 (C-19), 29.77 (C-20), 35.48 (C-21), 72.69 (C-22), 29.77 (C-23), 18.55 (C-24), 17.04 (C-25), 18.70 (C-26), 27.27 (C-27), 180.25 (C-28), 33.63 (C-29), 25.26 (C-30), 132.34 (Ar<u>C</u>H), 148.90 (C-1''), 123.48 (C-2''), 149.04 (C-3''), 149.04 (C-5''), 123.48 (C-6'').

ESI-MS (*m/z*): 558.3 (M-1).

Elemental anal.: $C_{36}H_{50}NO_4$ (559.3): cal. C 77.10%; H 8.99%; found: C 77.12%; H 8.98%.

Synthesis of 2-(3-nitrobenzylidene)-22*β*-hydroxy-3-oxoolean-12-en-28-oic acid (96)

To a solution of compound **86** (100 mg, 0.21 mM) in ethanolic potassium hydroxide solution (5% w/v, 25 ml), 3-nitrobenzaldehyde (1.1 eq.) was added and stirred at room temperature. After reaction completion solvent was removed *in vacuo* and the residue was diluted with water (15 ml). The mixture was acidified with dilute HCl and extracted with ethyl acetate (3 x 15 ml). The combined organic layer was dried over anhydrous sodium sulfate and evaporated to dryness. The residue was chromatographed over silica gel (100-200 mesh) and eluted with hexane : ethyl acetate (2:1) to obtain the **2-(3-nitrobenzylidene)-22*β*-hydroxy-3-oxoolean-12-en-28-oic acid 96** as brown solid (78.37 mg, 62.1%), R_f 0.12 (hexane : ethyl acetate :: 1:1), mp. 142-144 ^{0}C.

Analysis

IR (KBr) *v* max: 3376 (O-H), 2948 (C-H aliphatic), 1667 (C=O, arylidene), 1459 (N-O, asym), 1261 (N-O, sym) cm^{-1}.

^{1}H NMR (DMSO-d_6+$CDCl_3$, 400 MHz): δ 0.81 (s, 6H, 2 x CH_3), 0.99 (s, 3H, CH_3), 1.02 (s, 6H, 2 x CH_3), 1.17 (s, 3H, CH_3), 1.24 (s, 3H, CH_3), 2.92 (d, *J* = 12.68 Hz, 1H, C-18-H), 3.70 (s, 1H, C-22α-H), 4.38 (br s, 1H, C-22β-OH), 5.24 (s, 1H, C-12-H), 6.43-8.10 (m, 5H, Ar-H and vinylic H).

^{13}C NMR (DMSO-d_6+$CDCl_3$, 100 MHz): δ 35.73 (C-1), 132.56 (C-2), 206.16 (C-3), 38.36 (C-4), 51.00 (C-5), 22.33 (C-6), 29.87 (C-7), 38.67 (C-8), 44.73 (C-9), 35.49 (C-10),

23.89 (C-11), 120.89 (C-12), 148.38 (C-13), 41.93 (C-14), 27.34 (C-15), 22.40 (C-16), 41.99 (C-17), 41.14 (C-18), 44.36 (C-19), 29.30 (C-20), 33.81 (C-21), 72.54 (C-22), 29.05 (C-23),15.11 (C-24), 14.36 (C-25), 16.37 (C-26), 27.14 (C-27), 176.05 (C-28), 31.53 (C-29), 25.18 (C-30), 128.74 (ArCH), 128.74 (C-1''), 118.24 (C-2''), 135.74 (C-3''), 115.54 (C-4''), 120.89 (C-5''), 128.60 (C-6'').

ESI-MS (*m/z*): 600.4 (M-3).

Elemental anal.: $C_{37}H_{49}NO_6$ (600.4): cal. C 73.60%; H 8.18%; found: C 73.59%; H 8.19%.

Synthesis of 2-(4-fluorobenzylidene)-22*β*-hydroxy-3-oxoolean-12-en-28-oic acid (97)

To a solution of compound **86** (100 mg, 0.21 mM) in ethanolic potassium hydroxide solution (5% w/v, 25 ml), 4-fluorobenzaldehyde (1.1 eq.) was added and stirred at room temperature. After reaction completion solvent was removed *in vacuo* and the residue was diluted with water (15 ml). The mixture was acidified with dilute HCl and extracted with ethyl acetate (3 x 15 ml). The combined organic layer was dried over anhydrous sodium sulfate and evaporated to dryness. The residue was chromatographed over silica gel (100-200 mesh) and eluted with hexane : ethyl acetate (2:1) to obtain the **2-(4-fluorobenzylidene)-22*β*-hydroxy-3-oxoolean-12-en-28-oic acid 97** as yellow solid (89.9 mg, 74.4%), R_f 0.37 (hexane : ethyl acetate :: 1:1), mp.159-161 ^{0}C.

Analysis

IR (KBr) *ν* max: 3529 (O-H), 2949 (C-H aliphatic), 1672 (C=O, arylidene), 1020 (C-F) cm^{-1}.

^{1}H NMR (DMSO-d_6+$CDCl_3$, 400 MHz): δ 0.85 (s, 3H, CH_3), 0.87 (s, 6H, 2 x CH_3), 1.11 (s, 6H, 2 x CH_3), 1.13 (s, 3H, CH_3), 1.24 (s, 3H, CH_3), 2.96 (t, J = 13.64 Hz, 1H, C-18-H), 3.78 (s, 1H, C-22α-H), 4.23 (br s, 1H, C-22β-OH), 5.32 (s, 1H, C-12-H), 7.14 (t, J = 8.60 Hz, 2H, Ar-H), 7.40 (s, 1H, vinylic H), 7.46 (t, J = 8.04 Hz, 2H, Ar-H).

^{13}C NMR (DMSO-d_6+$CDCl_3$, 100 MHz): δ 38.65 (C-1), 135.34 (C-2), 206.48 (C-3), 41.08 (C-4), 52.15 (C-5), 22.25 (C-6), 31.46 (C-7), 41.91 (C-8), 51.11 (C-9), 38.16 (C-10), 25.09 (C-11), 120.76 (C-12), 143.77 (C-13), 44.45 (C-14), 27.28 (C-15), 23.10 (C-16), 44.70 (C-17), 43.43 (C-18), 45.95 (C-19), 29.79 (C-20), 35.68 (C-21), 72.65 (C-22), 29.26 (C-23), 16.22 (C-24), 14.91 (C-25), 19.84 (C-26), 27.03 (C-27), 176.33 (C-28), 33.68 (C-

29), 23.87 (C-30), 133.05 (ArCH), 132.01 (C-1''), 131.93 (C-2''), 115.26 (C-3''), 160.65 (C-4''), 115.05 (C-5''), 131.52 (C-6'');

ESI-MS (*m/z*): 575.3 (M-1).

Elemental anal.: $C_{37}H_{49}FO_4$ (576.4): cal. C 77.05%; H 8.56%; found: C 77.03%; H 8.58%.

Synthesis of 2-(3-phenylprop-2-en-1-ylidene)-22*β*-[(2-methyl-1-oxo-2-butenyl)oxy]-3-oxoolean-12-en-28-oic acid (98)

To a solution of compound **80** (100 mg, 0.18 mM) in ethanolic potassium hydroxide solution (5% w/v, 25 ml), cinnamic aldehyde (1.1 eq.) was added and stirred at room temperature. After reaction completion solvent was removed *in vacuo* and the residue was diluted with water (15 ml). The mixture was acidified with dilute HCl and extracted with ethyl acetate (3 x 15 ml). The combined organic layer was dried over anhydrous sodium sulfate and evaporated to dryness. The residue was chromatographed over silica gel (100-200 mesh) and eluted with hexane : ethyl acetate (4:1) to obtain the yellow solid as **2-(3-phenylprop-2-en-1-ylidene)-22*β*-[(2-methyl-1-oxo-2-butenyl)oxy]-3-oxoolean-12-en-28-oic acid 98** (85.2 mg, 71.1%), R_f (hexane : ethyl acetate :: 4:1), mp 145-147 ^{0}C.

Analysis

IR (KBr) *v* max: 2951 (C-H aliphatic), 1715 (C=O, ester), 1672 (C=O, arylidene) cm^{-1}.

^{1}H NMR (400 MHz, $CDCl_3$): δ 0.86 (s, 3H, CH_3), 0.91 (s, 6H, 2 x CH_3), 1.02 (s, 3H, CH_3), 1.11 (s, 3H, CH_3), 1.15 (s, 3H, CH_3), 1.18 (s, 3H, CH_3), 2.97 (dd, *J* = 9.24, 8.40 Hz, 1H, C-18-H), 5.10 (t, *J* = 2.68 Hz, 1H, C-22α-H), 5.34 (s, 1H, C-12-H), 6.00 (dd, *J* = 5.44 Hz, 1.44 Hz, 1H, C-3'-H), 6.94 (dd, *J* = 10.04, 3.44 Hz, 2H, ArCH, ArCHCH), 7.26 (d, *J* = 9.80 Hz, 1H, ArCHCHCH), 7.30 (dd, *J* = 5.32 Hz, 2.20 Hz, 1H, ArH), 7.36 (dd, *J* = 7.88, 1.6 Hz, 2H, ArH), 7.48 (d, *J* = 8.52 Hz, 2H, ArH).

^{13}C NMR (100 MHz, $CDCl_3$): δ 39.13 (C-1), 137.30 (C-2), 207.18 (C-3), 37.72 (C-4), 53.06 (C-5), 22.62 (C-6), 30.07 (C-7), 38.64 (C-8), 50.70 (C-9), 36.07 (C-10), 25.70 (C-11), 122.49 (C-12), 143.22 (C-13), 42.36 (C-14), 29.34 (C-15), 24.22 (C-16), 45.06 (C-17), 42.18 (C-18), 45.32 (C-19), 29.72 (C-20), 33.72 (C-21), 76.73 (C-22), 29.64 (C-23), 15.68 (C-24), 15.45 (C-25), 16.49 (C-26), 27.55 (C-27), 179.93 (C-28), 31.94 (C-29), 26.19 (C-30), 166.28 (C-1'), 128.79 (C-2') 140.70 (C-3'), 20.60 (C-4'), 14.15 (C-5'), 123.36

(ArCHCH), 132.65 (ArCH), 139.02 (ArCHCHCH), 136.67 (C-1''), 127.15 (C-2''), 128.79 (C-3''), 128.48 (C-4''), 128.84 (C-5''), 127.61 (C-6'').

ESI-MS (*m/z*): 665.4 (M-1).

Elemental anal.: $C_{44}H_{58}O_5$ (666.43): cal. C 79.24%; H 8.77%; found: C 79.25%; H 8.78%.

Synthesis of 2-(3-phenylprop-2-en-1-ylidene)-22*β*-[(3-methyl-1-oxo-2-butenyl)oxy]-3-oxoolean-12-en-28-oic acid (99)

To a solution of compound **81** (100 mg, 0.18 mM) in ethanolic potassium hydroxide solution (5% w/v, 25 ml), cinnamic aldehyde (1.1 eq.) was added and stirred at room temperature. After reaction completion solvent was removed *in vacuo* and the residue was diluted with water (15 ml). The mixture was acidified with dilute HCl and extracted with ethyl acetate (3 x 15 ml). The combined organic layer was dried over anhydrous sodium sulfate and evaporated to dryness. The residue was chromatographed over silica gel (100-200 mesh) and eluted with hexane : ethyl acetate (4:1) to obtain the yellow solid as **2-(3-phenylprop-2-en-1-ylidene)-22*β*-[(3-methyl-1-oxo-2-butenyl)oxy]-3-oxoolean-12-en-28-oic acid 99** as yellow solid (79.2 mg, 66.7%), R_f (hexane : ethyl acetate :: 4:1), mp. 159-161 ^{0}C.

Analysis

IR (KBr) *v* max: 2947 (C-H aliphatic), 1682 (C=O, arylidene) cm^{-1}.

^{1}H NMR ($CDCl_3$, 400 MHz): δ 0.82 (s, 3H, CH_3), 0.94 (s, 6H, 2 x CH_3), 1.04 (s, 3H, CH_3), 1.13 (s, 3H, CH_3), 1.18 (s, 3H, CH_3), 1.25 (s, 3H, CH_3), 2.97 (d, *J* = 20.84 Hz, 1H, C-18-H), 5.05 (s, 1H, C-22α-H), 5.45 (s, 1H, C-12-H), 5.57 (s, 1H, C-2'), 6.98 (q, *J* = 16.49, 15.44 Hz, 2H, ArCH, ArCHCH), 7.27 (d, *J* = 11.52 Hz, 1H, ArCHCHCH), 7.32 (d, *J* = 4.92 Hz, 1H, ArH), 7.35 (dd, *J* = 8.24, 7.64 Hz, 2H, ArH), 7.48 (d, *J* = 7.28 Hz, 2H, ArH).

^{13}C NMR ($CDCl_3$, 100 MHz): δ 39.14 (C-1), 138.69 (C-2), 207.13 (C-3), 39.14 (C-4), 53.07 (C-5), 20.24 (C-6), 31.88 (C-7), 42.19 (C-8), 50.69 (C-9), 38.56 (C-10), 24.03 (C-11), 122.48 (C-12), 143.24 (C-13), 45.06 (C-14), 27.55 (C-15), 22.61 (C-16), 45.34 (C-17), 42.21 (C-18), 46.06 (C-19), 30.06 (C-20), 37.71 (C-21), 75.94 (C-22), 29.63 (C-23), 63 (C-24), 15.45 (C-25), 16.53 (C-26), 26.18 (C-27), 179.95 (C-28), 36.08 (C-29), 25.69 (C-30), 166.32 (C-1'), 115.97 (C-2'), 157.32 (C-3'), 20.54 (C-4'), 14.47 (C-5'), 123.37 (ArCH),

136.69 (ArCHC), 140.69 (ArCHCCH), 137.29 (C-1''), 127.14 (C-2''), 132.66 (C-3''), 128.78 (C-4''), 128.83 (C-5''), 127.14 (C-6'').

ESI-MS (*m/z*): 665.4 (M-1).

Elemental anal.: $C_{44}H_{58}O_5$ (666.43): cal. C 79.24%, H 8.77%; found: C 79.27%, H 8.77%.

Synthesis of 2-(2-methyl-3-phenylprop-2-en-1-ylidene)-22*β*-[(2-methyl-1-oxo-2-butenyl) oxy]-3-oxoolean-12-en-28-oic acid (100)

To a solution of compound **80** (100 mg, 0.18 mM) in ethanolic potassium hydroxide solution (5% w/v, 25 ml), α-methyl-trans-cinnamic aldehyde (1.1 eq.) was added and stirred at room temperature. After reaction completion solvent was removed *in vacuo* and the residue was diluted with water (15 ml). The mixture was acidified with dilute HCl and extracted with ethyl acetate (3 x 15 ml). The combined organic layer was dried over anhydrous sodium sulfate and evaporated to dryness. The residue was chromatographed over silica gel (100-200 mesh) and eluted with hexane : ethyl acetate (4:1) to obtain the **2-(2-methyl-3-phenylprop-2-en-1-ylidene)-22*β*-[(2-methyl-1-oxo-2-butenyl)oxy]-3-oxo olean-12-en-28-oic acid 100** as light yellow solid (83.1 mg, 67.1%), R_f 0.66 (hexane : ethyl acetate :: 4:1), mp.152-154 ^{0}C.

Analysis

IR (KBr) *v* max: 2950 (C-H aliphatic), 1716 (C=O, ester), 1670 (C=O, arylidene) cm^{-1}.

^{1}H NMR ($CDCl_3$, 400 MHz): δ 0.84 (s, 3H, CH_3), 0.89 (s, 3H, CH_3), 1.00 (s, 3H, CH_3), 1.05 (s, 6H, 2 x CH_3), 1.09 (s, 3H, CH_3), 1.17 (s, 3H, CH_3), 3.07 (t, *J* =8.28 Hz, 1H, C-18-H), 5.03 (t, *J* = 7.68 Hz, 1H, C-22α-H), 5.31 (s, 1H, C-12-H), 5.92 (dd, *J* = 4.16, 1.12 Hz, 1H, C-2'-H), 7.11-7.17 (m, 3H, ArH), 7.20-7.34 (m, 4H, ArH).

^{13}C NMR ($CDCl_3$, 100 MHz): δ 38.47 (C-1), 138.75 (C-2), 206.96 (C-3), 39.23 (C-4), 55.31 (C-5), 19.49 (C-6), 30.04 (C-7), 39.23 (C-8), 50.61 (C-9), 37.72 (C-10), 24.20 (C-11), 122.50 (C-12), 143.10 (C-13), 45.97 (C-14), 26.46 (C-15), 23.52 (C-16), 46.89 (C-17), 42.00 (C-18), 47.43 (C-19), 27.57 (C-20), 36.78 (C-21), 75.89 (C-22), 26.92 (C-23), 15.63 (C-24), 15.10 (C-25), 19.49 (C-26), 26.14 (C-27), 179.62 (C-28), 33.68 (C-29), 25.78 (C-30), 166.29 (C-1'), 123.39 (C-2'), 155.48.10 (C-3'), 21.48 (C-4'), 20.53 (C-5'), 16.86 (ArCHCCH$_3$), 127.69 (ArCHC), 130.41 (ArCH), 143.10 (ArCHCCH), 138.75 (C-1''), 127.69 (C-2''), 129.30 (C-3''), 128.43 (C-4''), 129.30 (C-5''), 128.24 (C-6'').

ESI-MS (*m/z*): 679.6 (M-1).

Elemental anal.: $C_{45}H_{60}O_5$ (680.44): cal. C 79.37%, H 8.80%; found: C 79.35%, H 8.81%.

Synthesis of 2-(2-methyl-3-phenylprop-2-en-1-ylidene)-22*β*-[(3-methyl-1-oxo-2-butenyl)oxy]-3-oxoolean-12-en-28-oic acid (101)

To a solution of compound **81** (100 mg, 0.18 mM) in ethanolic potassium hydroxide solution (5% w/v, 25 ml), α-methyl-trans-cinnamic aldehyde (1.1 eq.) was added and stirred at room temperature. After reaction completion solvent was removed *in vacuo* and the residue was diluted with water (15 ml). The mixture was acidified with dilute HCl and extracted with ethyl acetate (3 x 15 ml). The combined organic layer was dried over anhydrous sodium sulfate and evaporated to dryness. The residue was chromatographed over silica gel (100-200 mesh) and eluted with hexane : ethyl acetate (4:1) to obtain the **2-(2-methyl-3-phenylprop-2-en-1-ylidene)-22*β*-[(3-methyl-1-oxo-2-butenyl)oxy]-3-oxoolean-12-en-28-oic acid 101** as light yellow solid (86.4 mg, 70.8%), R_f 0.64 (hexane : ethyl acetate :: 4:1), mp.167-169 ^{0}C.

Analysis

IR (KBr) *v* max: 2951 (C-H aliphatic), 1714 (C=O, ester), 1652 (C=O, arylidene) cm^{-1}.

^{1}H NMR ($CDCl_3$, 400 MHz): δ 0.77 (s, 3H, CH_3), 0.83 (s, 3H, CH_3), 0.96 (s, 6H, 2 x CH_3), 1.00 (s, 3H, CH_3), 1.06 (s, 3H, CH_3), 1.18 (s, 3H, CH_3), 3.04 (dd, *J* = 5.72, 2.39 Hz, 1H, C-18-H), 4.97 (t, *J* = 2.88 Hz, 1H, C-22α-H), 5.30 (t, *J* = 3.48 Hz, 1H, C-12-H), 5.49 (s, 1H, C-2'-H), 7.15-7.47 (m, 7H, ArH, ArC<u>H</u>, ArCHCC<u>H</u>).

^{13}C NMR ($CDCl_3$, 100 MHz): δ 38.47 (C-1), 138.82 (C-2), 206.77 (C-3), 39.23 (C-4), 55.31 (C-5), 19.49 (C-6), 30.04 (C-7), 39.23 (C-8), 50.61 (C-9), 37.72 (C-10), 24.20 (C-11), 122.50 (C-12), 143.10 (C-13), 45.97 (C-14), 26.46 (C-15), 23.52 (C-16), 46.89 (C-17), 42.00 (C-18), 47.43 (C-19), 27.57 (C-20), 36.78 (C-21), 75.89 (C-22), 26.92 (C-23), 15.63 (C-24), 15.10 (C-25), 16.91 (C-26), 26.14 (C-27), 179.58 (C-28), 33.68 (C-29), 25.78 (C-30), 166.30 (C-1'), 115.95 (C-2'), 157.20 (C-3'), 21.48 (C-4'), 20.53 (C-5'), 16.86 ($ArCH_2CH\underline{C}H_3$), 127.61 (Ar<u>C</u>H), 134.47 ($ArCH\underline{C}CH_3$), 143.10 ($ArCC\underline{C}H$), 138.82 (C-1''), 127.69 (C-2''), 129.44 (C-3''), 128.24 (C-4''), 130.47 (C-5''), 128.24 (C-6'').

ESI-MS (*m/z*): 679.6 (M-1).

Elemental anal.: $C_{45}H_{60}O_5$ (680.44): cal. C 79.37%; H 8.80%; found: C 79.38%, H 8.80%.

Synthesis of 2-(2-methyl-3-phenylprop-2-en-1-ylidene)-22*β*-hydroxy-3-oxoolean-12-en-28-oic acid (102)

To a solution of compound **86** (100 mg, 0.21 mM) in ethanolic potassium hydroxide solution (5% w/v, 25 ml), α-methyl-trans-cinnamic aldehyde (1.1 eq.) was added and stirred at room temperature. After reaction completion solvent was removed *in vacuo* and the residue was diluted with water (15 ml). The mixture was acidified with dilute HCl and extracted with ethyl acetate (3 x 15 ml). The combined organic layer was dried over anhydrous sodium sulfate and evaporated to dryness. The residue was chromatographed over silica gel (100-200 mesh) and eluted with hexane : ethyl acetate (2:1) to obtain the **2-(2-methyl-3-phenylprop-2-en-1-ylidene)-22*β*-hydroxy-3-oxoolean-12-en-28-oic acid 102** as yellow solid (85.1 mg, 68.3%), R_f 0.41 (hexane : ethyl acetate :: 1:1), mp.135-137 ^{0}C.

Analysis

IR (KBr) *v* max: 3416 (O-H), 2944 (C-H stretching), 1679 (C=O, arylidene) cm^{-1}.

^{1}H NMR ($CDCl_3$, 400 MHz): δ 0.78 (s, 3H, CH_3), 0.80 (s, 3H, CH_3), 0.83 (s, 3H, CH_3), 1.06 (s, 6H, 2 x CH_3), 1.08 (s, 3H, CH_3), 1.14 (s, 3H, CH_3), 2.93 (dd, *J* = 15.64, 4.56 Hz, 1H, C-18-H), 3.86 (s, 1H, C-22α-H), 5.34 (s, 1H, C-12-H), 7.11-7.46 (m, 7H, ArH, ArC<u>H</u>, ArCHCC<u>H</u>).

^{13}C NMR ($CDCl_3$, 100 MHz): δ 38.15 (C-1), 135.90 (C-2), 207.92 (C-3), 39.19 (C-4), 52.96 (C-5), 22.66 (C-6), 31.86 (C-7), 41.25 (C-8), 52.38 (C-9), 36.79 (C-10), 24.34 (C-11), 122.37 (C-12), 143.40 (C-13), 44.17 (C-14), 27.77 (C-15), 23.74 (C-16), 45.16 (C-17), 42.31 (C-18), 45.39 (C-19), 30.18 (C-20), 36.27 (C-21), 74.30 (C-22), 29.77 (C-23), 15.36 (C-24), 14.22 (C-25), 20.32 (C-26), 27.16 (C-27), 180.79 (C-28), 33.89 (C-29), 25.66 (C-30), 16.50 (ArCH$_2$CH<u>C</u>H$_3$), 128.25 (Ar<u>C</u>H), 130.42 (ArCH<u>C</u>CH$_3$), 137.55 (ArCHC<u>C</u>H), 133.63 (C-1''), 128.32 (C-2''), 130.21 (C-3''), 129.09 (C-4''), 129.32 (C-5''), 128.44 (C-6'').

ESI-MS (*m/z*): 597.4 (M-1).

Elemental anal.: $C_{40}H_{54}O_4$ (598.40): cal. C 80.22%; H 9.09% ; found: C 80.20%; H 9.08%.

Synthesis of 2-(3,4-dimethoxybenzylidene)-22*β*-hydroxy-3-oxoolean-12-en-28-oic acid (103)

To a solution of compound **86** (100 mg, 0.21 mM) in ethanolic potassium hydroxide solution (5% w/v, 25 ml), 3,4-dimethoxybenzaldehyde (1.1 eq.) was added and stirred at room temperature. After reaction completion solvent was removed *in vacuo* and the residue was diluted with water (15 ml). The mixture was acidified with dilute HCl and extracted with ethyl acetate (3 x 15 ml). The combined organic layer was dried over anhydrous sodium sulfate and evaporated to dryness. The residue was chromatographed over silica gel (100-200 mesh) and eluted with hexane : ethyl acetate (2:1) to obtain the **2-(3,4-dimethoxybenzylidene)-22*β*-hydroxy-3-oxoolean-12-en-28-oic acid 103** as yellow solid (93.1 mg, 72.1%), R_f 0.27 (hexane : ethyl acetate :: 1:1), mp. 195-197 ^{0}C.

Analysis

IR (KBr) *v* max: 3433 (O-H), 2946 (C-H aliphatic), 1686 (C=O, arylidene), 1272 (C-O-C, ether) cm^{-1}.

^{1}H NMR ($CDCl_3$, 400 MHz): δ 0.86 (s, 3H, CH_3), 0.89 (s, 3H, CH_3), 0.91 (s, 3H, CH_3), 1.11 (s, 6H, 2 x CH_3), 1.17 (s, 3H, CH_3), 1.21 (s, 3H, CH_3), 3.04 (d, *J* = 15.04 Hz, 1H, C-18-H), 3.85 (dd, *J* = 5.52, 2.84 Hz, 1H, C-22α-H), 3.90 (s, 3H, OCH_3), 3.91 (s, 3H, OCH_3), 5.40 (s, 1H, C-12-H), 6.90 (d, *J* = 8.44 Hz, 1H, Ar-H), 6.96 (d, *J* = 1.56 Hz, 1H, ArH), 7.07 (dd, *J* = 3.48, 1.44 Hz, 1H, ArH), 7.49 (s, 1H, vinylic H).

^{13}C NMR ($CDCl_3$, 100 MHz): δ 38.28 (C-1), 137.59 (C-2), 207.73 (C-3), 39.18 (C-4), 60.44 (C-5), 20.34 (C-6), 29.82 (C-7), 41.18 (C-8), 52.83 (C-9), 36.23 (C-10), 22.62 (C-11), 122.15 (C-12), 143.59 (C-13), 44.29 (C-14), 25.64 (C-15), 21.06 (C-16), 45.03 (C-17), 42.28 (C-18), 45.54 (C-19), 27.82 (C-20), 33.25 (C-21), 74.32 (C-22), 27.22 (C-23), 15.40 (C-24), 14.20 (C-25), 16.52 (C-26), 24.36 (C-27), 180.70 (C-28), 30.16 (C-29), 23.75 (C-30), 55.91 (OCH_3), 55.98 (OCH_3),128.85 (ArCH), 131.88 (C-1''), 110.18 (C-2''), 149.53 (C-3''), 148.63 (C-4''), 114.13 (C-5''), 123.49 (C-6'').

ESI-MS (*m/z*): 617.3 (M-1).

Elemental anal.: $C_{39}H_{54}O_6$ (618.84): cal. C 75.69%; H 8.80%; found: C 75.67%; H 8.81%.

Synthesis of 2-(2-methyl-3-phenylpropyl)-22*β*-hydroxy-3-oxoolean-12-en-28-oic acid (104)

To a solution of 2-(2-Methyl-3-phenylprop-2-en-1-ylidene)-22β-hydroxy-3-oxoolean-12-en-28-oic acid **102** (100 mg, 0.16 mM) in methanol (20 ml), palladium on carbon (0.15 mM) and ammonium formate (8.00 mM) was added and stirred at room temperature. After reaction completion the reaction mixture was filtered, dried over anhydrous sodium sulphate and evaporated to dryness. The residue was chromatographed over silica gel (100-200 mesh) and eluted with hexane : ethyl acetate (2:1) to obtain **2-(2-methyl-3-phenylpropyl)-22*β*-hydroxy-3-oxoolean-12-en-28-oic acid 104** as colourless solid (48.6 mg, 48.4%), R_f 0.44 (hexane : ethyl acetate :: 1:1), mp. 61-63 ^{0}C.

Analysis

IR (KBr) *v* max: 3466 (O-H), 2947 (C-H aliphatic), 1706 (C=O, keto) cm^{-1}.

^{1}H NMR ($CDCl_3$, 400 MHz): δ 0.78 (s, 3H, CH_3), 0.83 (s, 3H, CH_3), 0.85 (s, 1H, CH_3), 1.05 (s, 3H, CH_3), 1.07 (s, 3H, CH_3), 1.10 (s, 3H, CH_3), 1.14 (s, 3H, CH_3), 2.98 (dd, *J* = 20.08, 16.02 Hz, 1H, C-18-H), 3.84 (t, *J* = 3.00 Hz, 1H, C-22α-H), 5.31 (t, *J* = 3.44 Hz, 1H, C-12-H), 7.11-7.46 (m, 5H, ArH).

^{13}C NMR ($CDCl_3$, 100 MHz): δ 38.20 (C-1), 40.20 (C-2), 206.87 (C-3), 40.60 (C-4), 51.91 (C-5), 23.22 (C-6), 32.88 (C-7), 41.26 (C-8), 51.34 (C-9), 37.16 (C-10), 24.68 (C-11), 121.31 (C-12), 142.36 (C-13), 44.37 (C-14), 27.32 (C-15), 23.65 (C-16), 44.94 (C-17), 43.15 (C-18), 46.02 (C-19), 30.90 (C-20), 35.19 (C-21), 73.27 (C-22), 29.16 (C-23), 15.45 (C-24), 14.32 (C-25), 21.62 (C-26), 26.80 (C-27), 179.59 (C-28), 35.19 (C-29), 26.14 (C-30), 19.27 ($ArCH_2CH\underline{C}H_3$), 28.73 ($ArCH_2\underline{C}H$), 41.07 ($ArCH_2CH\underline{C}H_2$), 44.14 ($Ar\underline{C}H_2$), 134.85 (C-1''), 128.27 (C-2''), 132.58 (C-3''), 127.20 (C-4''), 129.37 (C-5''), 127.39 (C-6'').

ESI-MS (*m/z*): 601.3 (M-1).

Elemental anal.: $C_{40}H_{58}O_4$ (602.43): cal. C 79.69%; H 9.70%; found: C 79.68%; H 9.71%.

Synthesis of 2-(3,4-dimethoxybenzyl)-22*β*-hydroxy-3-oxoolean-12-en-28-oic acid (105)

To a solution of 2-(3,4-Dimethoxybenzylidene)-22β-hydroxy-3-oxoolean-12-en-28-oic acid **103** (100 mg, 0.16 mM) in methanol (20 ml), palladium on carbon (0.15 mM) and ammonium formate (8.00 mM) was added and stirred at room temperature. After reaction

completion the reaction mixture was filtered, dried over anhydrous sodium sulphate and evaporated to dryness. The residue was chromatographed over silica gel (100-200 mesh) and eluted with hexane : ethyl acetate (2:1) to obtain **2-(3,4-dimethoxybenzyl)-22*β*-hydroxy-3-oxoolean-12-en-28-oic acid 105** as white solid (59.2 mg, 58.9%), R_f 0.35 (hexane : ethyl acetate :: 1:1), mp. 103-105 ^{0}C.

Analysis

IR (KBr) *v* max: 3491 (O-H), 2947 (C-H aliphatic), 1709 (C=O, keto), 1253 (C-O-C, ether) cm^{-1}.

^{1}H NMR ($CDCl_3$, 400 MHz): δ 0.77 (s, 3H, CH_3), 0.80 (s, 3H, CH_3), 0.87 (s, 6H, 2 x CH_3), 0.99 (s, 3H, CH_3), 1.09 (s, 6H, 2 x CH_3), 2.97 (dd, *J* = 6.80, 3.88 Hz, 1H, C-18-H), 3.87 (s, 3H, OCH_3), 3.89 (s, 3H, OCH_3), 3.91 (s, 1H, C-22α-H), 5.32 (s, 1H, C-12-H), 6.70-6.88 (m, 3H, ArH).

^{13}C NMR ($CDCl_3$, 100 MHz): δ 35.52 (C-1), 32.79 (C-2), 217.23 (C-3), 37.07 (C-4), 62.67 (C-5), 21.68 (C-6), 28.68 (C-7), 38.32 (C-8), 51.33 (C-9), 33.65 (C-10), 22.43 (C-11), 121.80 (C-12), 141.94 (C-13), 41.02 (C-14), 26.14 (C-15), 21.98 (C-16), 41.14 (C-17), 40.19 (C-18), 45.04 (C-19), 28.68 (C-20), 33.60 (C-21), 73.35 (C-22), 28.35 (C-23), 14.53 (C-24), 13.11 (C-25), 15.70 (C-26), 24.65 (C-27), 179.73 (C-28), 29.09 (C-29), 23.35 (C-30), 54.77 (OCH_3), 54.81 (OCH_3), 30.89 (Ar$\underline{C}H_2$), 133.00 (C-1''), 108.62 (C-2''), 147.54 (C-3''), 146.81 (C-4''), 109.56 (C-5''), 117.73 (C-6'').

ESI-MS (*m/z*): 619.4 (M-1).

Elemental anal.: $C_{39}H_{56}O_6$ (620.41): C 75.45%; H 9.09%; found: C 75.43%; H 9.10%.

Synthesis of 2-(3-phenylpropyl)-22*β*-hydroxy-3-oxoolean-12-en-28-oic acid (106)

To a solution of 2-(3-Phenylprop-2-en-1-ylidene)-22β-hydroxy-3-oxoolean-12-en-28-oic acid **93** (100 mg, 0.17 mM) in methanol (20 ml), palladium on carbon (0.15 mM) and ammonium formate (8.00 mM) was added and stirred at room temperature. After reaction completion the reaction mixture was filtered, dried over anhydrous sodium sulphate and evaporated to dryness. The residue was chromatographed over silica gel (100-200 mesh) and eluted with hexane : ethyl acetate (2:1) to obtain **2-(3-phenylpropyl)-22β-hydroxy-3-oxoolean-12-en-28-oic acid 106** as semi solid (47.4 mg, 46.6%), R_f 0.43 (hexane : ethyl acetate :: 1:1).

Analysis

IR (KBr) *v* max: 3437 (O-H), 2944 (C-H aliphatic), 1700 (C=O, keto) cm^{-1}.

^{1}H NMR ($CDCl_3$, 400 MHz): δ 0.78 (s, 3H, CH_3), 0.89 (s, 3H, CH_3), 1.02 (s, 6H, 2 x CH_3), 1.07 (s, 3H, CH_3), 1.17 (s, 3H, CH_3), 1.22 (s, 3H, CH_3), 2.98 (t, *J* = 3.40 Hz, 1H, C-18-H), 3.89 (s, 1H, C-22α-H), 5.34 (t, *J* = 6.80 Hz, 1H, C-12-H), 7.14-7.17 (m, 2H, ArH), 7.24-7.28 (m, 3H, ArH).

^{13}C NMR ($CDCl_3$, 100 MHz): δ 40.05 (C-1), 41.05 (C-2), 216.84 (C-3), 47.57 (C-4), 51.61 (C-5), 18.50 (C-6), 32.82 (C-7), 39.98 (C-8), 45.98 (C-9), 35.63 (C-10), 24.61 (C-11), 121.15 (C-12), 142.04 (C-13), 44.96 (C-14), 28.68 (C-15), 23.29 (C-16), 51.36 (C-17), 41.19 (C-18), 45.72 (C-19), 30.72 (C-20), 38.39 (C-21), 73.26 (C-22), 26.73 (C-23), 22.58 (C-24), 15.26 (C-25), 17.04 (C-26), 26.12 (C-27), 179.80 (C-28), 35.23 (C-29), 28.21(C-30), 28.92 ($ArCH_2\underline{C}H_2$), 29.11($ArCH_2CH_2\underline{C}H_2$), 37.22 ($Ar\underline{C}H_2$), 141.54 (C-1''), 127.24 (C-2''), 127.36 (C-3''), 124.23 (C-4''), 127.36 (C-5''), 127.24 (C-6'').

ESI-MS (*m/z*): 587.4 (M-1).

Elemental anal.: $C_{39}H_{56}O_4$ (588.42): C 79.55%; H 9.59%; found: C 79.53%; H 9.60%.

3.4. *In-vitro* cytotoxicity study on NCI-60 cell lines and NCI's COMPARE analysis

The NCI *in-vitro* anticancer screening was two-stage process, beginning with the evaluation of selected compounds **80**, **81**, **84**, **85**, **86**, **87**, **92** and **93** against the NCI's 60 human tumor cell lines composite of nine different type of cancers at a single high dose (10 μM) concentration. The output from the single dose screen was reported as a mean graph and available for analysis by the NCI's COMPARE program. Compounds which exhibited significant growth inhibition were further evaluated against the same 60 human tumor cell lines at five concentration levels ranging from 0.01-100 μM concentration.

The human tumor cell lines of the cancer screening panel were grown in RPMI 1640 medium containing 5% fetal bovine serum and 2 mM L-glutamine. For a typical screening experiment, cells were inoculated into 96 well microtiter plates in 100 μL at plating densities ranging from 5,000 to 40,000 cells/well depending on the doubling time of individual cell lines. After cell inoculation, the microtiter plates were incubated at 37°C, 5 % CO_2, 95 % air and 100 % relative humidity for 24 h prior to addition of experimental drugs. After 24 h, two plates of each cell line were fixed *in situ* with trichloroacetic acid (TCA), to represent a measurement of the cell population for each cell line at the time of drug addition (Tz). Experimental drugs were solubilized in dimethyl sulfoxide at 400-fold

the desired final maximum test concentration and stored frozen prior to use. At the time of drug addition, an aliquot of frozen concentrate was thawed and diluted to twice the desired final maximum test concentration with complete medium containing 50 µg/ml gentamicin. Additional four, 10-fold or ½ log serial dilutions were made to provide a total of five drug concentrations plus control. Aliquots of 100 µl of these different drug dilutions were added to the appropriate microtiter wells already containing 100 µl of medium, resulting in the required final drug concentrations.

Following drug addition, the plates were incubated for an additional 48 h at 37°C, 5 % CO_2, 95 % air, and 100 % relative humidity. For adherent cells, the assay was terminated by the addition of cold TCA. Cells were fixed *in situ* by the gentle addition of 50 µl of cold 50 % (w/v) TCA (final concentration, 10 % TCA) and incubated for 60 minutes at 4°C. The supernatant was discarded, and the plates were washed five times with tap water and air dried. Sulforhodamine B (SRB) solution (100 µl) at 0.4 % (w/v) in 1 % acetic acid was added to each well, and plates were incubated for 10 minutes at room temperature. After staining, unbound dye was removed by washing five times with 1 % acetic acid and the plates were air dried. Bound stain was subsequently solubilized with 10 mM trizma base, and the absorbance was read on an automated plate reader at a wavelength of 515 nm. For suspension cells, the methodology was the same except that the assay is terminated by fixing settled cells at the bottom of the wells by gently adding 50 µl of 80 % TCA (final concentration, 16 % TCA). Using the seven absorbance measurements [time zero, (Tz), control growth, (C), and test growth in the presence of drug at the five concentration levels (Ti)], the percentage growth was calculated at each of the drug concentrations levels. Percentage growth inhibition was calculated as:

$$[(Ti-Tz)/(C-Tz)] \times 100 \text{ for concentrations for which } Ti \geq Tz$$

$$[(Ti-Tz)/Tz] \times 100 \text{ for concentrations for which } Ti < Tz$$

Three dose response parameters were calculated for each experimental agent. Growth inhibition of 50 % (GI_{50}) is calculated from $[(Ti-Tz)/(C-Tz)] \times 100 = 50$, which was the drug concentration resulting in a 50% reduction in the net protein increase (as measured by SRB staining) in control cells during the drug incubation. The drug concentration resulting in total growth inhibition (TGI) is calculated from Ti = Tz. The LC_{50} (concentration of drug resulting in a 50% reduction in the measured protein at the end

of the drug treatment as compared to that at the beginning) indicating a net loss of cells following treatment is calculated from [(Ti-Tz)/Tz] x 100 = -50. Values were calculated for each of these three parameters if the level of activity was reached; however, if the effect was not reached or is exceeded, the value for that parameter is expressed as greater or less than the maximum or minimum concentration tested [Boyd and Paull,1995].

The NCI's COMPARE algorithm utilizes the *in-vitro* antitumor results in determining and expressing the degree of similarity, or mean-graph profiles generated on a similar compound or different compounds [Shoemaker, 2006]. Dose response parameters were used as seed to calculate Pearson correlation coefficient (PCC) with various set compounds and prediction of probable molecular mechanistic targets.

3.5. Selective cancer cytotoxicity, mechanistic studies and docking analysis of novel congeners of lantadenes

3.5.1. Cell culture and MTT assay

The human leukemic cells HL-60, colorectal carcinoma cells HCT116, breast adenocarcinoma cells MCF7, human lung cancer cells A549 and African green monkey kidney fibroblast VERO cells were grown in RPMI medium supplemented with 10% fetal bovine serum and 1% penicillin-streptomycin (Gibco, Invitrogen, USA). For assay, phenol red-free RPMI medium (Sigma-Aldrich, USA) supplemented with 5% fetal bovine serum and 1% penicillin-streptomycin was used. HL-60 (15,000 cells/well), HCT116 and MCF7 (3000 cells/well), and A549 (4000 cells/well) were seeded into 96-well plates and incubated overnight for cell attachment. For treatment, compounds were added at concentrations ranging from 0.01 to 100 μM and incubated for 48 hours. At the end of incubation, 20 μl/well of 5 mg/mL thiazoyl blue tetrazolium bromide (MTT) (Amresco, USA) was added and cells were further incubated for 4 hours. Supernatant was then removed and the purple formazan which has formed was dissolved using 100 μl of DMSO (Fisher Scientific, UK). Absorbance was read at 570 nm using Spectra Max M4 microplate reader (Molecular Devices Inc., US).

3.5.2. NF-κB Luciferase assay

The A549 cells were cultured in 12-well plates and transiently co-transfected with 0.2μg of a pNF-*κ*B-Luc vector (Stratagene, La Jolla, CA) and 0.2 μg of pSV-*β*-galactosidase dissolved in 3μL lipofectamine™ or lipofectamine™ 2000 (Invitrogen,

Carlsbad, CA) as the internal control. The plasmids were transfected according to the manufacturer's instructions. After 6 h, the medium was changed to complete medium and cultured for 6 hours, and then the transfected cells were treated with different compounds in complete medium for 24 hours. The A549 cell extracts were harvested using 150μL of lysis buffer (Tropix, Inc., Bedford, MA) per well. To measure the luciferase and *β*-galactosidase activities, cell extracts (20μL each) were assayed separately using the Luciferase Assay Kit and Galacto-Light Plus™ system (Tropix, Inc.), respectively. Luciferase activity was measured and analyzed using an FB12 luminometer (Zylux Corporation, Oak Ridge, TN) [Liang *et al.,* 2009].

3.5.3. Akt kinase inhibition assay

AKT1/PKBa KinEASE^{TM} FP Fluorescein Green Assay kit for fluorescence polarization experiments and Akt1 enzyme were purchased from Upstate, Millipore Corporation (Charlottesville, VA). The enclosed experimental protocol of the KinEASE^{TM} kit was followed. Total reaction volume per well was 25μL. In Corning Costar 384-well black plates, various concentrations of compound in DMSO was diluted with buffer containing 50mM HEPES (pH 7.2), 0.01% BSA, 5mM $MgCl_2$, 1mM DTT. STK Substrate 3 (final concentration 10 μM) and Akt1 (concentration needed to achieve 70% activity) were added to each well and incubated for 10 min at 25 ^{0}C, ATP (final concentration 100μM) was added to start the reactions. After 1 h incubation at 25 ^{0}C, the reactions were quenched with 5 μL STK stop mix including the phosphorylated STK tracer, 5μL STK antibody mix were then added and the mixture were incubated for 6 h at 25 ^{0}C before reading. Fluorescence polarization were recorded by using a TECAN infinite® M1000 multimode reader at 25 ^{0}C, excitation: 470nm, emission: 530nm, z-position: 23,580μm. The data was fitted by using nonlinear regression in GraphPad Prism 5, and the IC_{50} values were obtained from the dose response curves. All data are obtained as average values from triplicate samples, and the experiments were repeated twice [Lindsley *et al.,* 2008].

3.5.4. Western blot analysis

The A549 cells (2 x 10^6 cells) were incubated at 37 ^{0}C for 12 hr in 2 mL of RPMI containing 10% FBS and the corresponding concentrations of each test compounds. After incubation, the cells were washed three times with PBS, dipped in 150 mL of ice-cold lysis buffer (20 mM HEPES, pH 7.4, 1% Triton-X 100, 10% glycerol, 1M sodium fluoride,

2.5mM *p*-nitrophenylene phosphate, 10 mg/mL of phenylmethylsulfonylfluoride, 1mM Na_3VO_4, 5mg/ mL of leupeptin, and 1mM EDTA) for 15 min, and disrupted with a Sonic Disrupter (UR-20P, TOMY). The lysis buffer containing the disrupted cells was centrifuged at 13,000 x g and 37 ^{0}C for 20 min. The supernatant fraction obtained was boiled for 5 min in 3 x sample buffer (50 mM Tris, pH 7.4, 4% SDS, 10% glycerol, 4% 2-mercaptoethanol, and 0.05 mg/mL of bromophenol blue) at a ratio of 2:1 (v/v), loaded on an acrylamide gel (8 or 10%) and subjected to electrophoresis (150 min at 125 V). The antibody for NF-κB and phospho-GSK3β(S9), was purchased from Santa Cruz Biotechnology and Cell Signalling Technologies respectively and Western blotting was carried out as described previously [Ban *et al.,* 2002]. The levels of each protein were quantified by scanning densitometry, and the individual band density value for each point was expressed as the relative density signal.

3.5.5. Docking analysis

The 2D structures of the compounds were constructed using ACD/ChemSketch 11.0 and prepared by using UCSF Chimera-1.6.1 [Pettersen *et al.,* 2004]. The 3D crystal structure of the nuclear factor kappa-B (NF-κB) P50 homodimer (PDB ID: 1NFK), structure of the NF-kappa B p50.p65 heterodimer bound to the interferon β-κB site (PDB ID: 1LE9) was obtained from the RCSB protein data bank (http://www.pdb.org). Automated molecular docking was performed to find out molecular interaction and optimized geometry by using docking software AutoDock 4.2. On the basis of Lamarckian genetic algorithm principle [Cosconati *et al.,* 2010] all docking parameters were set to default values.

3.6. Anti-melanoma activity and apoptotic studies of 2-(3-phenylprop-2-en-1-ylidene)-22β-hydroxy-3-oxoolean-12-en-28-oic acid (93)

3.6.1. *In-vitro* antitumor activity

3.6.1.1. Cell culture and cytotoxicity assay

The African green monkey kidney fibroblast (VERO) cells were grown in RPMI medium supplemented with 10% fetal bovine serum and 1% penicillin-streptomycin (Gibco, Invitrogen, USA). For assay, phenol red-free RPMI medium (Sigma-Aldrich, USA) supplemented with 5% fetal bovine serum and 1% penicillin-streptomycin was

used. The B16F10 (mouse melanoma cell) were maintained in Dulbecco's modified Eagle's medium (DMEM) supplemented with 10% fetal bovine serum (Hyclone Laboratories, Logan, USA), 100 U/ml penicillin (Sigma) and 100 µg/ml streptomycin (Sigma).

3.6.1.2. Morphology assessment

The B16F10 cells (1×10^5 cells/well) were seeded in 6-well plates and after 24 h of incubation; the cells were treated with different concentrations of compound **93** for 24 h. Then cells were then washed with PBS, fixed with 70% ethanol for 15 min and then washed with PBS. The cells were stained with DAPI (1 µg/ml) for 15 min, washed with PBS again, and then observed under a fluorescence microscope equipped with a Cool SNAP-Pro color digital camera.

3.6.1.3. DNA fragmentation assay

B16F10 cells were incubated with 0, 5 and 10µM of **93** for 24 h at 37 °C. DNA fragmentation was analyzed by electrophoresis as described earlier [Smith *et al.,* 1989]. Briefly, after exposure to trypsin, the cells (10^7 cells per sample) were washed with Tris-buffered saline (TBS) buffer (pH 7.6) and collected by centrifugation at 1000 *g* for 10 minutes. The pellet was re-suspended for 2 h at 50 °C in a lysing solution made up of 10 mM Tris-HCl (500 µL, pH 8.0), 150 mM NaCl, 10 mM ethylenediamine tetraacetic acid (EDTA, edetic acid), 0.4% sodium dodecyl sulfate (SDS) and 100 µg/ml proteinase K. The lysate was then extracted with equal volumes of phenol/ $CHCl_3$/ isoamyl alcohol (25:24:01). The DNA was precipitated with ethanol (EtOH), air-dried and dissolved in TE buffer (5mM Tris-HCl (pH 8.0) and 20 mM eidetic acid containing RNase A [0.1 mg/ml, Sigma]). The samples were run in agarose gel containing ethidium bromide (0.5 µg/ml) and were visualized under ultraviolet (UV) light.

3.6.1.4. Caspase-3 activity

Cells (1.5×10^6 cells/ml) were treated with compound **93** (at 5 and 10 µM) in 12-well plates for 24 h. Caspase-3 activity was measured using a Caspase-3 colorimetric assay kit (BioVision, USA). Briefly, compound **93** treated cells were washed with PBS, and were lysed with cell lysis buffer for 1 min on ice. Each cell lysate was centrifuged at 10000g for 1 min, and the supernatant was collected. After protein quantification using a DC protein assay kit (Bio-Rad Laboratories, USA), 50 µg protein was diluted to 50 µL with cell lysis

buffer and to that, 50 µL reaction buffer was added. The absorbance of each sample mixture was measured at 400 nm. Finally, 5 µL 4 mM DEVD-pNA (caspase-3 substrate) was added to the mixture and incubated at 37 °C for 1 h. The absorbance of the final reaction mixture was measured at the same wavelength.

3.6.1.5. Western blot analysis

The B16F10 cells (2 x 10^6 cells) were incubated at 37 ^{0}C for 12 hr in 2 mL of DMEM containing 10% FBS and the corresponding concentrations of test compound**.** After incubation, the cells were washed three times with PBS, dipped in 150 mL of ice-cold lysis buffer (20 mM HEPES, pH 7.4, 1% Triton-X 100, 10% glycerol, 1M sodium fluoride, 2.5mM *p*-nitrophenylene phosphate, 10 mg/mL of phenylmethylsulfonyl fluoride, 1mM Na_3VO_4, 5mg/ mL of leupeptin, and 1mM EDTA) for 15 min, and disrupted with a Sonic Disrupter (UR-20P, TOMY). The lysis buffer containing the disrupted cells was centrifuged at 13,000 x g and 37 ^{0}C for 20 min. The supernatant fraction obtained was boiled for 5 min in 3 x sample buffer (50 mM Tris, pH 7.4, 4% SDS, 10% glycerol, 4% 2-mercaptoethanol, and 0.05 mg/mL of bromophenol blue) at a ratio of 2:1 (v/v), loaded on an acrylamide gel (8 or 10%) and subjected to electrophoresis (150 min at 125 V). The antibody for NF-κB and c-jun, Bcl-2, Bax and caspase-3 was purchased from Santa Cruz Biotechnology and Cell Signalling Technologies respectively and Western blotting was carried out as described previously [Ban *et al.,* 2002]. The levels of each protein were quantified by scanning densitometry, and the individual band density value for each point was expressed as the relative density signal.

3.6.1.6. Flow cytometric analysis

The effects of compound **93** treatment on B16F10 cell cycle progression was determined by flow cytometric analysis. The DNA content was assessed by staining ethanol fixed cells with propidium iodide (PI). Briefly, the B16F10 cells were seeded in a 6 well plate at a density of 5× 10^5 cells per well and allowed to attach overnight. The cell growth medium was replaced with fresh medium dosed with various concentration of **93** or DMSO (control). After 24 h of incubation (37°C, 5% CO_2) the cells were harvested, washed twice with ice-cold PBS, fixed with 75% ethanol at 4 ^{0}C for 30 min, and then stained using a DNA staining kit with propidium iodide (Cycle Test Plus kit, Becton-Dickinson, San Jose, CA, USA). The DNA content at sub-G1, G1, S and G2/M phases was

then determined using a FACS Calibur (Becton-Dickinson, San Jose, CA, USA) and analyzed by Cell Quest software.

3.6.2. *In-vivo* antitumor activity

3.6.2.1. *In-vivo* anti-melanoma activity

B16F10 mouse melanoma cells were collected from cell cultures by trypsinization and then injected subcutaneously (1×10^6 cells) into the right flank region of C57BL/6 mice. After 24h of tumor induction, the mice were intraperitoneally injected with either olive oil vehicle alone (tumor control), 10mg/kg of **93** in olive oil or 5mg/kg cisplatin in PBS at 3 days intervals over 28 day treatment period. The length (A) and width (B) of the tumor from each mouse was measured every 3 days and the tumor volume was calculated using the formula, $V= AB^2/2$. After the treatment period, the animals were sacrificed and the tumors were removed and immediately weighed. The tumor inhibition ratio was calculated by the formula: inhibition ratio (%) = [(A-B)/A] × 100, whereby A was the average tumor weight of the negative control and B was the average tumor weight of the treated group. The death of each animal was recorded starting from the first day of tumor allograft. The percentage of surviving mice was determined at the designated time.

3.6.2.2. Liver enzymes quantification

To access the safety of compound **93** in animals, we evaluated a possible hepatotoxic effect, evaluating three enzymes associated with liver injury, the glutamic-oxalacetic transaminase (GOT), the glutamic pyruvic transaminase (ALT) and gamma glutamyl transferase (gamma-GT). The experimental procedure consists in a simple addition of the 50 µL of the serum sample to 1000 µL of commercial reagent for each tested enzyme [Stark *et al.,* 1986]. After 28 days of melanoma cells allograft and compound **93** treatments has started the blood was collect.

3.6.2.3. Effects on blood cells

The blood samples were collected after 28 days of tumor allograft from the axillary plexus of the animals in all experimental groups, which were used to perform blood and reticulocyte count, according to the techniques used in the Laboratory of Experimental Hematology of FCF/ USP [Fock *et al.,* 2008].

CHAPTER 4

RESULTS AND DISCUSSIONS

4.1. Synthesis and evaluation of C-2 arylidene congeners of lantadenes as anticancer agents

4.1.1. Extraction and isolation of lantadenes A & B

4.1.2. Synthesis of bioactive intermediates of lantadenes

4.1.3. Synthesis of C-2 arylidene congeners of lantadenes

4.1.4. *In-vitro* cytotoxicity and NCI's COMPARE analysis

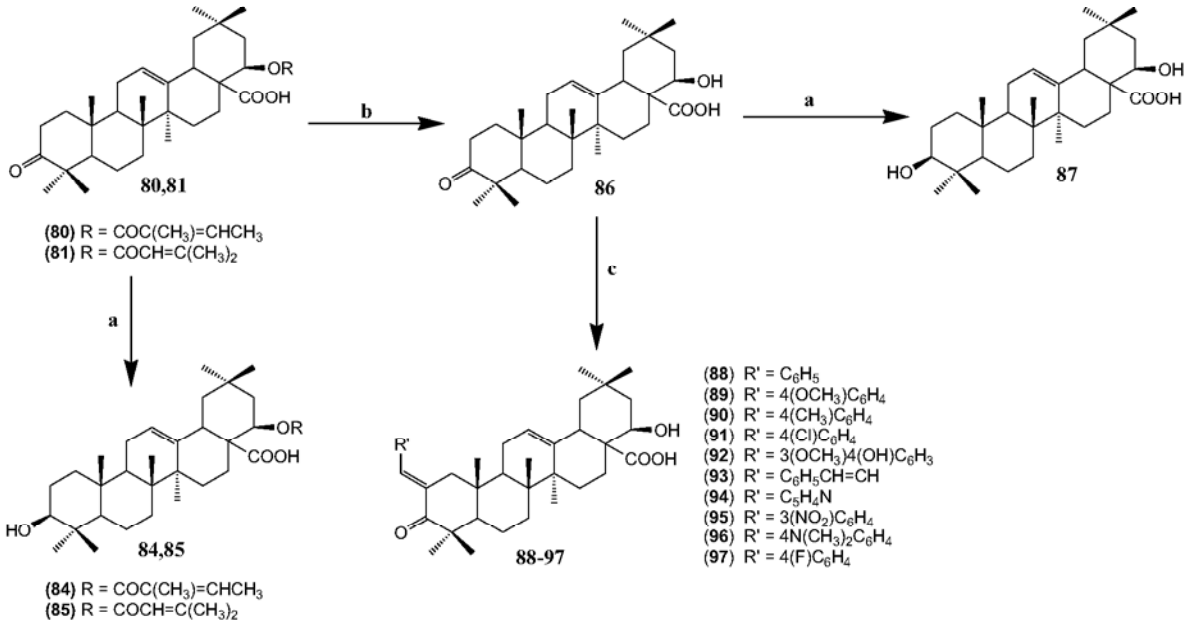

Scheme 1. (a) $NaBH_4$, CH_3OH/THF, r.t.; (b) KOH/CH_3OH, reflux; (c) R'CHO, KOH/CH_3OH, r.t.

4.1.1. Extraction and isolation of lantadenes A & B

The lantana leaves were dried in the shade and powdered. Lantana leaf powder was extracted with methanol and the extract obtained was treated with charcoal to remove the green pigments which gave golden yellow colored extract. The solvent was removed under reduced pressure and the residue was suspended in methanol-water (1:7) mixture and extracted with chloroform. The organic layer was dried over anhydrous sodium sulphate and the solvent was removed under reduced pressure. The solid residue obtained was recrystallized from methanol to obtain partially purified lantadenes as a white crystalline product. Partially purified lantadenes fraction was chromatographed on silica gel G column 100-200 mesh) using hexane-ethyl acetate (4:1) as the eluting solvent to obtain LA **80** and LB **81**.

The ESI-MS spectrum of **80** showed peak at m/z 551.3 (M-1) corresponding to the molecular formula $C_{35}H_{52}O_5$. Presence of keto and acid functionality was indicated by IR spectrum absorption bands at 1736.06 (C=O, keto) and 1702.14 cm^{-1} (C=O, acid). Seven tertiary methyl singlets (δ_H 1.17, 1.09, 1.05 x 2, 1.00, 0.85 and 0.82), δ_H 2.35-2.38 (m, 1H, C-2a-H), 2.51-2.60 (m, 1H, C-2b-H), 3.05 (d, *J* = 10.40 Hz, 1H, C-18-H), 5.38 (s, 1H, C-12-H) in the ^1H NMR spectrum and δ_C 122.49 (C-12), 143.10 (C-13), 179.29 (C-28), 217.72 (C-3) in the ^{13}C NMR spectrum revealed that it belongs to the oleanane series (pentacyclic triterpenoic acid). Presence of ester linkage with angeloyloxy group was characterized by absorption band at 1715.85 cm^{-1} (C=O, ester) in IR spectrum. The ^1H NMR showed a singlet at δ 5.09 for C-22α-H and quartet at δ_H 6.00 for C-3'-H. Similarly in ^{13}C NMR, the C-1', C-2' and C-3' were observed at δ_C 166.27, 127.59, 139.07 respectively. The presence of peak at m/z 469.3 by loss of $CH_3CH{=}CCH_3COOH$ confirmed the structure.

The ESI-MS spectrum of **81** showed peak at m/z 551.3 (M-1) corresponding to the molecular formula $C_{35}H_{52}O_5$. Presence of keto and acid functionality was indicated by IR spectrum absorption bands at 1738.61 (C=O, keto) and 1692.62 cm^{-1} (C=O, acid). Seven tertiary methyl singlets (δ_H 1.17, 1.09, 1.05 x 2, 1.00, 0.85 and 0.82), δ_H 2.35-2.39 (m, 1H, C-2a-H), 2.51-2.60 (m, 1H, C-2b-H), 3.02 (d, *J* = 9.96 Hz, 1H, C-18-H), 5.38 (s, 1H, C-12-H) in the ^1H NMR spectrum and δ_C 122.37 (C-12), 143.09 (C-13), 178.84 (C-28), 217.81 (C-3) in the ^{13}C NMR spectrum revealed that it belongs to the oleanane series (pentacyclic triterpenoic acid). Presence of ester linkage with dimethylacryloyloxy group was characterized by absorption band at 1712.29 cm^{-1} (C=O, ester) in IR spectrum. The ^1H NMR showed a singlet at δ_H 5.04 for C-22α-H and singlet at δ_H 5.55 for C-2'-H. Similarly in ^{13}C NMR, the C-1', C-2' and C-3' were observed at δ_C 165.32, 115.96, 165.32 respectively. The presence of peak at m/z 469.3 by loss of $(CH_3)_2C{=}CHCOOH$ confirmed the structure.

4.1.2. Synthesis of bioactive intermediates of lantadenes

4.1.2.1. Synthesis of reduced lantadene A (84) and reduced lantadene B (85)

One step reduction of LA and LB with $NaBH_4$ in CH_3OH: THF mixture (1:1) was done by stirring at room temperature to obtain corresponding reduced lantadene A **84**

(RLA) and reduced lantadene B **85** (RLB), respectively. The ESI-MS spectrum of **84** showed peak at m/z 553.4 (M-1) corresponding to the molecular formula $C_{35}H_{54}O_5$. Absence of 1736.06 cm^{-1} (C=O, keto) and δ_c 217.72 (C=O, C-3) while presence of δ_H 3.09 (t, *J* = 7.24 Hz, 1H, C-3α-H) and δ_C 79.12 (C-3β-OH) confirmed reduction process. Presence of 1717.87 cm^{-1} (ester, C=O) in IR spectrum, δ_H 4.99 (s, 1H, C-22α-H), 6.00 (q, *J* = 6.08 Hz, C-3'-H) in ^1H NMR spectrum, and δ_C 166.32 (C-1'), 127.68 (C-2'), 138.88 (C-3') in ^{13}C NMR spectrum indicated that $NaBH_4$ did not show any influence on C-22 angeloyloxy ester linkage and $\Delta^{2'}$ olefinic bond of LA. It was further confirmed by the presence of peak at m/z 471.3 by loss of $CH_3CH{=}CCH_3COOH$.

The ESI-MS spectrum of **85** showed peak at m/z 553.4 (M-1) corresponding to the molecular formula $C_{35}H_{54}O_5$. Absence of 1738.61 cm^{-1} (C=O, keto) and δ_C 217.81 (C=O, C-3) while presence of δ_H 3.15 (dd, *J* = 10.12, 2.96 Hz, 1H, C-3α-H) and δ_C 79.05 (C-3, Cβ-OH) confirmed the reduction process. Presence of 1717.98 cm^{-1} (C=O, ester) in IR spectrum, δ_H 4.96 (s, 1H, C-22α-H), 5.48 (s, 1H, C-3'-H) in ^1H NMR spectrum and δ_C 165.17 (C-1'), 115.99 (C-2'), 152.24 (C-3') in ^{13}C NMR spectrum indicated that $NaBH_4$ did not show any influence on C-22 dimethylacryloyloxy ester linkage and $\Delta^{2'}$ olefinic bond of LB. It was confirmed by presence of peak at m/z 471.3 by the loss of $(CH_3)_2C{=}CHCOOH$.

4.1.2.2. Synthesis of 22*β*-hydroxy-3-oxoolean-12-en-28-oic acid (86)

22*β*-Hydroxy-3-oxoolean-12-en-28-oic acid was obtained by the hydrolysis of partially purified lantadenes in ethanolic potassium hydroxide. The ESI-MS spectrum of **86** showed peak at m/z 469.3 (M-1) corresponding to the molecular formula $C_{30}H_{46}O_4$. It showed IR absorption bands at 3434 (O-H), 1701.98 cm^{-1} (C=O, acid). Absence of characteristic signals of angeloyloxy and dimethylacryloyloxy groups confirmed the cleavage of C-22 ester linkage. Presence of seven tertiary methyl singlets (δ_H 1.09, 1.05, 1.02, 0.99, 0.97, 0.83 and 0.78), δ_H 2.28-2.33 (m, 1H, C-2a-H), 2.44-2.51 (m, 1H, C-2b-H), 2.94 (dd, *J* = 16.72, 6.32 Hz, 1H, C-18-H), 3.85 (t, *J* = 3.24 Hz, 1H, C-22α-H), 5.29 (t, *J* = 3.44 Hz, 1H, C-12-H) in ^1H NMR spectrum and δ_C 122.41 (C-12), 143.28 (C-13), 180.70 (C-28) in ^{13}C NMR spectrum indicated that hydrolytic cleavage did not influence oleanane framework.

4.1.2.3. Synthesis of 3*β*,22*β*-dihydroxy-3-oxoolean-12-en-28-oic acid (87)

One step reduction of 22*β*-hydroxy-3-oxoolean-12-en-28-oic acid **86** with $NaBH_4$ in CH_3OH: THF mixture (1:1) was done by stirring at room temperature to obtain 3*β*,22*β*-dihydroxy-3-oxoolean-12-en-28-oic acid **87**. The ESI-MS spectrum of **87** showed peak at m/z 471.3 (M-1) corresponding to the molecular formula $C_{30}H_{48}O_4$. It showed IR absorption bands at 3446 (O-H) and 1701.98 cm^{-1} (C=O, acid). Presence of seven tertiary methyl singlets (δ_H 1.24, 1.10, 1.07, 0.93, 0.89, 0.85 and 0.73), δ_H 2.94 (dd, *J* = 16.72, 6.32 Hz, 1H, C-18-H), 3.07 (t, *J* = 6.48 Hz, 1H, C-3α-H), 3.07 (t, *J* = 6.48 Hz, 1H, C-3α-H), 3.58 (s, 2H, C-3β-OH and C-22α-H), 4.02 (br s, 1H, C-22β-OH), 5.23 (s, olefinic-H, C-12-H) in ^1H NMR spectrum and δ_C 120.99 (C-12), 143.78 (C-13), 176.30 (C-28) in ^{13}C NMR spectrum indicated that generation of C-3β-OH and hydrolytic cleavage did not influence oleanane framework. Physical properties of LA, LB and congeners are listed in Table 4.1. IR, ^1H NMR and ^{13}C NMR spectrum data of these compounds are listed in Table 4.2, 4.3 and 4.4, respectively.

Table 4.1 Physical properties of lantadenes and bioactive intermediates.

Compound name	TLC (R_f)	mp. (^0C)	Yield (%)
22*β*-[(2-methyl-1-oxo-2-butenyl)oxy]-3-oxoolean-12-en-28-oic acid **80**	0.63*	285-286	52
22*β*-[(3-methyl-1-oxo-2-butenyl)oxy]-3-oxyolean-12-en-28-oic acid **81**	0.61*	283-284	39
22*β*-[(2-methyl-1-oxo-2-butenyl)oxy]-3*β*-hydroxyolean-12-en-28-oic acid **84**	0.58*	278-279	83.7
22*β*-[(3-methyl-1-oxo-2-butenyl)oxy]-3*β*-hydroxyolean-2-en-28-oic acid **85**	0.56*	276-277	79.8
22*β*-hydroxy-3-oxoolean-12-en-28-oic acid **86**	0.35**	234-236	63.9
3*β*,22*β*-dihydroxy-3-oxoolean-12-en-28-oic acid **87**	0.32**	210-212	70.7

(* Hexane: Ethyl acetate :: 4:1; ** Hexane: Ethyl acetate :: 1:1)

Table 4.2 IR spectral data (cm^{-1}) of lantadenes and bioactive intermediates.

Code	O-H	C-H aliphatic	C=O, C-3 keto	C=O, ester
80	-	2952	1702	1715
81	-	2950	1692	1712
84	3482	2948	-	1717
85	3480	2949	-	1717
86	3434	2946	1703	-
87	3446	2948	-	-

Table 4.3 ^{1}H NMR spectral data (δ) of lantadenes and bioactive intermediates.

Code	C-12-H	C-22α-H	C-18-H	C-3α-H	Tertiary methyl proton(s)
80	5.38	5.09	3.05	-	1.17, 1.09, 1.05 (2), 1.00, 0.85, 0.82
81	5.37	5.04	3.02	-	1.17, 1.09, 1.05 (2), 1.00, 0.88, 0.83
84	5.31	4.99	3.00	3.09	1.16, 0.99, 0.94, 0.89 (2), 0.80, 0.73
85	5.29	4.96	2.94	3.15	1.09, 0.93 (2), 0.85, 0.81, 0.71 (2)
86	5.29	3.85	2.94	-	1.09, 1.05, 1.02, 0.99, 0.97, 0.83, 0.78
87	5.23	4.00	2.94	3.07	1.24, 1.10, 1.07, 0.93, 0.89, 0.85, 0.73

Table 4.4 ^{13}C NMR spectral data (δ) of lantadenes and bioactive intermediates.

Carbon no.	**80**	**81**	**84**	**85**	**86**	**87**
1	37.32	38.54	38.74	38.75	39.28	38.09
2	34.14	33.75	37.04	33.77	34.16	27.04
3	217.72	217.81	79.12	79.05	217.84	77.20
4	38.45	39.16	46.02	38.75	47.44	38.29
5	55.29	55.30	55.17	55.18	55.30	54.79
6	21.48	21.50	20.60	19.20	19.54	17.89
7	30.19	32.26	32.60	30.57	32.22	32.41
8	39.21	39.24	38.74	39.24	39.15	40.23
9	50.59	50.57	47.62	50.52	46.90	51.02

Table 4.4 cont.

Carbon No.	**80**	**81**	**84**	**85**	**86**	**87**
10	36.78	37.63	37.69	38.44	36.79	37.91
11	24.19	25.77	24.21	25.89	24.32	23.89
12	122.49	122.37	122.64	122.85	122.41	120.99
13	143.10	143.09	143.11	143.05	143.28	143.78
14	45.94	45.97	39.21	46.03	42.13	41.62
15	26.44	27.46	28.10	27.47	27.80	27.31
16	23.51	24.13	25.90	25.89	23.56	22.89
15	26.44	27.46	28.10	27.47	27.80	27.31
16	23.51	24.13	25.90	25.89	23.56	22.89
17	46.88	46.87	50.55	47.63	52.32	46.03
18	41.99	42.07	38.40	41.92	41.23	41.09
19	47.45	47.45	41.86	50.52	46.02	47.09
20	30.05	30.07	30.04	30.07	30.15	29.78
21	33.69	36.77	38.31	37.04	38.00	36.52
22	75.84	75.20	76.20	75.00	74.34	72.72
23	27.56	27.59	27.56	28.10	26.48	27.93
24	16.84	16.85	17.01	16.97	21.48	15.60
25	15.67	15.16	15.18	15.59	15.13	15.01
26	19.48	19.52	18.23	18.26	16.93	16.67
27	26.14	26.44	27.13	27.16	25.75	26.79
28	179.28	178.84	179.66	177.10	180.70	176.30
29	32.19	34.16	33.72	31.01	33.88	33.70
30	25.79	26.28	26.17	26.30	27.16	25.37
C1’	166.26	165.32	166.32	165.17	-	-
C2’	127.58	115.96	127.68	115.99	-	-
C3’	139.06	157.15	138.88	152.24	-	-
C4’	15.10	20.25	15.00	20.24	-	-
C5’	20.58	23.56	23.43	24.12	-	-

4.1.3. Synthesis of C-2 arylidene congeners of lantadenes (88-97)

The sequence steps involved in the synthesis of C-2 arylidene congeners of 22*β*-hydroxy-3-oxoolean-12-en-28-oic acid **86** is described in Scheme 1. Claisen-Schmidt reaction of **86** with several requisite aldehydes were done under mild basic conditions at room temperature. The reaction mixture after processing and column chromatography gave desired compounds **88-97**. The characteristic IR spectrum band of O-H stretch were in the range of 3662-3224 cm^{-1}, C-H aliphatic stretch were in the range of 2998-2946 cm^{-1} and *α,β*-unsaturated carbonyl functionality were observed in the range of 1691-1627 cm^{-1} and are listed in Table 4.6. The ^{1}H NMR spectra of these compounds showed signals for seven tertiary methyl protons in the range of δ_H 0.78-1.25. Signals of methine bridge protons appeared in the range of δ_H 6.85-7.55 as singlet (s) or double-doublet (dd). The C-12-H olefinic proton appeared as either singlet or triplet in range of δ_H 5.24-5.44, while remaining other important characteristic protons are represented in Table 4.7. The ^{13}C NMR chemical shift value of all carbon atoms are listed in Table 4.8.

Table 4.5 Physical properties of C-2 arylidene congeners of lantadenes (88-97).

Compound name	TLC (R_f)	mp. (^0C)	Yield %)
2-Benzylidene-22*β*-hydroxy-3-oxoolean-12-en-28-oic acid **88**	0.39*	152-154	71.2
2-(4-Methoxybenzylidene)-22*β*-hydroxy-3-oxoolean-12-en-28-oic acid **89**	0.37*	188-191	65.8
2-(4-Methylbenzylidene)-22*β*-hydroxy-3-oxoolean-12-en-28-oic acid **90**	0.38*	165-167	81.4
2-(4-Chlorobenzylidene)-22*β*-hydroxy-3-oxoolean-12-en-28-oic acid **91**	0.37*	132-134	67.8
2-(4-Hydroxy-3-methoxybenzylidene)-22*β*-hydroxy-3-oxoolean-12-en-28-oic acid **92**	0.24*	147-149	74.6
2-(3-Phenylprop-2-en-1-ylidene)-22*β*-hydroxy-3-oxoolean-12-en-28-oic acid **93**	0.39*	90-92	86.7
2-(4-Dimethylaminobenzylidene)-22*β*-hydroxy-3-oxoolean-12-en-28-oic acid **94**	0.31*	175-177	70.6

Table 4.5 cont.

Compound name	TLC (R_f)	mp. (^{0}C)	Yield %)
2-(Pyridine-4-ylmethylidene)-22*β*-hydroxy-3-oxoolean-12-en-28-oic acid **95**	0.18*	123-125	64.7
2-(3-Nitrobenzylidene)-22*β*-hydroxy-3-oxoolean-12-en-28-oic acid **96**	0.12*	142-144	62.1
2-(4-Fluorobenzylidene)-22*β*-hydroxy-3-oxoolean-12-en-28-oic acid **97**	0.37*	159-161	74.4

(* Hexane: Ethyl acetate :: 1:1)

Table 4.6 IR spectral data (cm^{-1}) of C-2 arylidene congeners of lantadenes (88-97).

Code	O-H	C-H aliphatic	C=O, C-3 keto
88	3525	2952	1671
89	3501	2951	1688
90	3473	2949	1675
91	3224	2946	1627
92	3437	2969	1691
93	3662	2998	1686
94	3456	2998	1668
95	3479	2948	1667
96	3376	2948	1667
97	3529	2949	1672

Table 4.7 ^{1}H NMR spectral data (δ) of C-2 arylidene congeners of lantadenes (88-97).

Code	C-12-H	C-22α-H	C-18-H	C-3α-H	Tertiary methyl proton(s)
88	7.53	5.39	3.92	3.02	1.21, 1.18, 1.14, 1.12, 0.90, 0.87, 0.85
89	7.44	5.33	3.85	2.93	1.14, 1.10, 1.05 (2), 0.83, 0.78 (2)
90	7.42	5.34	3.81	2.99	1.21, 1.14, 1.12 (2), 0.88 (2), 0.85
91	7.19	5.34	3.87	2.97	1.18, 1.14, 1.10, 1.06, 0.84, 0.79 (2)
92	7.48	5.39	3.92	3.02	1.21, 1.17, 1.13, 1.08, 0.91, 0.89, 0.85
93	6.93 (2), 7. 25 (1)	5.44	3.93	3.05	1.25, 1.20, 1.15 (2), 1.14, 0.97, 0.94
94	7.46	5.34	3.86	2.98	1.14, 1.10, 1.05 (2), 0.83, 0.80, 0.79
95	6.85	5.26	3.73	2.93	1.10, 1.08, 1.04, 0.99, 0.93, 0.84, 0.79
96	6.43	5.24	3.70	2.92	1.24, 1.17, 1.02 (2), 0.99, 0.81(2)
97	7.40	5.32	3.78	2.96	1.24, 1.13, 1.11 (2), 0.87(2), 0.85

Table 4.8 ^{13}C NMR spectral data (δ) of C-2 arylidene congeners of lantadenes (88-97).

Carbon no.	88	89	90	91	92	93	94	95
1	39.23	39.20	38.65	39.30	38.12	39.19	38.21	38.4
2	137.59	137.48	138.21	140.24	137.59	136.68	138.65	156
3	207.92	207.83	207.09	207.74	207.70	207.33	207.59	203
4	41.29	41.20	41.03	41.30	39.20	41.22	40.23	41.0
5	53.00	52.82	52.19	52.95	52.34	53.06	52.75	52.4
6	22.70	22.63	20.94	22.64	22.64	22.63	22.66	21.2
7	31.90	31.87	31.45	31.85	30.18	31.94	31.92	31.9
8	42.35	42.32	41.89	42.32	41.28	42.33	41.25	41.3
9	52.42	52.40	51.18	52.39	46.10	52.42	52.44	51.1
10	38.18	38.18	38.13	38.20	36.26	38.24	37.09	38.1
11	24.38	24.34	23.87	25.64	24.35	24.36	25.73	27.0
12	122.44	122.36	120.81	122.33	122.34	122.38	122.51	120
13	143.14	143.48	143.76	143.38	143.43	143.42	143.49	144
14	45.20	45.01	44.44	45.19	44.27	45.08	44.85	43.8
15	27.82	27.80	27.28	27.77	27.78	27.79	27.83	27.8

Table 4.8 cont.

Carbon no.	88	89	90	91	92	93	94	95
16	23.78	23.79	22.23	23.74	23.75	23.76	23.84	23.8
17	45.44	45.47	44.76	45.39	45.06	45.35	45.59	43.8
18	44.21	44.39	43.61	44.13	42.28	42.42	42.35	42.0
19	46.14	46.14	45.92	46.07	45.55	46.11	46.19	45.7
20	30.22	30.19	29.76	30.17	29.83	30.19	30.22	29.7
21	36.32	36.20	35.66	36.29	33.89	36.07	36.14	35.4
22	74.36	74.31	72.76	74.35	74.33	74.33	74.34	72.6
23	29.83	29.93	29.28	29.72	29.69	29.64	30.11	29.7
24	16.59	16.56	16.19	16.43	16.52	16.61	15.46	18.5
25	15.40	15.41	14.88	15.37	15.41	15.50	16.59	17.0
26	20.36	20.35	19.84	20.30	20.34	20.29	20.42	18.7
27	27.20	27.19	26.98	27.16	27.16	27.20	27.23	27.2
28	180.74	180.85	176.47	180.88	180.36	180.74	180.98	180
29	33.93	33.91	33.61	33.87	31.83	33.90	33.95	33.6

Table 4.8 cont.

Carbon no.	88	89	90	91	92	93	94	95
30	25.71	25.68	23.11	24.35	25.68	25.64	24.41	25.2
Ar-R^1	-	-	-	-	-	-	-	-
Ar-R^2	-	55.35 (OCH_3)	25.10 (CH_3)	-	55.98 (OCH_3)	-	39.31 (NCH_3) 39.24 (NCH_3)	-
Ar-R^3	-	-	-	-	-	-	-	-
Ar-C	135.95	132.33	132.43	136.17	131.91	132.76	132.62	132
Ar-C-C	-	-	-	-	-	123.37	-	-
Ar-C-C-C	-	-	-	-	-	140.66	-	-
C1''	133.67	128.61	132.38	134.18	128.85	137.25	123.97	148
C2''	128.49	132.33	128.80	128.70	110.86	127.15	132.62	123
C3''	130.47	113.96	129.96	131.57	149.51	128.84	111.78	149
C4''	128.59	159.88	136.68	134.32	148.64	128.79	150.40	-
C5''	130.47	113.96	129.96	128.86	114.09	128.82	111.78	149
C6''	128.49	131.44	128.80	127.84	123.47	127.13	128.94	123

4.1.4. *In-vitro* cytotoxicity and NCI's COMPARE analysis

Lantadenes and congeners **80**, **81**, **84-87**, **92** and **93** were selected by National Cancer Institute, Bethesda, Maryland, USA for evaluation of *in vitro* anticancer activity. In first stage, they were evaluated at a single high dose concentration (10 μM) on a panel of 60 human tumor cell lines. Results were reported as mean-graph of the percentage growth of the treated human cancer cells, and presented as percentage growth inhibition (GI %), and are illustrated in Table 4.9. Results indicated that compound **84** showed lethality against leukemia cell HL-60 (TB), non-small cell lung cancer cells HOP-92, NCI-H322M, CNS cancer cells SF-295, SNB-19, melanoma UACC-62, renal cancer cell 786-0, A498, UO-31 and breast cancer cell HS 578T, while compound **80** showed lethality against leukemia cell HL-60 (TB) at 10 μM concentration.

In second stage, compounds **80**, **81**, **84**, **85** and **93** were further evaluated at 10-fold dilutions of five concentrations (0.01-100 μM) on same 60 human tumor cell lines panels. *In vitro* anticancer activity of compounds **80**, **81**, **84**, **85** and **93** were compared with NCI standard anticancer agents Cisplatin (CDDP, NSC 119875), and results are illustrated in Table 4.10. Mean graph mid point (MG_MID) value of compound **84** (MG_MID -5.69) was higher than standard cisplatin (MG_MID -5.66), while compound **93** (MG_MID -5.52) was comparable to cisplatin. Cytotoxic potential of compounds were observed in order of **84** > **93** > **81** > **80** > **85** and GI_{50} value <5 μM for more than 80% cancer cell lines.

Among individual cell lines compound **80** was active against leukemia cell HL-60 (TB) (log GI_{50} -5.73), non-small cell lung cancer cell A594/ATCC (log GI_{50} -5.55), colon cancer cell COLO 205 (log GI_{50} -5.58), melanoma cell SK-MEL-5 (log GI_{50} -5.91), renal cancer cell RXF 393 (log GI_{50} -5.62), prostate cancer cell MDA-MB-468 (log GI_{50} -5.59); **81** against leukemia cell RPMI-8226 (log GI_{50} -5.83), non-small cell lung cancer cell A549/ATCC (log GI_{50} -6.10), colon cancer cell KM12 (log GI_{50} -6.06), CNS cancer cell SF-295 (log GI_{50} -5.77), melanoma cell SK-MEL-5 (log GI_{50} -5.82), renal cancer cell A498 (log GI_{50} -5.80), prostate cancer cell PC-3 (log GI_{50} -5.81), breast cancer cell MDA-MB-468 (log GI_{50} -5.64); **84** against leukemia cell RPMI-8226 (log GI_{50} -5.73), non-small cell lung cancer cell A549/ATCC (log GI_{50} -5.92), colon cancer cell KM12 (log GI_{50} -5.87), CNS cancer cell U251 (log GI_{50} -5.80), melanoma cell UACC-62 (log GI_{50} -5.81), ovarian cancer cell SK-OV-3 (log GI_{50} -5.73), renal cancer cell A498 (log GI_{50} -5.81),

prostate cancer cell PC-3 (log GI_{50} -5.87), breast cancer cell MDA-MB-231/ATCC (log GI_{50} -5.78); **85** against leukemia cell RPMI-8226 (log GI_{50} -5.61), non-small cell lung cancer cell A549/ATCC (log GI_{50} -6.36), colon cancer cell KM12 (log GI_{50} -6.06), CNS cancer cell SF-295 (log GI_{50} -5.84), melanoma cell UACC-62 (log GI_{50} -5.71), renal cancer cell RXF 393 (log GI_{50} -5.59), breast cancer cell HS 578T (log GI_{50} -5.52), and **93** against leukemia cells SR (log GI_{50} -5.61), MOLT-4 (log GI_{50} -5.61), non-small cell lung cancer cell HOP-92 (log GI_{50} -5.72), colon cancer cell COLO 205 (log GI_{50} -5.70), CNS cancer cell SF-295 (log GI_{50} -5.62), melanoma cell SK-MEL-5 (log GI_{50} -5.76), ovarian cancer cell OVCR-3 (log GI_{50} -5.69), renal cancer cell A498 (log GI_{50} -5.59), prostate cancer cell PC-3 (log GI_{50} -5.52), breast cancer cell MDA-MB-231/ATCC (log GI_{50} -5.69).

The structure activity relationship (SAR) revealed that: (1) anticancer activity of compounds **80**, **81**, **84-87**, **92** and **93** were sensitive to the nature of structural modification of 3-oxoolean-12-en-28-oic acid template; (2) 3-oxo reduction of compound **80** resulted in 3β-hydroxy-22β-(angeloyloxy)-olean-12-en-28-oic acid **84** with drastic change in mean percentage growth (60.54→ 28.66), mean $LogGI_{50}$ value (-5.37→ -5.69) and negative value of growth percent against various cancer cell lines indicated improvement in hydrophilicity enhances solubility and cytotoxicity of compound; (3) 3-oxo reduction of compound **81** and **87** to 3β-hydroxy-22β-(dimethylacryloyloxy)-olean-12-en-28-oic acid **85** and 3β,22β-dihydroxy-3-oxoolean-12-en-28-oic acid **86**, respectively did not show any significant change in growth percentage and mean $LogGI_{50}$; (4) cleavage of 22β-angeloyloxy and 22β-dimethylacryloyloxy side chain of compound **80** and **81**, respectively caused reduction in the growth percentage inhibition which indicates that side chains were also play a critical role in cytotoxicity; (5) integration of cinnamoyl functionality at C-2 position of compound **87** results in 2-(3-phenylprop-2-en-1-ylidene)-22β-hydroxy-3-oxoolean-12-en-28-oic acid **93** caused reduction in growth percentage from 90.58% to 58.19% and with mean $LogGI_{50}$ -5.52 M indicated the significance of cinnamoyl functionality and its role in Michel interaction; (6) integration of vanillyl functionality did not show any significant changes in growth percentage of human tumor cell lines. On the basis of logarithmic cytostatic parameter (GI_{50}), cytotoxic potential of compounds were obtain in sequence of **84** > **93** > **81** > **80** > **85**.

Table 4.9 Percentage growth inhibition (GI %) of *in-vitro* subpanel tumor cell lines at 10 μM concentration of compounds **80**, **81**, **84-87**, **92** and **93**. Bold values represent to point out the active compounds and lethal effect.

Cell lines	% Growth Inhibition (GI %)[a]							
	80	**81**	**84**	**85**	**86**	**87**	**92**	**93**
Leukemia								
CCRF-CEM	**56.40**	**74.67**	**54.21**	**72.64**	12.46	11.64	17.96	**80.09**
HL-60 (TB)	**L**	**89.76**	**L**	**86.02**	24.82	18.04	28.86	**61.24**
K-562	**55.90**	**55.01**	**64.14**	**54.76**	23.17	-	28.80	**67.64**
MOLT-4	**56.72**	**63.45**	**58.56**	**50.42**	21.30	21.73	36.67	**55.56**
RPMI-8226	**83.35**	**80.42**	**78.90**	**76.29**	29.81	10.67	40.48	**84.39**
SR	30.53	47.89	38.09	29.79	16.32	21.99	12.89	37.37
Non-small cell lung cancer								
A549/ATCC	**60.79**	**77.84**	**72.64**	**76.49**	20.99	12.45	28.25	**77.32**
EKVX	**50.67**	**58.78**	**63.50**	**52.31**	-	-	11.52	**60.64**
HOP-62	24.36	39.78	**75.67**	46.27	11.34	-	-	37.19
HOP-92	**56.26**	**71.59**	**L**	**57.05**	24.63	-	29.14	**50.77**
NCI-H226	18.04	21.76	**57.93**	21.31	-	-	-	27.72
NCI-H23	42.01	46.63	35.29	36.63	-	-	15.01	40.31
NCI-H322M	31.45	46.00	**L**	40.27	-	-	-	28.14
NCI-H460	48.51	**52.93**	**64.87**	49.73	-	-	-	**54.23**
NCI-H522	33.92	42.69	**50.27**	32.35	19.11	-	19.16	**52.27**
Colon cancer								
COLO 205		21.99	28.97	**71.77**	31.89	-	-	-
HCC-2998		38.65	47.18	**73.62**	37.96	-	-	-

Table 4.9 cont.

Cell lines	% Growth Inhibition (GI%)[a]							
	80	**81**	**84**	**85**	**86**	**87**	**92**	**93**
HCT-116	**66.02**	**73.42**	**80.02**	**72.81**	21.16	17.27	15.23	**82.51**
HCT-15	**69.79**	**81.38**	**78.81**	**74.92**	24.64	-	23.53	**64.83**
HT29	32.08	42.71	44.25	**50.66**	16.81	-	14.48	48.26
KM12	**59.99**	**69.61**	**78.26**	**65.67**	12.3	-	16.00	**68.16**
SW-620	31.30	37.26	**60.88**	33.12	-	-	-	44.23
CNS cancer								
SF-268	25.94	27.00	**74.06**	-	-	-	-	29.31
SF-295	**72.35**	nt	**L**	**55.41**	19.34	-	23.49	**76.48**
SF-539	21.79	35.03	**57.01**	45.29	-	-	-	-
SNB-19	40.65	42.68	**L**	14.36	-	-	-	26.64
SNB-75	13.06	30.01	**88.05**	26.82	-	-	17.89	27.91
U251	39.85	**61.76**	**61.79**	**60.75**	10.82	-	15.26	**66.40**
Melanoma								
LOX IMVI	38.22	48.76	**57.26**	46.77	-	11.05	11.59	38.61
MALME-3M	19.56	14.63	**64.77**	-	12.88	-	18.88	15.46
M14	36.25	19.70	**71.32**	-	-	-	-	27.10
MDA-MB-435	12.21	10.42	35.09	-	-	-	-	27.69
SK-MEL-2	22.91	21.82	45.91	13.50	-	-	-	35.43
SK-MEL-28	17.30	-	**66.33**	11.74	-	-	-	25.80
SK-MEL-5	**61.27**	**52.07**	46.77	38.48	12.22	-	11.89	26.30
UACC-257	29.98	26.09	39.42	-	-	-	-	38.02

Table 4.9 cont.

Cell lines	% Growth Inhibition (GI %)[a]							
	80	**81**	**84**	**85**	**86**	**87**	**92**	**93**
UACC-62	**50.14**	42.17	**L**	32.76	19.53	11.79	25.02	49.63
Ovarian cancer								
IGROV1	28.38	37.70	**64.87**	21.68	-	-	-	39.16
OVCAR-3	37.42	38.67	**68.01**	26.09	-	-	-	42.66
OVCAR-4	23.06	28.74	36.77	29.29	14.10	-	16.19	45.79
OVCAR-5	-	-	36.05	-	-	-	-	-
OVCAR-8	36.32	44.91	42.32	40.14	19.22	-	20.23	**57.02**
NCI/ADR-RES	26.94	40.02	30.16	45.45	-	-	-	23.78
SK-OV-3	-	-	**58.16**	10.56	-	-	-	14.32
Renal cancer								
786-0	**55.55**	**55.87**	**L**	38.24	13.77	13.77	-	21.9
A498	23.78	-	L	-	-	-	-	-
ACHN	46.11	**56.08**	**91.88**	**53.67**	-	-	14.39	**58.10**
CAKI-1	**51.60**	**53.16**	**70.54**	**64.44**	15.18	15.18	21.23	**57.05**
RXF 393	11.53	15.43	**77.23**	14.79	-	-	-	15.94
SN12C	47.63	57.37	**94.23**	49.15	16.65	16.65	12.51	**54.48**
TK-10	16.66	21.94	33.2	20.06	-	-	-	11.67
UO-31	**57.36**	**57.97**	**L**	39.14	13.87	13.87	24.08	**59.71**
Prostate cancer								
PC-3	**62.84**	**63.13**	**66.72**	**54.58**	40.74	23.53	27.82	**58.49**
DU-145	17.41	25.55	25.06	13.41	-	-	-	28.78

Table 4.9 cont.

Cell lines	% Growth Inhibition (GI %)[a]							
	80	**81**	**84**	**85**	**86**	**87**	**92**	**93**
Breast cancer								
MCF7	45.3	**50.68**	38.99	37.29	18.61	-	22.54	**66.18**
MDA-MB-31/ATCC	24.29	28.53	**77.76**	18.66	-	-	-	31.11
HS 578T	21.21	20.43	**L**	14.52	-	-	-	41.62
BT-549	**55.97**	30.39	**73.91**	21.94	10.12	-	-	30.00
T-47D	36.10	38.39	24.30	13.31	19.16	-	18.86	**62.39**
MDA-MB-468	49.18	35.79	33.91	-	-	**88.76**	-	27.39

[a] -, GI <10%; nt, not tested; L, compound proved lethal to the cancer cell line.

Table 4.10 *In-vitro* anticancer activity of compounds **80**, **81**, **84**, **85** and **93** against NCI's 60 human cancer cell lines and comparison with standard cisplatin.

Cell lines	Compound/ growth inhibitory activity (log GI_{50})					
	80	**81**	**84**	**85**	**93**	Cisplatin
Leukemia						
CCRF-CEM	-5.46	-5.67	-5.64	-5.55	-5.55	-5.60
HL-60 (TB)	-5.73	-5.66	-5.66	-5.60	-5.54	-5.74
K-562	-5.33	-5.46	-5.58	-5.47	-5.43	-5.60
MOLT-4	-5.48	-5.53	-5.69	-5.52	-5.61	-5.75
RPMI-8226	-5.70	-5.83	-5.73	-5.61	-5.59	-5.60
SR	-5.52	-5.43	-5.67	-6.30	-5.61	-6.49
Non-small cell lung cancer						
A549/ATCC	-5.55	-6.10	-5.92	-6.36	-5.55	-5.60

Table 4.10 cont.

Cell lines	Compound/ growth inhibitory activity (log GI_{50})					
	80	**81**	**84**	**85**	**93**	Cisplatin
HOP-62	-4.69	-5.03	-5.73	-5.13	-5.33	-5.60
HOP-92	-5.92	-5.77	-5.85	-5.82	-5.72	-5.72
NCI-H226	-5.33	-5.25	-5.77	-5.29	-5.56	-5.60
NCI-H23	-5.34	-5.40	-5.62	-5.14	-5.48	-5.93
NCI-H23	-5.34	-5.40	-5.62	-5.14	-5.48	-5.93
NCI-H322M	-5.40	-5.54	-5.75	-5.44	-5.46	-5.60
NCI-H460	-5.44	-5.66	-5.55	-5.51	-5.57	-5.82
NCI-H522	-5.49	-5.50	-5.66	-5.38	-5.61	-5.60
Colon cancer						
COLO 205	-5.58	-5.44	-5.68	-5.44	-5.70	-5.70
HCC-2998	-5.48	-5.52	-5.73	-5.43	-5.53	-5.60
HCT-116	-5.44	-5.63	-5.61	-5.57	-5.54	-5.60
HCT-15	-5.50	-5.89	-5.59	-5.81	-5.49	-5.60
HT29	-5.36	-5.40	-5.67	-5.37	-5.57	-5.60
KM12	-5.45	-6.06	-5.87	-6.06	-5.52	-5.60
SW-620						
CNS cancer						
SF-268	-5.22	-5.28	-5.22	-5.23	-5.47	-5.60
SF-295	-5.56	-5.77	-5.56	-5.84	-5.62	-5.67
SF-539	-5.19	-5.32	-5.19	-5.05	-5.54	-5.60
SNB-19	-5.33	-5.37	-5.33	-5.31	-5.39	-5.74
SNB-75	-4.85	-5.11	-4.85	-4.89	-5.37	-5.60
U251	-5.40	-5.54	-5.40	-5.58	-5.59	-5.60

Table 4.10 cont.

Cell lines	Compound/ growth inhibitory activity (log GI_{50})					
	80	**81**	**84**	**85**	**93**	Cisplatin
LOX IMVI	-5.11	-5.20	-5.47	-5.04	-5.72	-5.71
MALME-3M	-5.10	-4.94	-5.74	-4.86	-5.59	-
M14	-5.34	-5.19	-5.74	-5.11	-5.43	-5.60
MDA-MB-435	-5.28	-5.21	-5.66	-4.92	-5.48	-5.60
Melanoma						
SK-MEL-28	-4.89	-4.93	-5.72	-5.31	-5.36	-5.60
SK-MEL-5	-5.91	-5.82	-5.75	-5.54	-5.76	-5.60
UACC-257	-5.32	-5.30	-5.67	-4.84	-5.58	-5.60
UACC-62	-5.76	-5.61	-5.73	-5.71	-5.75	-5.60
Ovarian cancer						
IGROV1	-5.17	-5.27	-5.64	-5.20	-5.38	-5.67
OVCAR-3	-5.23	-5.39	-5.71	-5.15	-5.69	-5.60
OVCAR-4	-5.25	-5.30	-5.75	-5.07	-5.41	-5.60
OVCAR-5	-4.74	-5.18	-5.47	-4.80	-5.53	-5.60
OVCAR-8	-5.30	-5.42	-5.72	-5.33	-5.47	-5.60
NCI/ADR-RES	-5.29	-5.43	-5.66	-5.23	-5.48	-5.60
SK-OV-3	-4.74	-4.78	-5.73	-4.89	-5.42	-5.60
Renal cancer						
786-0	-5.46	-5.43	-5.74	-5.51	-5.46	-5.60
A498	-5.69	-5.80	-5.81	-5.55	-5.59	-5.60
ACHN	-5.31	-5.52	-5.74	-5.53	-5.44	-5.65
CAKI-1	-5.41	-5.42	-5.61	-5.47	-5.45	-5.97
RXF 393	-5.62	-5.48	-5.75	-5.59	-5.58	-5.60

Table 4.10 cont.

Cell lines	Compound/ growth inhibitory activity (log GI_{50})					
	80	**81**	**84**	**85**	**93**	Cisplatin
SN12C	-5.46	-5.51	-5.79	-5.54	-5.54	-5.60
TK-10	-5.27	-5.15	-5.65	-4.97	-5.43	-5.60
UO-31	-5.46	-5.53	-5.78	-5.43	-5.47	-6.85
Prostate cancer						
PC-3	-5.60	-5.81	-5.87	-5.44	-5.52	-5.60
DU-145	-5.23	-5.29	-5.67	-5.11	-5.37	-5.60
Breast cancer						
MCF7	-5.44	-5.48	-5.51	-5.21	-5.49	-5.60
MDA-MB- 31/ATCC	-5.23	-5.39	-5.78	-5.34	-5.69	-5.60
HS 578T	-5.29	-5.38	-5.67	-5.52	-5.48	-5.60
BT-549	-5.33	-5.32	-5.71	-5.18	-5.42	-5.60
T-47D	-5.21	-5.29	-4.93	-4.78	-5.42	-5.60
MDA-MB-468	-5.59	-5.64	-5.77	-5.38	-5.48	-
MG-MID	**-5.37**	**-5.45**	**-5.69**	**-5.35**	**-5.52**	**-5.67**

[a] MG_MID = mean graph midpoint = arithmetical mean value for all tested cell lines.

NCI's COMPARE analyses of test compounds with various set of compounds were done to find out probable molecular mechanistic targets and results are illustrated in Table 4.11. Results indicated that compound **80** showed PCC $\geq$ 0.6 with target vector NSC S24819 (PCC = 0.648), S224124 (PCC = 0.623), NSC S623093 (PCC = 0.612), NSC S267712 (PCC = 0.607), NSC S627708 (PCC = 0.602), compound **81** with NSC S175636 (PCC = 0.782) and compound **93** with NSC S24819 (PCC = 0.648), NSC S623093 (PCC = 0.612), NSC S267712 (PCC = 0.607), NSC S627708 (PCC = 0.602). No molecular targets have been reported in literature for these target vectors. However, on the basis of *in vitro* cytotoxicity data, lantadenes along with cinnamoyl and vanillyl functionality integrated

congeners were further explored for selective cancer cytotoxicity and selective NF-κB and Akt inhibitory potential.

Table 4.11 NCI's COMPARE analysis for tested compounds[a]

Comp. No.	PCC	Target	Target vector NSC	No. of common cell lines	Target mechanism of action[b]
80	0.648	Peltatin B	S24819	46	-
80	0.623		S224124	44	-
80	0.612		S623093	48	-
80	0.607	Resibufogenin	S267712	46	-
80	0.602		S627708	41	-
81	0.782		S175636	43	-
93	0.648	Peltatin B	S24819	46	-
93	0.612		S623093	48	-
93	0.607	Resibufogenin	S267712	46	-
93	0.602		S627708	41	-

[a]Only correlations with PCC ≥ 0.6 were selected as significant.

[b]Putative mechanism of action were searched from literature sources.

4.2. Synthesis, selective cancer cytotoxicity and mechanistic studies of novel congeners of lantadenes

4.2.1. Synthesis of C-2 arylidene/aryl and C-22-acyloxy congeners of 22*β*-hydroxy-3-oxoolean-12-en-28-oic acid

4.2.2. Selective *in-vitro* cytotoxicity and molecular mechanistic studies

4.2.3. Docking analysis

4.2.1. Synthesis of C-2 arylidene/aryl and C-22-acyloxy congeners of 22*β*-hydroxy-3-oxoolean-12-en-28-oic acid

The sequence steps involved in the synthesis of novel congeners of lantadenes and site specific reduced congeners are described in Scheme 2. Claisen-Schmidt reaction between lantadenes **80**, **81** and **86** with several requisite aldehydes were done under mild basic conditions at room temperature. The reaction mixture after processing and column

chromatography gave desired compounds. The characteristic IR spectrum band of O-H stretch were observed in the range of 3662-3224 cm^{-1}, C-H aliphatic stretch at 2998-2944 cm^{-1} and α,β-unsaturated carbonyl functionality were showed in range of 1690-1640 cm^{-1} (Table 4.13). The ^{1}H NMR spectra of these compounds showed signals for seven tertiary methyl protons in the range of δ_H 0.77-1.25. Signals of methine bridge protons appeared in the range of δ_H 6.85-7.55 as singlet (s) or double-doublet (dd). The C-12-H olefinic proton appeared as either singlet or triplet in range of δ_H 5.24-5.44, while remaining other important characteristic protons are represented in Table 4.14. The ^{13}C NMR chemical shift value of all carbon atoms are listed in Table 4.15.

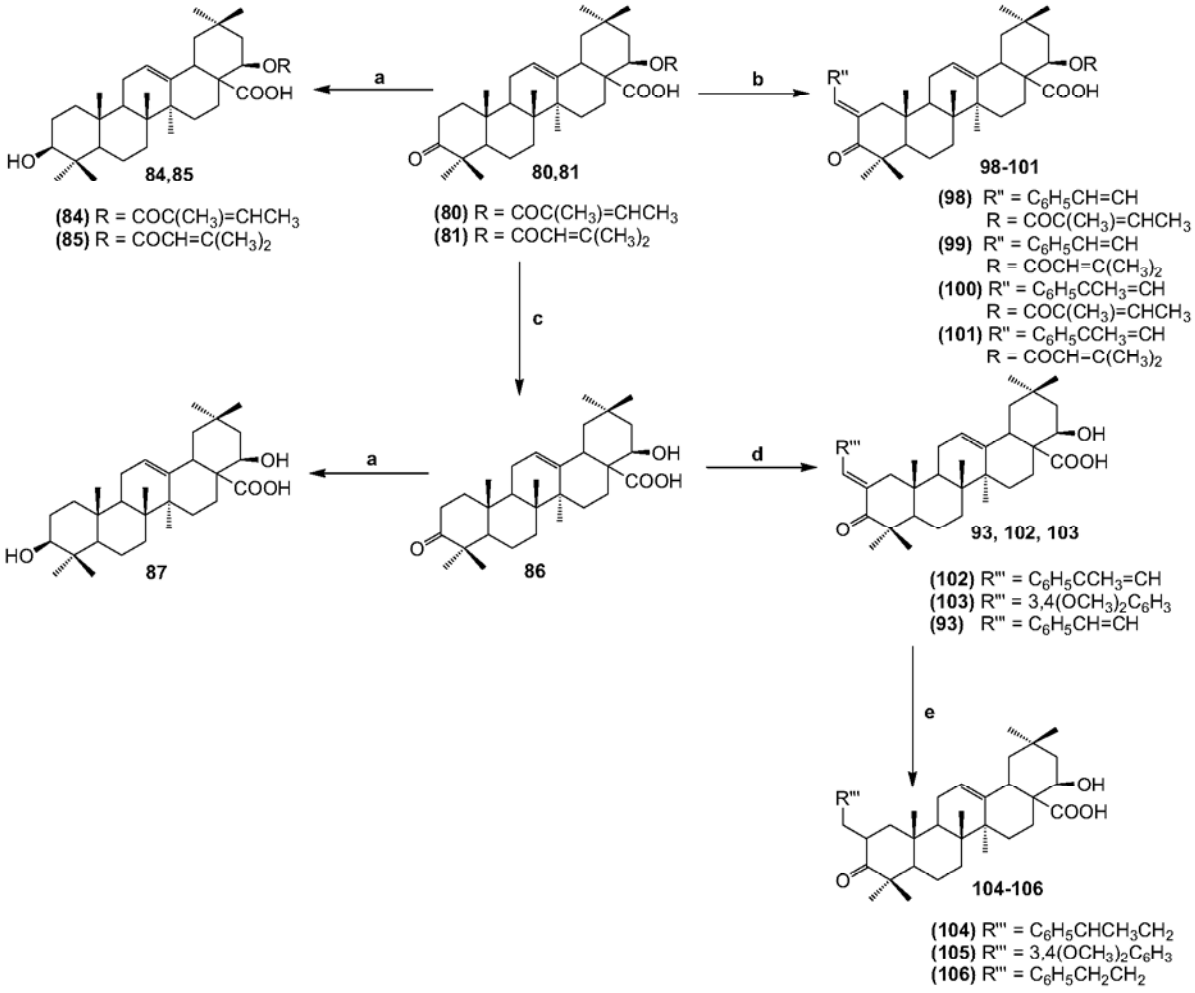

Scheme 2. (a) $NaBH_4$, CH_3OH/THF, r.t.; (b) R''CHO, KOH/CH_3OH, r.t.; (c) KOH/CH_3OH, reflux; (d) R'''CHO, KOH/CH_3OH, r.t.; (e) Pd/C, $HCOONH_4$, r.t.

Table 4.12 Physical properties of C-2 arylidene/aryl and C-22-acyloxy congeners of 22*β*-hydroxy-3-oxoolean-12-en-28-oic acid (98-106).

Compound name	TLC (R_f)	mp. (^{0}C)	Yield (%)
2-(3-Phenylprop-2-en-1-ylidene)-22*β*-[(2-methyl-1-oxo-2-butenyl)oxy]-3-oxoolean-12-en-28-oic acid **98**	0.68**	145-147	71.1
2-(3-Phenylprop-2-en-1-ylidene)-22*β*-[(3-methyl-1-oxo-2-butenyl)oxy]-3-oxoolean-12-en-28-oic acid **99**	0.65**	159-161	66.7
2-(2-Methyl-3-phenylprop-2-en-1-ylidene)-22*β*-[(2-methyl-1-oxo-2-butenyl)oxy]-3-oxoolean-12-en-28-oic acid **100**	0.66**	152-154	67.1
2-(2-Methyl-3-phenylprop-2-en-1-ylidene)-22*β*-[(3-methyl-1-oxo-2-butenyl)oxy]-3-oxoolean-12-en-28-oic acid **101**	0.64**	167-169	70.8
2-(2-Methyl-3-phenylprop-2-en-1-ylidene)-22*β*-hydroxy-3-oxoolean-12-en-28-oic acid **102**	0.41*	135-137	68.3
2-(3,4-Dimethoxybenzylidene)-22*β*-hydroxy-3-oxoolean-12-en-28-oic acid **103**	0.27*	195-197	72.1
2-(2-Methyl-3-phenylpropyl)-22*β*-hydroxy-3-oxoolean-12-en-28-oic acid **104**	0.44*	61-63	48.4
2-(3,4-Dimethoxybenzyl)-22*β*-hydroxy-3-oxoolean-12-en-28-oic acid **105**	0.35*	103-105	58.9
2-(3-Phenylpropyl)-22*β*-hydroxy-3-oxoolean-12-en-28-oic acid **106**	0.43*	Semi-solid	46.6

(* Hexane: Ethyl acetate :: 1:1; ** Hexane: Ethyl acetate :: 4:1)

Table 4.13 IR spectral data (cm^{-1}) of C-2 arylidene/aryl and C-22-acyloxy congeners of 22*β*-hydroxy-3-oxoolean-12-en-28-oic acid (98-106).

Code	O-H	C-H aliphatic	C=O, C-3 keto	C=O, ester
98	-	2951	1672	1715
99	-	2947	1682	1718
100	-	2950	1670	1716
101	-	2951	1652	1714
102	3416	2944	1679	-
103	3433	2946	1686	-
104	3466	2947	1706	-
105	3491	2947	1709	-
106	3437	2944	1700	-

Table 4.14 ^{1}H NMR spectral data (δ) of C-2 arylidene/aryl and C-22-acyloxy congeners of 22*β*-hydroxy-3-oxoolean-12-en-28-oic acid (98-106).

Code	Vinylic-H	C-12-H	C-22α-H	C-18-H	Tertiary methyl proton (s)
98	6.94 (2), 7.26 (1)	5.34	5.10	2.97	1.18, 1.15, 1.11, 1.02, 0.91 (2), 0.86
99	6.98 (2), 7.27 (1)	5.45	5.05	2.97	1.25, 1.18, 1.13, 1.04, 0.94 (2), 0.82
100	7.11-7.34	5.31	5.03	3.07	1.17, 1.09, 1.05 (2), 1.00, 0.89, 0.84
101	7.15-7.47	5.30	4.97	3.04	1.18, 1.06, 1.00, 0.96 (2), 0.83, 0.77
102	7.11-7.46	5.34	3.86	2.93	1.14, 1.08, 1.06 (2), 0.83, 0.80, 0.78
103	7.49	5.40	3.85	3.04	1.21, 1.17, 1.11 (2), 0.91, 0.89, 0.86
104		5.31	3.84	2.98	1.14, 1.10, 1.07, 1.05, 0.85, 0.83, 0.78
105		5.32	3.91	2.97	1.09 (2), 0.99, 0.87 (2), 0.80, 0.77
106		5.34	3.89	2.98	1.22, 1.17, 1.07, 1.02 (2), 0.89, 0.78

Table 4.15 ^{13}C NMR of C-2 arylidene/aryl and C-22-acyloxy congeners of 22*β*-hydroxy-3-oxoolean-12-en-28-o

Carbon no.	98	99	100	101	102	103	104	105
1	39.13	39.14	38.47	38.47	38.15	38.28	38.20	35.52
2	137.30	138.69	138.75	138.82	135.90	137.59	40.20	32.79
3	207.18	207.13	206.96	206.77	207.92	207.73	216.87	217.2
4	37.72	39.14	39.23	39.23	39.19	39.18	40.60	37.07
5	53.06	53.07	55.31	55.31	52.96	60.44	51.91	62.67
6	22.62	20.24	19.49	19.49	22.66	20.34	23.22	21.68
7	30.07	31.88	30.04	30.04	31.86	29.82	32.88	28.68
8	38.64	42.19	39.23	39.23	41.25	41.18	41.26	38.32
9	50.70	50.69	50.61	50.61	52.38	52.83	51.34	51.33
10	36.07	38.56	37.72	37.72	36.79	36.23	37.16	33.65
11	25.70	24.03	24.20	24.20	24.34	22.62	24.68	22.43
12	122.49	122.48	122.50	122.50	122.37	122.15	121.31	121.8
13	143.22	143.24	143.10	143.10	143.40	143.59	142.36	141.9
14	42.36	45.06	45.97	45.97	44.17	44.29	44.37	41.02
15	29.34	27.55	26.46	26.46	27.77	25.64	27.32	26.14
16	24.22	22.61	23.52	23.52	23.74	21.06	23.65	21.98

Table 4.15 cont.

Carbon no.	98	99	100	101	102	103	104	105
17	45.06	45.34	46.89	46.89	45.16	45.03	44.94	41.14
18	42.18	42.21	42.00	42.00	42.31	42.28	43.15	40.19
19	45.32	46.06	47.43	47.43	45.39	45.54	46.02	45.04
20	29.72	30.06	27.57	27.57	30.18	27.82	30.90	28.68
21	33.72	37.71	36.78	36.78	36.27	33.25	35.19	33.60
22	76.73	75.94	75.89	75.89	74.30	74.32	73.27	73.35
23	29.64	29.63	26.92	26.92	29.77	27.22	29.16	28.35
24	15.68	-	15.63	15.63	15.36	15.40	15.45	14.53
25	15.45	15.45	15.10	15.10	14.22	14.20	14.32	13.11
26	16.49	16.53	19.49	16.91	20.32	16.52	21.62	15.70
27	27.55	26.18	26.14	26.14	27.16	24.36	26.80	24.65
28	179.93	179.95	179.62	179.58	180.79	180.70	179.59	179.7
29	31.94	36.08	33.68	33.68	33.89	30.16	35.19	29.09
30	26.19	25.69	25.78	25.78	25.66	23.75	26.14	23.35
Ar-R^1	-	-	-	-	-	55.91 (OCH_3)	-	54.77
Ar-R^2	-	-	-	-	-	55.98 (OCH_3)	-	54.81

Table 4.15 cont.

Carbon no.	98	99	100	101	102	103	104	105
Ar-R^3								
Ar-CH	132.65	123.37	130.41	127.61	128.25	128.85	44.14	30.89
Ar-C-C	123.36	136.69	127.69	134.47	130.42	-	28.73	-
Ar-C-C-C	139.02	140.69	143.10	143.10	137.55	-	41.07	-
C1''	136.67	137.29	138.75	138.82	133.63	131.88	134.85	133.0
C2''	127.15	127.14	127.69	127.69	128.32	110.18	128.27	108.6
C3''	128.79	132.66	129.30	129.44	130.21	149.53	132.58	147.5
C4''	128.48	128.78	128.43	128.24	129.09	148.63	127.20	146.8
C5''	128.84	128.83	129.30	130.47	129.32	114.13	129.37	109.5
C6''	127.61	127.14	128.24	128.24	128.44	123.49	127.39	117.7
C1'	166.28	166.32	166.29	166.30	-	-	-	-
C2'	128.79	115.97	123.39	115.95	-	-	-	-
C3'	140.70	157.32	155.48	157.20	-	-	-	-
C4'	20.60	20.54	21.48	21.48	-	-	-	-
C5'	14.15	14.47	20.53	20.53	-	-	-	-

4.2.2. Selective *in-vitro* cytotoxicity and molecular mechanistic studies

The isolated Lantadene A and B **(80**, **81)** along with synthesized congeners **(84-87**, **93**, **98-106)** were screened for anticancer activity against panel of cancer cell lines including HCT-116 (Colon cancer), HL-60 (Leukemia), MCF-7 (Breast cancer) and A549 (Lung cancer). The results of cytotoxicity studies are shown in Table 4.16. The parent compound **80** and **81** showed cytotoxicity with IC_{50} in the range of 1.19 to 3.62μM. The reduction of compound **80** and **81** to corresponding reduced metabolites **84** and **85**, respectively resulted in the increase of cytotoxic activity. The compounds **84** and **85** showed marked selectivity towards lung cancer cell line (A549) with IC_{50} 0.43 and 0.79μM, which inferred improved solubility of compounds. The compound **80** and **81** are structurally different at C-22 position via ester linkage and hydrolysis of ester side chain leads to compound **86**. The cytotoxicity of compound **86** decreased significantly in comparison to parent compounds and it showed that *α,β* unsaturated carbonyl group in the side chain may be playing an important role in binding with receptor site. Further, reduction of compound **86** to **87** did not alter the cytotoxicity to much extent. The C-2 arylidene congeners of **80** and **81** showed marked cytotoxicity in comparison to parent compounds.

The compound **98** and **99** showed significant cytotoxicity against HCT-116, A549 and HL-60 in the range of IC_{50} 0.18 to 1.28μM. The compound **93, 102** and **103** were the C-2 arylidene congeners of compound **86**, and in this series compound **103** showed selective toxicity towards HL-60 cells with IC_{50} 0.65μM. The reduction of compound **102**, **103** and **93** yielded compound **104-106** with marked decrease in the activity. This reflected the importance of double bond in the C-2 congeners. These congeners **(80**, **81**, **84-87**, **93**, **98-106)** showed selective toxicity towards cancer cells and were found non toxic to normal cells (VERO) with IC_{50} >50 μM and at the same time, these congeners showed better cytotoxicity profile than standard drug cisplatin. The cytotoxicity results showed that, C-22 ester chain was critical for the activity and reduction of C-3 oxo group to hydroxyl group increased the activity whereas, reduction of C-2 arylidene to C-2 aryl group led to decrease in the activity.

All compounds were evaluated for their effects on the NF-κB signalling pathway (Figure 4.1) in A549 cells. The four compounds **(84**, **85**, **98** and **99)** which were more active than compound **80** and **81** against the tested tumor cell lines also showed more

potent suppression of NF-κB activation in A549 lung cancer cells. The most potent compound **98** was selected to evaluate its effect on NF-κB protein expression at cellular level via western blotting and compound **98** showed suppression of NF-κB expression in dose dependent manner (Figure 4.2).

A fluorescence polarization based assay was performed by using AKT1/ PKBαKinEASE^{TM} FP Fluorescein Green Assay kit (Upstate, Millipore Corporation) to obtain the IC_{50} values. The compound **84**, **85**, **98** and **99** showed marked Akt1 kinase inhibition, with an IC_{50} of 1.20, 1.08, 0.84 and 0.96μM respectively (Table 4.17). In order to further evaluate the effect of the found inhibitor on cellular Akt signalling, the phosphorylation state of Akt downstream substrate GSK3β in A549 cell were examined in the presence or absence of representative compound **98** which was found to be the most potent compound against A549 cell growth (IC_{50}, 0.48μM) and Akt activity (IC_{50}, 0.84μM) in current study. After treatment with various concentrations of **98** (0.125, 0.25, 0.5 and 1.0 μM), the A549 cell was lysed and analyzed by western blot as shown in Figure 4.3, the phosphorylation of GSK3β was significantly suppressed by compound **98** in a dose dependent manner.

Table 4.16 Antiproliferative activity of compounds **80**, **81**, **84-87**, **93**, **98-106** against 4 cancer cell lines and normal cell line[a] (IC_{50} μM).

Compound	HCT-116	A549	MCF-7	HL-60	VERO
80	3.62±0.84	2.84±0.72	3.60±1.02	1.87±0.87	>50
81	2.45±0.36	1.19±0.28	3.09±0.76	2.19±0.42	>50
84	2.35±0.62	0.79±0.01	3.29±0.92	2.21±0.42	>50
85	2.67±0.68	0.43±0.03	6.18±1.42	2.52±0.82	>50
86	>10	>10	>10	3.30±0.54	>50
87	>10	>10	>10	2.58±0.72	>50
98	0.60±0.02	0.48±0.04	2.51±0.42	0.18±0.04	>50
99	0.84±0.04	0.54±0.02	2.36±0.38	1.28±0.56	>50

Table 4.16 cont.

Compound	HCT-116	A549	MCF-7	HL-60	VERO
99	0.84±0.04	0.54±0.02	2.36±0.38	1.28±0.56	>50
100	1.96±0.02	2.31±0.96	2.78±0.42	1.20±0.32	>50
101	1.48±0.34	9.36±2.30	3.05±1.45	1.41±0.02	>50
102	2.23±0.86	2.08±0.54	3.16±0.92	1.10±0.48	>50
103	1.74±0.56	2.25±0.72	3.31±1.02	0.65±0.25	>50
93	2.92±0.78	2.80±0.80	3.23±0.76	2.92±0.84	>50
104	>10	>10	>10	3.45±1.04	>50
105	>10	>10	>10	>10	>50
106	>10	>10	>10	2.58±0.86	>50
Cisplatin	17.5±4.42	21.3±3.62	18.4±4.86	2.40±1.62	0.03±0.00

[a] Data shown are the average values from at least two independent experiments with standard error (SE).

Table 4.17 Akt1 kinase inhibition activity[a].

Compound	IC_{50} (μM)
84	1.20±0.24
85	1.08±0.20
98	0.84±0.04
99	0.96±0.06

[a] Data shown are the average values from two independent experiments with standard error (SE).

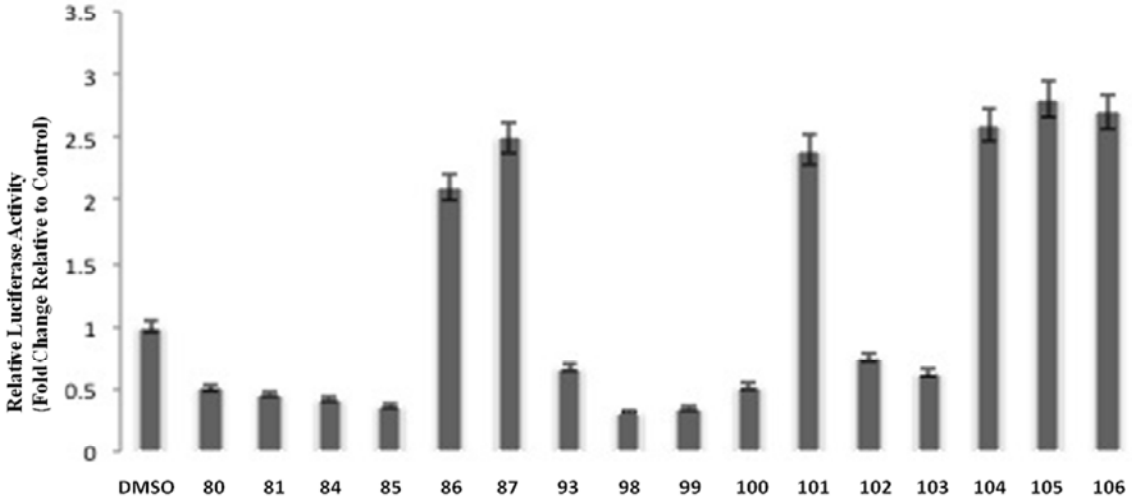

Figure 4.1 Inhibitory effects of compound **80**, **81**, **84-87**, **98-106** on NF-κB signaling in A549 cells.

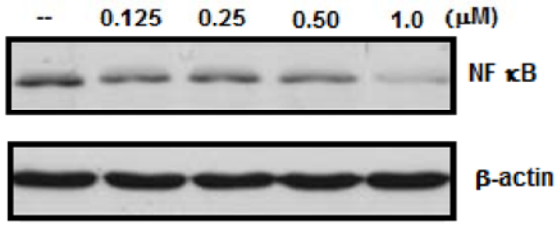

Figure 4.2 Inhibitory effects of compound **98** on NF-κB expression in A549 cells.

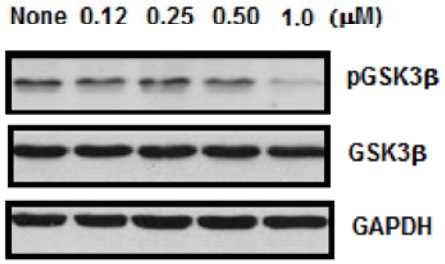

Figure 4.3 Effect of compound **98** on phosphorylation of Akt downstream substrate GSK3β at cellular level. A549 cells were pretreated with compound **98** for 12h, cell lysates were prepared and analyzed for the phosphorylation state of the Akt kinase downstream substrate GSK3β via western blot.

4.2.3. Docking analysis

The X-ray crystal structures of the NF-κB p50-p50 homodimer (from 1NFK) was used for docking analysis. The stereo view of NF-κB p50-p50 homodimer complexed with compound **98** is described in Figure 4.4a. Improvement in biological activity of compound **80** on integration of cinnamoyl functionality was supported by final intramolecular energy and comparative docking analysis results. Final intramolecular energy of compound **98** (-11.16 kcal/mol) was higher than compound **80** (-8.62 kcal/mol) which showed that integration of cinnamoyl functionality improved binding interaction and biological activity. Visual inspection of the docked structure of compound **80** was surrounded by charged residues involved in hydrogen bonding interactions such as C-3 carbonyl group (C=O) projecting toward the hydroxyl functionality of carbonyl group of Lys 293, forming a H-bond (H...O: 2.191 Å) interaction. Similarly, oxygen of carboxyl group (C=O) formed hydrogen bonding with Lys 241 (H…O: 2.243 Å) and oxygen atom of carbonyl group of side chain form hydrogen bonding with hydrogen atom of Arg 305 (H…O: 2.690 Å).

Binding interactions of compound **98** with NF-κB p50-p50 homodimer are described in Figure 4.4b. Visual inspection indicated that integration of cinnamoyl functionality on compound **80** slightly change in binding position and improvement in binding interactions, which favour to improve the biological activities. The C-3 carbonyl group (C=O) of compound **98** projecting toward the hydroxyl functionality of carbonyl group of Lys 272, forming a H-bond (H...O: 2.612 Å) interactions. Similarly, oxygen of carboxyl group (C=O) formed hydrogen bonding with Gln 306 (H…O: 1.448 Å), oxygen atom of hydroxyl of acid functionality formed hydrogen bonding with Gln 274 (H…O: 2.203 Å), and oxygen atom of carbonyl group of side chain form hydrogen bonding with hydrogen atom of Ser 246 (H…O: 3.190 Å). Generation of new hydrophobic interaction (which is not showed in Figure 4.4b in order to highlight hydrogen bonding interactions) of oleanane template and cinnamoyl functionality with Phe 307 which also favour improved biological activities.

4.3. Anti-melanoma activity of 2-(3-phenylprop-2-en-1-ylidene)-22β-hydroxy-3-oxoolean-12-en-28-oic acid 93

4.3.1. *In-vitro* antitumor activity and apoptotic studies

In-vitro anti-melanoma activity of compound **93** was evaluated on B16F10 melanoma cells and was observed with 0.84 μM GI_{50}. The morphological changes and cell death in B16F10 cells were observed by using DAPI staining at 5 and 10 μM concentrations (Figure 4.5). Uniform normal morphology was seen in the control group, whereas, fragmented chromatin and apoptotic bodies were seen in the cells treated with compound **93**. In addition, a typical DNA strand-break was observed by means of gel electrophoresis. The B16F10 cancer cells were incubated in the presence of **93** at 5 and 10μM concentrations for 24h and DNA was isolated from B16F10 cells. The characteristic 'ladder' pattern of apoptosis was observed at 10 μM of **93** (Figure 4.6). It is known that caspases are specific proteases of apoptosis, particularly caspase-3; therefore, we further examined the effects of compound **93** on the activation of caspase-3, an active executor of apoptosis. The compound **93** (5 and 10μM) induced the activation of caspase-3 in B16F10 cells after 24 h of incubation (Figure 4.7). Effect of compound **93** on various transcription factors involved in apoptosis, an immunoblot was carried out using Bcl-2, NF-κB, c-jun, caspase-3 proteins and bax. The treatment of B16F10 cells with compound **93** (5 and 10μM) down-regulated the expression of bcl-2, c-jun and NF-κB whereas, the expression of bax and caspase-3 were up-regulated in B16F10 cells (Figure 4.8).

In order to assess whether compound **93** induced growth inhibition of the cells was mediated *via* alterations in cell cycle regulation and apoptosis, the effect of compound **93** on cell cycle distribution was evaluated. We examined the effect after 24 h treatment of different concentrations of **93** on B16F10 cell cycle progression and as shown in Table 4.18 & Figure 4.9, compound **93** treatments resulted in a dose dependent accumulation of cells in sub G1 phase. At the dose of 10μM of **93**, the percentage of total cells in sub G1 phase reached 39.74% as compared to 1.62% in the control group. Concomitantly, there was a significant decrease of the number of cells in the G1, S and G2/M phases to 31.81, 15.67 and 12.78% as compared to 73.82, 12.62 and 11.94% in the control group, respectively. These results indicated that compound **93** induced typical apoptosis by sub G1 cell cycle arrest in B16F10 cells.

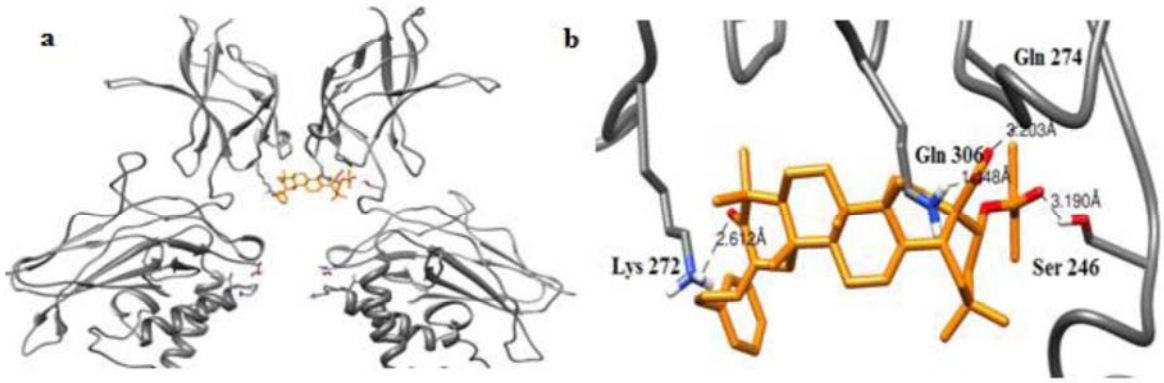

Figure 4.4. (**a**) Stereo view of 3D crystal structure of NF-κB p50-p50 homodimer (1NFK) complexed with compound **98**. (**b**) Hydrogen bond interactions of compound **98** with amino acid residue of Ser 246, Lys 272, Gln 274 and Gln 306.

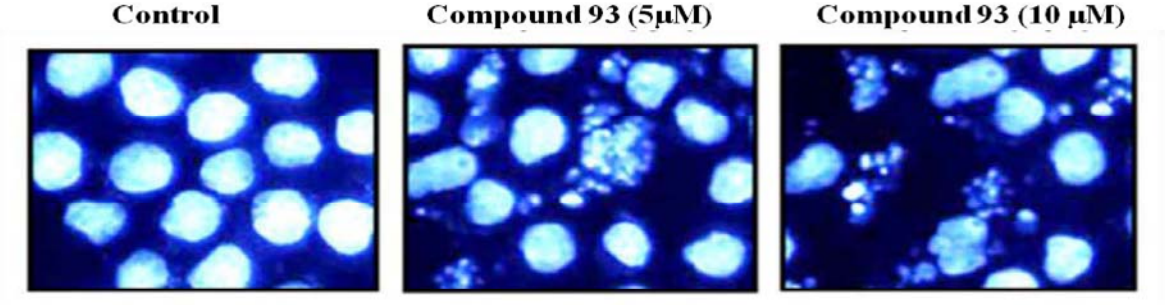

Figure 4.5 Apoptosis observed by DAPI staining. Marked morphological changes such as apoptotic bodies, nuclear fragmentation were seen at 5 and 10μM treatment of **93** after 24h.

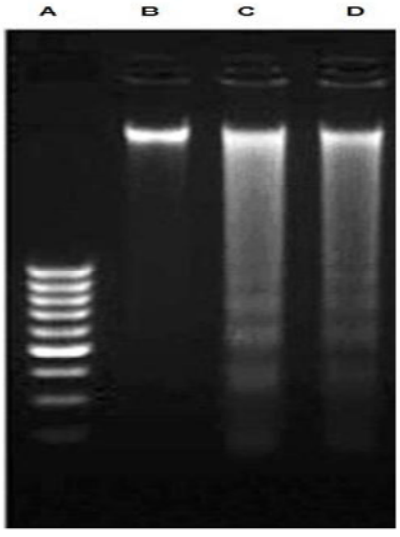

Figure 4.6 Dose-dependent induction of DNA fragmentation by **93** in B16F10 cells. (A) DNA marker, (B) control cells, (C) cells treated with 5μM of **93**, (D) cells treated with 10μM of **93**.

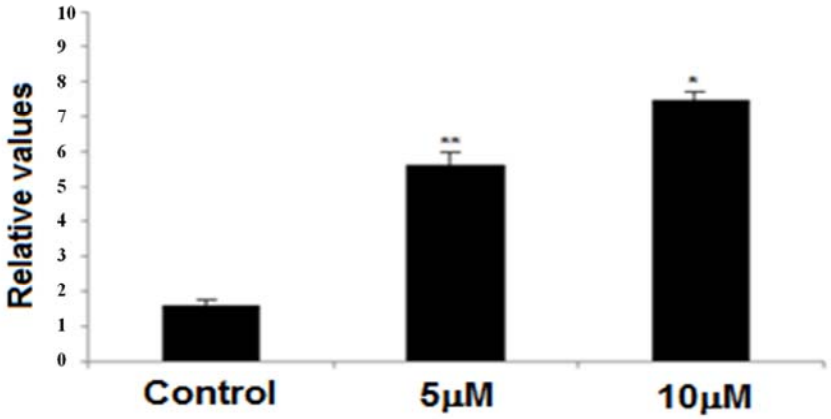

Figure 4.7 Caspase-3 activation by **93** at 5 and 10 μM after 24 hours.

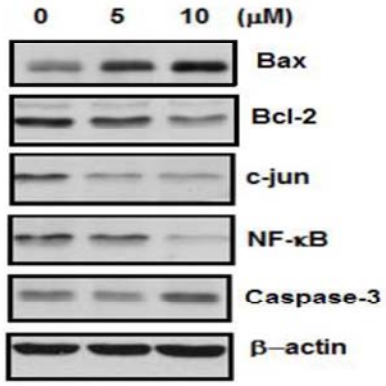

Figure 4.8 Expression of transcription factors detected by western blotting before and after cells was treated with 5 and 10μM of **93.**

Table 4.18 Effects of compound **93** on the cell cycle distribution in B16F10 cells by flow cytometry.

Number of cells (%)

Compound **93** (μM)	Sub G1	G1	S	G2/M
0	1.62	73.82	12.62	11.94
5	12.51	42.86	17.94	26.69
10	39.74	31.81	15.67	12.78

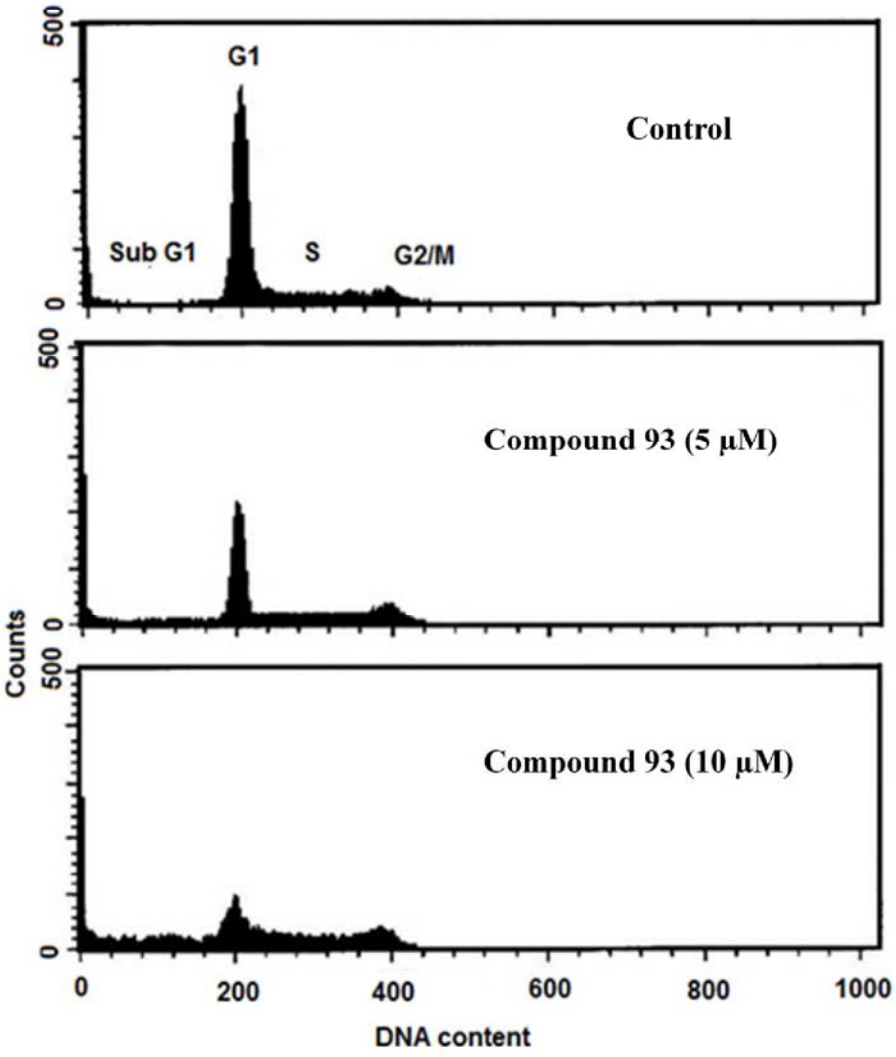

Figure 4.9 Effect of compound **93** on cell cycle. B16 F10 cells were treated with compound **93** at 5 and 10 µM for 24 h. The cells were stained with propidium iodide and the cell cycle.

4.3.2. *In-vivo* antitumor activity

4.3.2.1. *In-vivo* anti-melanoma activity

To investigate the effect of compound **93** on melanoma growth *in-vivo*, B16F10 tumor cells were subcutaneously inoculated into C57BL/6 mice. After, 24 h tumor inoculation the animals were systematically treated with **93**, cisplatin and vehicle. The tumor volumes, tumor weight of the control, **93** and cisplatin treated groups after tumor induction are described in Table 4.19 and Figure 4.10. The compound **93** at 10 mg/kg body weight on a 4 week administration schedule exhibited 62.78 ± 20.72 % prevention of tumor growth. The weight (1.98 ± 0.42 g) and volume (2480.62.04 ± 880.60 mm^3) of the

tumors in the **93** treated group (10 mg/kg body weight) at the end of 4 weeks was significantly lower when compared with the control ($p < 0.01$). The **93** at a dose of 10 mg/kg inhibited tumor proliferation more effectively than the positive control (38.72 ± 12.32%), cisplatin (5 mg/kg). The mice treated with **93** demonstrated prolonged survival time in comparison with cisplatin and control groups (*P<0.01)*, which showed the beneficial effects of **93** (Figure 4.11).

Table 4.19 Evaluation of tumor volume, weight and % inhibition of B16F10 solid tumor in mice treated with compound **93.**

Group	Tumor volume (mm^3) on 28^{th} day	Tumor weight (g)	Tumor weight % inhibition
Control	5230.42± 1220.62	5.32 ±1.20	-
Compound 93	2480.62 ± 880.60**	1.98 ± 0.42**	62.78±20.72
Cisplatin	4664.24 ± 1456.72*	3.26 ± 1.62*	38.72±12.32

Values are mean ± standard deviation, n=10. Comparisons between control and treatment groups were performed by Dunnett's test. *p* values **< 0.01, *< 0.05.

Figure 4.10 Morphology of tumors isolated after 28 days of study.

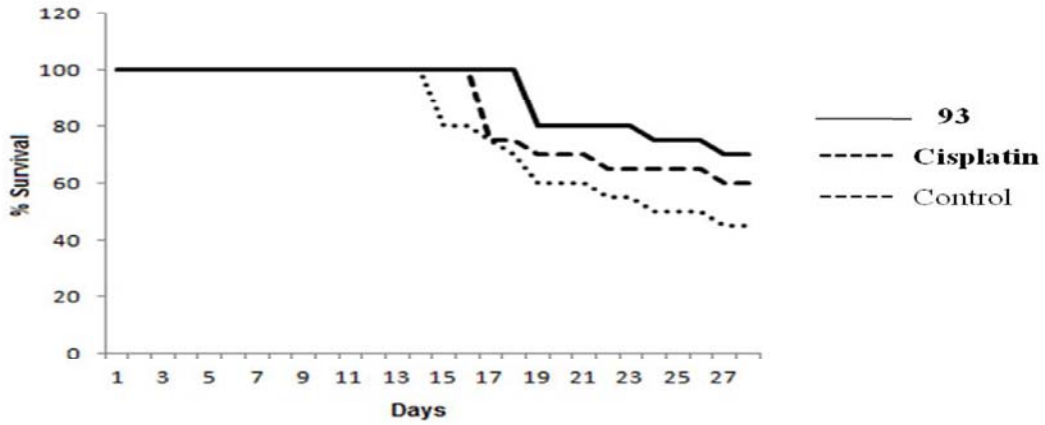

Figure 4.11 Effect of compound **93** and cisplatin on survival rate (%). Differences between groups became significant on day 15 **(P <0.01)* reaching to ** *P <0.001* on day 28.

4.3.2.2. Effects on liver enzymes

To access the liver injury after treatment of compound **93** and cisplatin in mice, the liver transaminases were studied. The results showed that there was significant decrease in the level GOT, Gamma- GT and ALT in tumor control group and cisplatin group. Whereas, there was significant improvement in the level of ALT, GOT and Gamma GT in compound **93** treated groups in comparison with tumor control group (Table 4.20).

Table 4.20 Effect of compound **93** on liver enzymes.

Groups	GOT(U/L)	ALT (U/L)	Gamma-GT (U/L)
Control	30.2 ± 4.2	18.6 ± 2.8	24.8 ± 8.2
Tumor Control	18.4 ± 4.8	12.4 ± 4.4	16.6 ± 3.2
Compound **93**	28.8 ±6.2*	16.2 ± 3.2**	22.6 ± 6.8*
Cisplatin	20.6 ±4.2**	14.8 ± 4.2*	18.8 ± 6.4**

Data are expressed as mean ± S.E.M. of ten animals per group.* denotes significant difference from respective tumor control at $p < 0.05$, ** denotes significant difference from respective tumor control at $p < 0.01$.

4.3.2.3. Effects on Blood cells

The treatment of compound **93** and cisplatin to the tumor bearing mice resulted no major change in the haemoglobin in comparison with control (vehicle treated group), whereas, there was decrease in the haemoglobin content in cisplatin and tumor control group. The percent eosinophils decreased significantly in cisplatin and tumor control, but there was significant *(P<0.05)* increase in compound **93** treated group. The total leukocyte count decreased significantly in tumor control and cisplatin group, whereas, the compound **93** treated group showed improved leukocyte count (Table 4.21).

Table 4.21 Effect of compound **93** on blood profile.

Groups	Haemoglobin (g/dL)	Total Leukocytes ($10^3/mm^3$)	Eosinophils (%)
Control	12.4 ±1.2	5.4 ±0.4	6.8± 1.4
Tumor Control	7.6 ± 2.3	3.2 ± 0.2	2.8 ± 0.8
Compound **93**	11.8 ± 2.4*	4.2 ± 1.2**	7.6 ± 1.6*
Cisplatin	9.6 ± 1.6*	3.8 ± 0.4*	5.4 ± 0.8*

Data are expressed as mean ± S.E.M. of ten animals per group.* denotes significant difference from respective tumor control at $p < 0.05$, ** denotes significant difference from respective tumor control at $p < 0.01$.

CHAPTER 5

CONCLUSIONS

Nature is an abundant source of structurally diver's constituents as they have been generated by mixed biosynthesis have been found to exhibit unusual properties and biological activity as a different molecular segment act cooperatively to control and modulate confirmation, recognition, communication, transportation and solubility and other properties. Development of hybrid systems opened a new way to discover and development of new drug candidates against cancer and other diseases as hybrid systems are constructs of different molecular entities, natural or unnatural, to generate functional molecules in which the characteristics of various components are modulated, amplified or give rise to entirely new properties.

Lantana camara L. (Verbenaceae) a weed of tropical and subtropical part of the world, is rich source of oleanane type of pentacyclic triterpenoids. Lantadene A and lantadene B emerged as potential candidates to be developed as anticancer agents as they have shown selective cancer cytotoxicity, non-toxic towards normal cells (VERO), chemopreventive potential against two stage carcinogenesis in mice model along with their role in apoptosis via down regulation regulation of transcription factors NF-κB, Bcl-2 and c-jun and upregulation of caspase-3 and Bax. In order to further pharmacophore optimization within the frame of cancer, various C-2 arylidene/aryl congeners of lantadenes have been synthesized and screened for their anticancer potential. The compound **84** and **93** were found most active out of isolated and synthesized congeners of lantadenes. The GI_{50} value of compound **84** and **93** was <5 μM against more than 80% cancer cell lines. The mean graph midpoint (MG_MID) value of compound **84** (MG_MID -5.69) was higher than standard cisplatin (MG_MID -5.66) while comparable in case of compound **93** (MG_MID -5.52). The NCI's COMPARE analysis showed that these compounds were in significant number of correlations with activity patterns of mechanistic set of compounds (PCC ≥ 0.60). These compounds could be considered as a useful template for future development to obtain more potent antitumor agent(s).

Several new C-arylidene/aryl and C-22-ayloxy congeners of 22*β*-hydroxy-3-oxoolean-12-en-28-oic acid with integrated cinnamoyl and vanillyl functionality were synthesized and showed marked selective toxicity against cancer cells and inhibited the activation of NF-κB and Akt1 signaling in A549 cells. The structure activity relationship revealed that C-22 ester chain was critical for the activity and reduction of C-3 oxo group

to hydroxyl group increased the activity whereas, reduction of C-2 arylidene to C-2 aryl group led to decrease in the activity. The molecular docking of the NF-κB p50-p50 homodimer with lead molecule showed high binding affinity and it can be inferred from results that lead molecule can be developed as potent anticancer compound.

The cinnamoyl integrated 22*β*-hydroxy-3-oxoolean-12en-28-oic acid **93** showed marked and selective cytotoxicity against panel of melanoma cell lines whereas it was found non toxic towards normal cells (VERO). The compound **93** induced apoptosis in B16F10 cells by down-regulation of NF-κB, c-jun, Bcl-2 and up-regulation caspase-3 and Bax expression. The compound **93** also demonstrated beneficial in B16F10 allograft mice model. The compound **93** showed significant reduction of tumor growth and tumor weight *in vivo,* with improved survival rate in comparison to tumor control and standard drug cisplatin. The compound **93** showed better safety profile than standard drug cisplatin in terms of haematological parameters and liver enzymes levels. The compound **93** has the potential to be developed as anti-melanoma agent.

CHAPTER 6

REFERENCES

Aggarwal B. B. and Shishodia S., "Molecular targets of dietary agents for prevention and therapy of cancer," *Biochem. Pharmacol.*, vol. 71, pp. 1397-1421, 2006.

Ahmed N. *et al.,* "Synthesis, characterization, and estrogen receptor binding affinity of flavone-, indole-, and furan-estradiol conjugates," *Bioorg. Med. Chem. Lett.*, vol. 17, pp. 3212-3216, 2007.

Akiyama N. *et al.,* "Up-regulation of cytosolic phospholipase A2alpha expression by N, N diethyldithiocarbamate in PC12 cells; involvement of reactive oxygen species and nitric oxide," *Toxicol. Appl. Pharmacol.,* vol. 215, pp. 218-227, 2006.

Allen D. and Smith Q. R., "Characterization of the blood-brain barrier choline transporter using the in situ rat brain perfusion technique," *J. Neurochem.*, vol. 76, pp. 1032-1041, 2001.

Al-Malaika S. and Suharty N., "Reactive processing of polymers: mechanisms of grafting reactions of functional antioxidants on polyolefins in the presence of a coagent," *Polym. Degrad. Stab.,* vol. 49, pp. 77-89, 1995.

Altun A. and Ugur-Altun B., "Melatonin: therapeutic and clinical utilization," *Int. J. Clin. Pract.*, vol. 61, pp. 835-845, 2007.

Atabek M. E. *et al.,* "Oxidative stress in childhood obesity," *J. Pediatr. Endocrinol. Metab.,* vol. 17, pp. 1063-1068, 2004.

Atkinson D. and Lehrle R., "A model polymer-bound antioxidant system for lubricants. *Eur. Poly. J.,* vol. 28, pp. 1569-1575. 1992.

Baburaj K. *et al.,* "HOCGO and DMACGO. Two coumarin derived alpha-dicarbonyls suitable as pH and polarity sensitive fluorescent reporters for proteins that can be targeted at reactive arginines," *Biochim. Biophys. Acta.*, vol. 1199, pp. 253-265, 1994.

Balogun E. *et al.,* "Curcumin activates the haem oxygenase-1 gene via regulation of Nrf2 and the antioxidant-responsive element," *Biochem. J.* vol. 371, pp. 887-895, 2003.

Balunas M. J. and Kinghorn A. D., "Drug discovery from medicinal plants," *Life Sciences*, vol. 78, pp. 431-441, 2005.

Ban H.S., "Inhibition of prostaglandin E2 production by taiwanin C isolated from the root of *Acanthopanax chiisanensis* and the mechanism of action," *Biochem Pharmacol.,* vol. 64, pp. 1345–1354, 2002.

Banerjee S. *et al.,* "Multi-target therapy of cancer by genistein," *Cancer Lett.*, vol. 269, pp. 226-242, 2008.

Beaulieu P. L. *et al.,* "Viral polymerase inhibitors," *Int. Patent Appl.* WO 02/04425. Boehringer Ingelheim (Canada) Ltd. 2002.

Belluti F. *et al.,* "Design, synthesis and anticancer activities of stilbene-coumarin hybrid compounds: Identification of novel proapoptotic agents," *Bioorg. Med. Chem.,* vol. 18, pp. 3543-3550, 2010.

Bodine P. V. *et al.,* "Estrogenic effects of 7alpha-methyl-17alpha-ethynylestradiol: a newly discovered tibolone metabolite," *Steroids*, vol. 67, pp. 681-686, 2002.

Bolanos J. P. *et al.,* "Mitochondria and reactive oxygen and nitrogen species in neurological disorders and stroke: therapeutic implications," *Adv. Drug Deliv. Rev*., vol. 61, pp. 1299-1315, 2009.

Boyd M. R. and Paull K. D., "The NCI In Vitro Anticancer Drug Discovery Screen," *Drug Dev. Res*., vol. 34, pp. 91-109, 1995.

Brush C. K., "Fluorescein Labelled Phosphoramidites," US Patent 5,583,236.

Chang L. and Karin M., "Mammalian MAP kinase signaling cascades," *Nature,* vol. 410, pp. 37-40, 2001.

Chandra V. *et al.,* "First structural evidence of a specific inhibition of phospholipase A2 by α-tocopherol (vitamin E) and its implications in inflammation: crystal structure of the complex formed between phospholipase A2 and α-tocopherol at 1.8 Å resolution," *J. Mol. Biol*., vol. 320, pp. 215-222, 2002.

Cheng Y. *et al.,* "Phosphatidylcholine-specific phospholipase C, p53 and ROS in the association of apoptosis and senescence in vascular endothelial cells," *FEBS Lett.,* vol. 580, pp. 4911-4915, 2006.

Chin Y. W. *et al.,* "Drug Discovery From Natural Sources," The AAPS Journal, vol. 8, pp. E239-E253, 2006.

Choo Q. L. *et al.,* "Isolation of a cDNA clone derived from a blood-borne non-A, non-B viral hepatitis genome," *Science*, vol. 244, pp. 359-362, 1989.

Chu F. *et al.,* "Potent inactivation of representative members of each PKC isozyme subfamily and PKD via S-thiolation by the tumorpromotion/progression antagonist glutathione but not by its precursor cysteine," *Carcinogenesis*, vol. 22, pp. 1221-1229, 2001.

Conboy L. *et al.,* "Curcumin-induced degradation of PKC delta is associated with enhanced dentate NCAM PSA expression and spatial learning in adult and aged Wistar rats," *Biochem. Pharmacol*. Vol. 77, pp. 1254-1265, 2009.

Conner E. M. and Grisham M. B., "Inflammation, free radicals, and antioxidants," *Nutrition*, vol. 12, pp. 274-277, 1996.

Cosconati S. *et al.,* "Virtual Screening with AutoDock: Theory and Practice," *Expert Opin. Drug Discov*., vol. 5, pp. 597-607, 2010.

Cragg G. M. and Newman D. J. "Plants as a sources of anti-cancer agents," *J Ethnopharmacol*., vol. 100, pp. 72-79, 2005.

Crespo I. *et al.,* "A comparison of the effects of kaempferol and quercetin on cytokine-induced pro-inflammatory status of cultured human endothelial cells," *Br. J. Nutr*., vol. 100, pp. 968-976, 2008.

Croall D. E. and DeMartino G. N., "Calcium-activated neutral protease (calpain) system: structure, function, and regulation," *Physiol. Rev.*, vol. 71, pp. 813-847, 1991.

Cross J. V. and Templeton D. J., "Oxidative stress inhibits MEKK1 by site-specific glutathionylation in the ATP-binding domain," *Biochem. J.*, vol. 381, pp. 675-683, 2004.

Curcio M. *et al.,* "Poly(2-hydroxyethyl methacrylate)-quercetin conjugate as biomaterial in ophthalmology: An "ab initio" study," *J. Funct. Biomaterials*, vol. 2, pp. 1-17, 2011.

Decker M. *et al.,* "Design, synthesis and pharmacological evaluation of hybrid molecules out of quinazolinimines and lipoic acid lead to highly potent and selective butyrylcholinesterase inhibitors with antioxidant properties," *Bioorg. Med. Chem.*, vol. 16, pp. 4252-4261, 2008.

De Francesco R. *et al.,* "Approaching a new era for hepatitis C virus therapy: inhibitors of the NS3-4A serine protease and the NS5B RNA-dependent RNA polymerase," *Antiviral Res.*, vol. 58, pp. 1-16, 2003.

De La Torre M. D. L. *et al.,* "Synthesis of [60] fullerene-quercetin dyads," *Tetrahedron Lett.*, vol. 43, pp. 4617-4620, 2002.

De La Torre M. D. L. *et al.,* "Fullerene-flavonoid dyads," *Tetrahedron*, vol. 60, pp. 3581-3592, 2004.

Detsi A. *et al.,* "Design and synthesis of novel quinolinone-3-aminoamides and their α-lipoic acid adducts as antioxidant and Anti-inflammatory Agents," *J. Med. Chem.,* vol. 50, pp. 2450-2458, 2007.

Dhanak D. *et al.,* Novel anti-infectives. Int. Patent Appl. WO 01/85172. Smithkline Beechham Corporation, Int. 2001.

Di Virgilio F., "New pathways for reactive oxygen species generation in inflammation and potential novel pharmacological targets," *Curr. Pharm. Des.,* vol. 10, pp. 1647-1652, 2004.

Dugan L. L. and Quick K. L. "Reactive oxygen species and aging: evolving questions," *Sci. Aging. Knowledge Environ.,* vol. 26, pp. 20, 2005.

Dugan L. L. *et al.,* "Carboxyfullerenes as neuroprotective agents," Proc. Natl. Acad. Sci. USA," *Neurobiology*, vol. 94, pp. 9434-9439, 1997.

Dugan L. L. *et al.,* "Fullerene-based antioxidants and neurodegenerative disorders," *Parkinsonism Relat. Disord.*, vol. 7, pp. 243-246, 2001.

el Amouri H. *et al.,* "Syntheses and affinities of novel organometallic-labeled estradiol congeners: a structure-affinity relationship. *J. Med. Chem.*, vol. 35, pp. 3130-3135, 1992.

Eldaw A. and Khalfan H. A., "Aminomethyl coumarin acetic acid and fluorescein isothiocyanate in detection of leishmanial antibodies: a comparative study," *Trans. R. Soc. Trop. Med. Hyg.*, vol. 82, pp. 561-562, 1988.

Enes R. F. *et al.,* "Synthesis and antioxidant activity of [60] fullerene-flavonoid conjugates," *Tetrahedron*, vol. 65, pp. 253-262, 2009.

Fang L. *et al.,* "Design and synthesis of tacrine-ferulic acid hybrids as multi-potent anti-Alzheimer drug candidates," *Bioorg. Med. Chem. Lett.*, vol. 18, pp. 2905-2909, 2008.

Farombi E. O. *et al.,* "Curcumin attenuates dimethyl nitrosamine-induced liver injury in rats through Nrf2-mediated induction of heme oxygenase-1," *Food Chem. Toxicol.*, vol. 46, pp.1279-1287, 2008.

Figueiredo-Gonzalez M. *et al.,* "Pattern recognition of three Vitis vinifera L. red grapes varieties based on anthocyanin and flavonol profiles, with correlations between their biosynthesis pathways," *Food Chem.*, vol. 130, pp. 9-19, 2012.

Filardo E. J. *et al.,* "Estrogen-induced activation of Erk-1 and Erk-2 requires the G protein-coupled receptor homolog, GPR30, and occurs via trans-activation of the epidermal growth factor receptor through release of HB-EGF," *Mol. Endocrinol.*, vol. 14, pp. 1649-1660, 2000.

Fisher B. *et al.,* Endometrial cancer in tamoxifen-treated breast cancer patients: findings from the National Surgical Adjuvant Breast and Bowel Project (NSABP) B-14. *J. Natl. Cancer Inst.*, vol. 86, pp. 527-537, 1994.

Fock R. A. *et al.*, "Protein energy malnutrition modifies the production of interleukin-10 in response to lipopolysaccharide (LPS) in a murine model," *J. Nutr. Sci. Vitaminol*, vol. 54, pp. 371-377, 2008.

Furukawa S. *et al.,* "Increased oxidative stress in obesity and its impact on metabolic syndrome," *J. Clin. Invest.,* vol. 114, pp. 1752-1761, 2004.

Garcia G. *et al.,* "Losartan-Antioxidant Hybrids: Novel Molecules for the Prevention of Hypertension-Induced Cardiovascular Damage," *J. Med. Chem.*, vol. 52, pp. 7220-7227, 2009.

Gelderman K. A. *et al.,* "Rheumatoid arthritis: the role of reactive oxygen species in disease development and therapeutic strategies," *Antioxid. Redox Signal.,* vol. 9, pp. 1541-1567, 2007.

Gupta M. *et al.,* "Studies on hepatic injury and antioxidant enzyme activities in rat subcellular organelles following in vivo ischemia and reperfusion," *Mol. Cell. Biochem.*, vol.176, pp. 337-347, 1997.

Goll D. E. *et al.,* "The calpain system," *Physiol. Rev.,* vol. 83, pp. 731-801, 2003.

Hahm E. R. *et al.,* "New and known symmetrical curcumin congeners inhibit the formation of Fos-Jun-DNA complex," *Cancer Lett.,* vol. 184, pp. 89-96, 2002.

Hajnoczky G. *et al.,* "Mitochondrial calcium signalling and cell death: approaches for assessing the role of mitochondrial Ca^{2+} uptake in apoptosis," *Cell Calcium.,* vol. 40, pp. 553-560, 2006.

Halliwell B., "Free radicals, reactive oxygen species and human disease: a critical evaluation with special reference to atherosclerosis," *Br. J. Exp. Pathol.,* vol. 70, pp. 737-757, 1989.

Hashimoto H. *et al.,* "Preparation of heterocyclic compounds as remedies for hepatitis C," Int. Patent Appl. WO 01/47883. Japan Tobacco Inc. 2001.

Harvey A. L., "Natural Product in drug discovery," *D.D.T.,* vol. 13, pp. 19-20, 2008.

Hauptmann N. *et al.,* "The metabolism of tyramine by monoamine oxidase A/B causes oxidative damage to mitochondrial DNA," *Arch. Biochem. Biophys.,* vol. 335, pp. 295-304, 1996.

Haurani M. J. and Pagano P. J., "Adventitial fibroblast reactive oxygen species as autacrine and paracrine mediators of remodeling: Bellwether for vascular disease?," *Cardiovasc. Res.,* vol. 75, pp. 679-689, 2007.

Hensley K. *et al.,* "Reactive oxygen species as causal agents in the neurotoxicity of the Alzheimer's disease associated amyloid beta peptide," *Ann. N. Y. Acad. Sci.,* vol. 786, pp. 120-134, 1996

Hsu H. C. *et al.,* "Water-Soluble Hexasulfobutyl [60] Fullerene Inhibits Plasma Lipid Peroxidation by Direct Association with Lipoproteins," *J. Cardiovas. Pharmacol*., vol. 36, pp. 423-427. 2000.

Huryn M. D. and Wipf P., " Natural product chemistry and anticancer drug discovery," *Cancer Drug Design and Discovery*, pp. 107-130, 2008.

Hussain A. R. *et al.,* "Curcumin suppresses constitutive activation of nuclear factor-kappa B and requires functional Bax to induce apoptosis in Burkitt's lymphoma cell lines," *Mol. Cancer Ther*., vol. 7, pp. 3318-3329, 2008.

Hwu J. R. *et al.,* "Synthesis of new benzimidazole-coumarin conjugates as anti-hepatitis C virus agents," *Antiviral Res*., vol. 77, pp. 157-162, 2008.

Inada A. *et al.,* "Inhibitory effects of Lantadenes and related triterpinoids on Epstein-Barr virus activation," *Planta Med*., vol. 61, pp. 558-559, 1995.

Inoue M. *et al.,* "Mitochondrial generation of reactive oxygen species and its role in aerobic life," *Curr. Med. Chem.,* vol. 10, pp. 2495-2505, 2003.

Jahan M. S. and McKinny K. S., "Radiation-sterilization and subsequent oxidation of medical grade polyethylene: An ESR study," *Nuclear Instruments and Methods in Physics Research Section B: Beam Interactions with Materials and Atoms*, vol. 151, pp. 207-212, 1999.

Jaiyesimi I. A. *et al.,* "Use of tamoxifen for breast cancer: twenty-eight years later. *J. Clin. Oncol.,* vol. 13, pp. 513-529, 1995.

Jeremy J. Y. *et al.,* "Reactive oxygen species, vascular disease and cardiovascular surgery," *Curr. Vasc. Pharmacol*., vol. 2, pp. 229-236, 2004.

Kagan V. E. *et al.,* "Dihydrolipoic acid - a universal antioxidant both in the membrane and in the aqueous phase. Reduction of peroxyl, ascorbyl and chromanoxyl radicals," *Biochem. Pharmacol*., vol. 44, pp. 1637-1649, 1992.

Kalkhambkar R. G. *et al.,* "Synthesis and biological activities of some new fluorinated coumarins and 1-aza coumarins," *Eur. J. Med. Chem*., vol. 43, pp. 2178-2188, 2008.

Kamp D. W. *et al.,* "The role of free radicals in asbestos-induced diseases," *Free Radic. Biol. Med*., vol. 12, pp. 293-315, 1992.

Kambhampati S. *et al.,* "Activation of protein kinase C delta by all-trans-retinoic acid," *J. Biol .Chem.*, vol. 278, pp. 32544-32551, 2003.

Kang E. S. *et al.,* "Up-regulation of aldose reductase expression mediated by phosphatidylinositol 3-kinase/Akt and Nrf2 is involved in the protective effect of curcumin against oxidative damage," *Free. Radic. Biol. Med.*, vol. 43, pp. 535-545, 2007.

Kaur J. *et al.,* "Chemopreventive activity of lantadenes on two-stage carcinogenesis model in Swiss albino mice: AP-1 (c-jun), NF κB (p65) and p55 expression by ELISA and immunohistochemical localization," *Mol Cell Biochem.,* vol. 314, pp. 1-8, 2008.

Kaur J. *et al.,* "Antitumor activity of Lantadenes in DMBA/TPA induced skin tumors in mice: Expression of transcription factors," *Am J Biomed Sci.*, vol. 2, pp. 79-90, 2010.

Kempna P. *et al.,* "Inhibition of HMC-1 mast cell proliferation by vitamin E: involvement of the protein kinase B pathway," *J. Biol. Chem.*, vol. 279, pp. 50700-50709, 2004.

Koufaki M. *et al.,* "Bifunctional Agents for Reperfusion Arrhythmias: Novel Hybrid Vitamin E/Class I Antiarrhythmics," *Bioorg. Med. Chem.*, vol. 11, pp. 5209-5219, 2003.

Koufaki M. *et al.,* "Synthesis of chroman analogues of lipoic acid and evaluation of their activity against reperfusion arrhythmias," *Bioorg. Med. Chem.*, vol. 12, pp. 4835-4841, 2004.

Koufaki M. *et al.,* Design and synthesis of 1,2-dithiolane congeners and evaluation of their neuroprotective activity. *Bioorg. Med .Chem. Lett.*, vol. 17, pp. 4223-4227, 2007.

Labbe D. *et al.,* "The flavonols quercetin, kaempferol, and myricetin inhibit hepatocyte growth factor induced medulloblastoma cell migration," *J. Nutr.*, vol. 139, pp. 646-652, 2009.

Leonarduzzi G. *et al.,* "Targeting tissue oxidative damage by means of cell signaling modulators: the antioxidant concept revisited," *Pharmacol. Ther.*, vol. 128, pp. 336-74, 2010.

Lee T. T. *et al.,* "Suksdorfin: an anti-HIV principle from Lomatium suksdorfii, its structure-activity correlation with related coumarins, and synergistic effects with anti-AIDS nucleosides," *Bioorg. Med. Chem.*, vol. 2, pp. 1051-1056, 1994.

Lee K. S. *et al.,* "Synthesis and biological evaluation of chromone carboxamides as calpain inhibitors. *Bioorg. Med. Chem. Lett.*, vol. 15, pp. 2857-2860, 2005.

Leonard S. S. *et al.,* "Metal-induced oxidative stress and signal transduction," *Free Radic. Biol. Med.,* vol. 37, pp. 1921-1942, 2004.

Levine R. L. and Stadtman E. R., "Oxidative modification of proteins during aging," *Exp. Gerontol.,* vol. 36, pp. 1495-1502, 2001.

Linnewiel K. *et al.,* "Structure activity relationship of carotenoid congeners in activation of the electrophile/antioxidant response element transcription system," *Free Radic. Biol. Med.*, vol. 47, pp. 659-667, 2009.

Lipton P., "Ischemic Cell Death in Brain Neurons," *Physiol. Rev.*, vol. 79, pp. 1431-1568, 1999.

Li C. and Jackson R. M., "Reactive species mechanisms of cellular hypoxia-reoxygenation injury," *Am. J. Physiol. Cell. Physiol.*, vol. 282, pp. C227-C241, 2002.

Liang, J. A. *et al.,* "Vanillin inhibits matrix metalloproteinase-9expression through down-regulation of nuclear factor-kappaB signaling pathway in human hepatocellular carcinoma cells," *Mol Pharmacol.*, vol.75, pp. 151-157, 2009.

Lindsley C. W. *et al.,* "The PI3K/Akt pathway: Recent progress in the development of ATP-competitive and allosteric Akt kinase inhibitors," *Curr. Cancer Drug Targets,* vol. 8, pp. 7-18, 2008.

Mahmmoud Y. A., "Modulation of protein kinase C by curcumin; inhibition and activation switched by calcium ions," *Br. J. Pharmacol.*, vol. 150, pp. 200-208, 2007.

McCall M. R. and Frei B., "Can antioxidant vitamins materially reduce oxidative damage in humans?," *Free Radic. Biol. Med.*, vol. 26, pp. 1034-1053, 1999.

Mehta G. and Singh V., "Hybrid systems through natural product leads: An approach towards new molecular entities," *Chem. Soc. Rev.*, vol. 31, pp. 324-334, 2002.

Melagraki G. *et al.,* "Synthesis and evaluation of the antioxidant and anti-inflammatory activity of novel coumarin-3-aminoamides and their alpha-lipoic acid adducts," *Eur. J. Med. Chem.*, vol. 44, pp. 3020-3026, 2009.

Milacic V. *et al.,* "Curcumin inhibits the proteasome activity in human colon cancer cells in vitro and in vivo," *Cancer Res.*, vol. 68, pp. 7283-7292, 2008.

Min Y. D. *et al.,* "Quercetin inhibits expression of inflammatory cytokines through attenuation of NF-kappaB and p38 MAPK in HMC-1 human mast cell line," *Inflamm. Res.*, vol. 56, pp. 210-215, 2007.

Morel Y. and Barouki R., "Repression of gene expression by oxidative stress," *Biochem. J.*, vol. 342, pp. 481-496, 1999.

Morton J. R. *et al.,* "ChemInform Abstract: Addition of Free Radicals to C_{60}," *ChemInform*, vol. 29, pp. 33-39, 1998.

Moulton P. J., "Inflammatory joint disease: the role of cytokines, cyclooxygenases and reactive oxygen species," *Br. J. Biomed. Sci.,* vol. 53, pp. 317-324, 1996.

Multhaup G. *et al.,* "Reactive oxygen species and Alzheimer's disease," *Biochem. Pharmacol.,* vol. 54, pp. 533-539, 1997.

Muralikrishna A. R. and Hatcher J. F. "Phospholipase A2, reactive oxygen species, and lipid peroxidation in cerebral ischemia," *Free Radic. Biol. Med.,* vol. 40, pp. 376-387, 2006.

Muhammad S. *et al.,* "Reactive oxygen species in diabetes- induced vascular damage, stroke, and Alzheimer's disease," *J. Alzheimers Dis*., vol. 16, pp. 775-785, 2009.

Musa M. A. *et al.,* "Synthesis and antiproliferative activity of coumarin-estrogen conjugates against breast cancer cell lines. *Lett. Drug Des. Discov*., vol. 6, pp.133-138, 2009.

Moudgil R. *et al.,* "The role of k^+ channels in determining pulmonary vascular tone, oxygen sensing, cell prolifcration, and apoptosis: implications in hypoxic pulmonary vasoconstriction and pulmonary artcrial hypertension," *Microcirculation,* vol. 13, pp. 615-632, 2006.

Nakamura K. *et al.,* "Redox regulation of a src family protein tyrosine kinase p56lck in T cells," *Oncogene.,* vol. 8, pp. 3133-3139, 1993.

Nielsen A. T. *et al.,* "Organic reactions," John Wiley, New York, pp.1-438, 1968.

Nishikawa H. *et al.,* "Inhibition of NADPH oxidase subunits translocation by tea catechin EGCG in mast cell," *Biochem. Biophys. Res. Commun*., vol. 362, pp. 504-509, 2007.

Noguchi M. *et al.,* "Development of novel water-soluble photocleavable protective group and its application for dcsign of photo rcsponsivc paclitaxcl prodrugs," *Bioorg. Med. Chem*., vol. 16, pp. 5389-5397, 2008.

Nomura E. *et al.,* "Synthesis of Novel Polyphenols Consisted of Ferulic and Gallic Acids, and Their Inhibitory Effects on Phorbol Ester-Induced Epstein–Barr Virus Activation and Superoxide Generation" *Bioorg. Med. Chem*., vol. 10, pp. 1069-1075, 2002.

Ochoa W. F. *et al.,* "Retinoic acid binds to the C2-domain of protein kinase C (alpha)," *Biochemistry,* vol. 42, pp. 8774-8779, 2003.

O'Hara K. A. *et al.,* "Selective activation of Src family kinases and JNK by low levels of chromium (VI)," *Toxicol. Appl. Pharmacol*., vol. 190, pp. 214-223, 2003.

Okuno H. *et al.,* "Escape from redox regulation enhances the transforming activity of Fos," *Oncogene,* vol. 8, pp. 695-701, 1993.

Opletalova V., "Chalcones and their heterocyclic congeners as potential therapeutic agents in bacterial diseases," *Ceska. Slov. Farm*., vol. 49, pp. 278-284, 2000.

Ortiz C. *et al.,* "Hydrophilic acrylic biomaterials derived from vitamin E with antioxidant properties," *J. Biomed. Mater. Res*., vol. 45, pp. 184-191, 1999.

Ozcelik B. *et al.,* "Prevention of paclitaxel and cisplatin induced ovarian damage in rats by a gonadotropin-releasing hormone agonist," *Fertil. Steril*., vol. 93, pp. 1609-1614, 2010.

Packer L. *et al.,* "Neuroprotection by the metabolic antioxidant alpha-lipoic acid," *Free Radic. Biol. Med.*, vol. 22, pp. 359-378, 1997.

Perez-Gregorio M. R. *et al.,* "Influence of alcoholic fermentation process on antioxidant activity and phenolic levels from mulberries (Morus nigra L.)," *LWT - Food Sci. Tech.*, vol. 44, pp. 1793-1801, 2011.

Pettersen E. F. *et al.,* "UCSF Chimera--a visualization system for exploratory research and analysis," *J. Comput. Chem.*, vol. 25, pp. 1605-1612, 2004.

Poli G. *et al.,* "Oxidative stress and cell signaling," *Curr. Med. Chem.,* vol. 11, pp. 1163-1182, 2004.

Qanungo S. *et al.,* "Glutathione supplementation potentiates hypoxic apoptosis by S-glutathionylation of p65-NFkappaB," *J. Biol. Chem.*, vol. 282, pp. 18427-18436, 2007.

Rani P. *et al.,* "Synthesis and antiinflammatory activity of heterocyclic indole congeners," *Eur. J. Med. Chem.*, vol. 39, pp. 449-452, 2004.

Reiter R. J. *et al.,* "Free radical-mediated molecular damage. Mechanisms for the protective actions of melatonin in the central nervous system," *Ann. N. Y. Acad. Sci.,* vol. 939, pp. 200-215, 2001.

Reynaert N. L. *et al.,* "Dynamic redox control of NF-kappaB through glutaredoxin-regulated S glutathionylation of inhibitory kappaB kinase beta," *Proc. Natl. Acad. Sci.* U S A, vol. 103, pp. 13086-13091, 2006.

Ricciarelli R. *et al., alpha*-"Tocopherol specifically inactivates cellular protein kinase C alpha by changing its phosphorylation state," *Biochem. J.*, vol. 334, pp. 243-249, 1998.

Roussaki M. *et al.,* "A novel synthesis of 3-aryl coumarins and evaluation of their antioxidant and lipoxygenase inhibitory activity," *Bioorg. Med. Chem. Lett.*, vol. 20, pp. 3889-3892, 2010.

Saville M. W. *et al.,* "Treatment of HIV-associated Kaposi's sarcoma with paclitaxel," *Lancet*, vol. 346, pp. 26-28, 1995.

Sashidhara K. V. *et al.,* "Synthesis and in vitro evaluation of novel coumarin-chalcone hybrids as potential anticancer agents," *Bioorg. Med. Chem. Lett.*, vol. 20, pp. 7205-7211, 2010.

Schmitz M. L. *et al.,* "Molecular analysis of mitogen-activated protein kinase signaling pathways induced by reactive oxygen intermediates," *Methods Enzymol.*, vol. 352, pp. 53-61, 2002.

Schreck R. *et al.,* "Reactive oxygen intermediates as apparently widely used messengers in the activation of the NF-kappa B transcription factor and HIV-1," *EMBO J.,* vol. 10, pp. 2247-2258, 1991.

Shakibaei M. *et al.,* "Resveratrol suppresses interleukin-1beta-induced inflammatory signaling and apoptosis in human articular chondrocytes: potential for use as a novel nutraceutical for the treatment of osteoarthritis," *Biochem. Pharmacol.*, vol. 76, pp. 1426-1439, 2008.

Simonian N. A. and Coyle J. T. "Oxidative stress in neurodegenerative diseases," *Annu. Rev. Pharmacol Toxicol.*, vol. 36, pp. 83-106, 1996.

Singla A. K. *et al.,* "Paclitaxel and its formulations," *Int. J. Pharm.*, vol. 235, pp. 179-192, 2002.

Sharma M. *et al.,* "Lantadene A-induced apoptosis in human leukemia HL-60 cells," *Ind J Pharmacol.,* vol. 39, pp. 140-144, 2007a.

Sharma M. *et al.,* Synthesis, cytotoxicity and antitumor activity of Lantadene A congeners," *Chem Biodiver.*, vol. 4, pp. 932-939, 2007b.

Sharma M. *et al.,* "Synthesis and antitumor activity of novel pentacyclic triterpenoid Lantadene D," *Letters in Drug Design & Discovery*, vol. 4, pp. 201-206, 2007c.

Sharma M. *et al.,* "Design, synthesis and evaluation of Lantadene A congener with hydroxyl functionality in ring A as an antitumour agent," *Nat Prod Res.,* vol. 25, pp. 387- 396, 2011.

Sharma M. *et al.,* "Lantadenes and their esters as potential antitumor agents," *J Nat Prod.*, vol. 71, pp. 1222-1227, 2008.

Sharma O. P. *et al.,* "Isolation and partial purification of lantana (Lantana camara L.) toxins," *Toxicol. Lett.,* vol. 37, pp. 165-172, 1987.

Shoemaker R. H., "The NCI60 human tumour cell line anticancer drug screen," *Nat. Rev. Cancer.*, vol. 6, pp. 813-823, 2006.

Smith J. *et al.*, "Antibodies to CD3/T-cell receptor complex induce death by apoptosis in immature T cells in thymic cultures," *Nature (Lond),* vol. 337, pp. 181-184, 1989.

Spizzirri U. G. *et al.,* "Synthesis of antioxidant polymers by grafting of gallic acid and catechin on gelatin," *Biomacromolecules*, vol. 10, pp. 1923-1930, 2009.

Spizzirri U. G. *et al.,* "Antioxidant-polysaccharide conjugates for food application by eco-friendly grafting procedure," *Carbohydrate Polymers*, vol. 79, pp. 333-340, 2010.

Stark A. A. *et al.*, "Gamma-glutamyl transpeptidase in murine lymphomas. *Eur. J. Cancer Clin. Oncol.*" vol. 22, pp. 77-87, 1986.

Stanway S. J. *et al.,* "Phase I Study of STX 64 (667 Coumate) in Breast Cancer Patients: The First Study of a Steroid Sulfatase Inhibitor," *Clin. Cancer Res.*, vol. 12, pp. 1585, 2006.

Stadtman E. R., "Protein oxidation in aging and age-related diseases," *Ann. N. Y. Acad. Sci.,* vol. 928, pp. 22-38, 2001.

Stepp J. R. and Moerman D. E., "The importance of weeds in ethnopharmacology," *J Ethnopharmacol.,* vol. 75, pp. 25-31, 2001.

Stratford M. R. and Dennis M. F., "Measurement of incorporation of bromodeoxyuridine into DNA by high performance liquid chromatography using a novel fluorescent labelling technique," *Int. J. Radiat. Oncol. Biol. Phys*., vol. 22, pp. 485-487, 1992.

Suzuki Y. J. *et al.,* "Thioctic acid and dihydrolipoic acid are novel antioxidants which interact with reactive oxygen species," *Free Radic. Res. Commun*., vol. 15, pp. 255-263, 1991.

Tabner B. J. *et al.,* "Production of reactive oxygen species from aggregating proteins implicated in Alzheimer's disease, Parkinson's disease and other neurodegenerative diseases," *Curr. Top. Med. Chem*., vol. 1, pp. 507-517, 2001.

Tailor N. and Sharma M. "Antioxidant hybrid compounds: a promising therapeutic intervention in oxidative stress induced diseases," *Mini. Rev. Med. Chem.,* vol. 13, pp. 280-297, 2013.

Takeda Y. *et al.,* "Morroniside cinnamic acid conjugates as an anti-inflammatory agent," *Bioorg. Med. Chem. Lett*., vol. 20, pp. 4855-4857, 2010.

Tappia P. S. *et al.,* "Oxidative stress and redox regulation of phospholipase D in myocardial disease," *Free Radic. Biol. Med.,* vol. 41, pp. 349-361, 2006.

Teillet F. *et al.,* "Flavonoids as RTK inhibitors and potential anticancer agents," *Med. Res. Rev*., vol. 28, pp. 715-745, 2008.

Thannickal V. J. and Fanburg B. L., "Reactive oxygen species in cell signaling," *Am. J. Physiol. Lung Cell Mol. Physiol*., vol. 279, pp. L1005-L1028, 2000.

Thevenin B. J. *et al.,* "A novel photoactivatable cross-linker for the functionally-directed region-specific fluorescent labeling of proteins," *Eur. J. Biochem*., vol. 206, pp. 471-477, 1992.

Thomas M. P. *et al.,* "Ion channel blockade attenuates aggregated alpha synuclein induction of microglial reactive oxygen species: relevance for the pathogenesis of Parkinson's disease," *J. Neurochem.,* vol. 100, pp. 503-519, 2007.

Todeschini A. R. *et al.,* "Synthesis and evaluation of analgesic, antiinflammatory and antiplatelet properties of new 2-pyridylarylhydrazone congeners," *Eur. J. Med. Chem*., vol. 33, pp. 189-199, 1998.

Valko M. *et al.,* "Metals, toxicity and oxidative stress," *Curr. Med. Chem.,* vol. 12, pp. 1161-1208, 2005.

Venkatachalam S. R. *et al.,* "Synthesis, pulse radiolysis, and in vitro radioprotection studies of melatoninolipoamide, a novel conjugate of melatonin and α-lipoic acid," *Bioorg. Med. Chem*., vol. 14, pp. 6414-6419, 2006.

Velu C. S. *et al.,* "Human p53 is inhibited by glutathionylation of cysteines present in the proximal DNA-binding domain during oxidative stress," *Biochemistry*, vol. 46, pp. 7765-7780, 2007.

Vissers M. C. *et al.,* "Modulation of hypoxia-inducible factor-1 alpha in cultured primary cells by intracellular ascorbate," *Free Radic. Biol. Med*., vol. 42, pp. 765-772, 2007.

Walker E. H. *et al.,* "Structural determinants of phosphoinositide 3-kinase inhibition by wortmannin, LY294002, quercetin, myricetin, and staurospirin," *Mol. Cell.*, vol. 6, pp. 909-919, 2000.

Wang I. C. *et al.,* "C_{60} and Water-Soluble Fullerene Congeners as Antioxidants Against Radical-Initiated Lipid Peroxidation," *J. Med. Chem.,* vol. 42, pp. 4614-4620, 1999.

Wasley A. and Alter M. J., "Epidemiology of hepatitis C: geographic differences and temporal trends," *Semin. Liver Dis.*, vol. 20, pp. 1-16, 2000.

Welch K. D. *et al.,* "Modification of ferritin during iron loading," *Free Radic. Biol. Med.,* vol. 31, pp. 999-1006, 2001.

Wells G. *et al.,* Fluorescent 7-diethylaminocoumarin pyrrolobenzodiazepine conjugates: Synthesis, DNA interaction, cytotoxicity and differential cellular localization. *Bioorg. Med. Chem. Lett.*, vol. 18, pp. 2147-2151, 2008.

Wilson J. N. *et al.,* "Reactive oxygen species in acute respiratory distress syndrome," *Heart Lung*, vol. 30, pp. 370-375, 2001.

Woo Y. J. *et al.,* "Development of Selective Butyrylcholinesterase Inhibitors Using (R)-Lipoic Acid-Polyphenol Hybrid Molecules," *Bull. Korean Chem. Soc.*, vol. 32, pp. 2997-3002, 2011.

Yan L. J. *et al.,* "Efficacy of hypochlorous acid scavengers in the prevention of protein carbonyl formation," *Arch. Biochem. Biophys.*, vol. 327, pp. 330-334, 1996.

Yang S. and Meyskens F., "Alterations in activating protein 1 composition correlate with phenotypic differentiation changes induced by resveratrol in human melanoma," *Mol. Pharmacol.*, vol. 67, pp. 298-308, 2005.

Yoshizumi M. *et al.,* "Signal transduction of reactive oxygen species and mitogen-activated protein kinases in cardiovascular disease," *J. Med. Invest.,* vol. 48, pp. 11-24, 2001.

Yoo Y. J. *et al.,* "Synthesis of cinnamoyl ketoamides as hybrid structures of antioxidants and calpain inhibitors," *Bioorg. Med. Chem. Lett.,* vol. 21, pp. 2850-2854, 2011.

Yu R. *et al.,* "Resveratrol inhibits phorbol ester and UV-induced activator protein1 activation by interfering with mitogen-activated protein kinase pathways," *Mol. Pharmacol.*, vol. 60, pp. 217-22, 2001.

Yu S. H. *et al.,* "Preparation and characterization of radical and pH-responsive chitosan-gallic acid conjugate drug carriers," *Carbohydrate Polymers*, vol. 84, pp. 784-802, 2011.

Youk H. J. *et al.,* "Enhanced anticancer efficacy of a-tocopheryl succinate by conjugation with polyethylene glycol," *J. Control. Release*, vol. 107, pp. 43-52, 2005.

Zhao J. *et al.,* "Upregulating of Fas, integrin beta4 and P53 and depressing of PC-PLC activity and ROS level in VEC apoptosis by safrole oxide," *FEBS Lett.,* vol. 579, pp. 5809-5813, 2005.

Zingg J. M., "Modulation of signal transduction by vitamin E," *Mol. Aspects. Med.*, vol. 28, pp. 481-506, 2007.

PUBLICATIONS

1. Tailor N. K. *et al.,* "Synthesis and *in-vitro* anticancer activities of C-2 arylidene congeners of lantadenes", *Eur. J. Med. Chem.*, vol. 64, pp. 285-291, 2013 [I.F. 3.34].

2. Tailor N. K. *et al.,* "Synthesis, selective cancer cytotoxicity and mechanistic studies of novel congeners of lantadenes," *Anticancer Agents Med. Chem.* 2012 Dec 24. [Epub ahead of print], [I.F. 2.862].

3. Tailor N. and Sharma M., "Antioxidant Hybrid Compounds: A Promising Therapeutic Intervention in Oxidative Stress Induced Diseases," *Mini. Rev. Med. Chem.* Vol. 13, pp. 280-297, 2012. [IF 2.528].

4. Tailor N. K. *et al.,* "Effective melanoma inhibition by synthetic pentacyclic triterpenoid 2-(3-phenylprop-2-en-1-ylidene)-22β-hydroxy-3-oxoolean-12-en-28-oic acid: An *in-vitro* and *in-vivo* study," *J. Envior. Pathol. Toxicol. Oncol.* (In Press) [I.F. 1.107].